PhD Program in Translational and Molecular Medicine

DIMET

(XXVIII cycle)

University of Milano-Bicocca

School of Medicine and Faculty of Science

Induced pluripotent stem cells (iPSCs) for modelling mucopolysaccharidosis type I (Hurler syndrome)

Tutor: Dott.ssa Marta SERAFINI

Co-tutor: Prof. Andrea BIONDI

Dr. Anna Montagna

Matr. No.774873

Academic year 2014-2015

A me: un traguardo personale!

A tutte le ragazze del Tettamanti!

TABLE OF CONTENTS

CHAPTER 1

General Introduction

1.The disease

1.1 Lysosomal Storage Disorders

Lysosomal storage disorders (LSDs) are a significant subgroup of inherited metabolic disorders characterized by disruption of normal lysosomal function and consequent accumulation of incompletely degraded macromolecules.

Most LSDs result from mutations in genes that encode soluble lysosomal acid hydrolases; some of them are caused, instead, by genetic defects in proteins essential for the function of the lysosomal system such as receptors, activator proteins, membrane proteins or transporters. Lysosomal disorders are autosomal recessive, except for Fabry, Hunter and Danon diseases, which are X-linked [1]. To date, nearly 60 different diseases have been recognized and more than 50 different proteins were identified as causing LSDs, and the list continue to grow;[2, 3] These disorders are individually rare and affect between 1:25,000 to less than 1: 250,000 live births, but the combined frequency of LSDs as a group is almost 1 incident in every 8,000 live births, that makes them an important public health problem worldwide [2, 4].

LSDs are usually classified based on the nature of the stored material and broad categories include (Table 1):

- Mucopolysaccharidoses (MPSs)
- Sphingolipidoses
- Oligosaccharidoses and Glycoproteinoses
- Glicogen storage diseases
- Mucolipidoses

OMIM	Disease	Defective protein	Main storage material(s)	Preliminary test	Gene symbol	MIM ID	Diagnostic test
Mucopolysaccharidoses (MPSs)							
607014 607015 607016	MPS I (Hurler, Scheie, Hurler/Scheie)	α-Iduronidase	Dermatan sulphate, heparan sulphate	GAGs (U)	IDUA	252800	BGT, MGT
309900	MPS II (Hunter)	Iduronate sulphatase	Dermatan sulphate, heparan sulphate	GAGs (U)	IDS	309900	BGT, MGT
252900	MPS III A (Sanfilippo A)	Heparan sulphamidase	Heparan sulphate	GAGs (U)	SGSH	605270	BGT, MGT
252920	MPS III B (Sanfilippo B)	Acetyl-α-glucosaminidase	Heparan sulphate	GAGs (U)	NAGLU	609701	BGT, MGT
252930	MPS III C (Sanfilippo C)	Acetyl CoA: α-glucosaminide N-acetyltransferase	Heparan sulphate	GAGs (U)	HGSNAT	610453	BGT, MGT
252940	MPS III D (Sanfilippo D)	N-acetyl glucosamine-6-sulphatase	Heparan sulphate	GAGs (U)	GNS	607664	BGT, MGT
253000	MPS IV A (Morquio A)	Acetyl galactosamine-6-sulphatase	Keratan sulphate, chondroitin 6-sulphate	GAGs (U)	GALNS	612222	BGT, MGT
253010	MPS IV B (Morquio B)	β-Galactosidase	Keratan sulphate	GAGs (U)	GLB1	611458	BGT, MGT
253200	MPS VI (Maroteaux-Lamy)	Acetyl galactosamine 4-sulphatase (arylsulphatase B)	Dermatan sulphate	GAGs (U)	ARSB	611542	BGT, MGT
253220	MPS VII (Sly)	β-Glucuronidase	Dermatan sulphate, heparan sulphate, chondroitin 4-sulphate	GAGs (U)	GUSB	611499	BGT, MGT
601492	MPS IX (Natowicz)	Hyaluronidase	Hyaluronan	–	HYAL1	607071	BGT, MGT
Sphingolipidoses							
301500	Fabry	α-Galactosidase A	Globotriaosylceramide	–	GLA	300644	BGT, MGT
228000	Farber	Acid ceramidase	Ceramide	–	ASAH1	613468	BGT, MGT
230500 230600 230650	Gangliosidosis GM1 (Types I, II, III)	GM1-β-galactosidase	GM1 ganglioside, Keratan sulphate, oligo, glycolipids	Oligos (U)	GLB1	611458	BGT, MGT
272800	Gangliosidosis GM2, Tay-Sachs	β-Hexosaminidase A	GM2 ganglioside, oligo, glycolipids	–	HEXA	606869	BGT, MGT
268800	Gangliosidosis GM2, Sandhoff	β-Hexosaminidase A + B	GM2 ganglioside, oligos	–	HEXB	606873	BGT, MGT
230800 230900 231000	Gaucher (Types I, II, III)	Glucocerebrosidase	Glucocerebroside	Chitot* (U)	GBA	606463	BGT, MGT
245200	Krabbe	β-Galactocerebrosidase	Galactocerebroside	–	GALC	606890	BGT, MGT
250100	Metachromatic leucodystrophy	Arylsulphatase A	Sulphatides	Sulphatides (U)	ARSA	607574	BGT, MGT
257200 607616	Niemann-Pick (type A, type B)	Sphingomyelinase	Sphingomyelin	–	SMPD1	607608	BGT, MGT
Oligosaccharidoses (glycoproteinoses)							
208400	Aspartylglucosaminuria	Glycosylasparaginase	Aspartylglucosamine	Oligos (U)	AGA	**613228**	BGT, MGT
230000	Fucosidosis	α-Fucosidase	Glycoproteins, glycolipids, fucose-rich oligos	Oligos (U)	FUCA1	**612398**	BGT, MGT
248500	α-Mannosidosis	α-Mannosidase	Mannose-rich oligos	Oligos (U)	MANBA1	609458	BGT, MGT
248510	β-Mannosidosis	β-Mannosidase	Man(β1 → 4)GlcNAc	Oligos (U)	MANBA	609489	BGT, MGT
609241	Schindler	N-acetylgalactosaminidase	Sialylated/ asialoglycopeptides, glycolipids	Oligos (U)	NAGA	104170	BGT, MGT
256550	Sialidosis	Neuraminidase	Oligos, glycopeptides	Bound SA (U), Oligos (U)	NEU1	608272	BGT, MGT
Glycogenoses							
232300	Glycogenosis II, Pompe	α-1,4-glucosidase (acid maltase)	Glycogen	CK (S)	GAA	606800	BGT, MGT
Lipidoses							
278000	Wolman/CESD	Acid lipase	Cholesteryl esters	–	LIPA	613497	BGT, MGT
Non-enzymatic lysosomal protein defect							
272750	Gangliosidosis GM2, activator defect	GM2 activator protein	GM2 ganglioside, oligos	–	GM2A	613109	MGT
249900	Metachromatic leucodystrophy	Saposin B	Sulphatides	Sulphatides (U)	PSAP	176801	MGT
611721	Krabbe	Saposin A	Galactocylceramide	–	PSAP	176801	MGT
610539	Gaucher	Saposin C	Glucocylceramide	–	PSAP	176801	MGT
Transmembrane protein defect							
Transporters							
269920 604369	Salla acid storage disease, infantile form (SIASD) and adult form (Salla)	Sialin	Salla acid	Free SA (U)	SLC17A5	604322	MGT
219800	Cystinosis	Cystinosin	Cystine	–	CTNS	606272	MGT
257220	Niemann-Pick Type C1	Niemann-Pick type 1 (NPC1)	Cholesterol and sphingolipids	Chitot* (U)	NPC1	607623	Filipin test, MGT
607625	Niemann-Pick, Type C2	Niemann-Pick type 2 (NPC2)	Cholesterol and sphingolipids	Chitot* (U)	NPC2	601015	Filipin test, MGT
Structural Proteins							
300257	Danon	Lysosome-associated membrane protein 2	Cytoplasmatic debris and glycogen	–	LAMP2	309060	MGT
252650	Mucolipidosis IV	Mucolipin	Lipids	–	MCOLN1	605248	MGT
Lysosomal enzyme protection defect							
256540	Galactosialidosis	Protective protein cathepsin A (PPCA)	Sialyloligosaccharides	Bound SA (U), Oligos (U)	CTSA	613111	BGT*, MGT
Post-translational processing defect							
272200	Multiple sulphatase deficiency	Multiple sulphatases	Sulphatides, glycolipids, GAGs	Sulphatides (U), GAGs (U)	SUMF1	607939	BGT*, MGT

Table 1. List of lysosomal storage disorders (LSDs) providing information about the defective protein and the main storage material(s) of each disease [5].

Alternatively, LSDs can also be classified according to the type of protein deficiency, i.e. lysosomal hydrolases, transmembrane proteins, co-factors or coactivators required for lysosomal enzyme function, proteins protecting lysosomal enzymes, proteins involved in post-translational processing of lysosomal enzymes, enzymes involved in targeting mechanisms for protein localization to the lysosome, proteins involved in intracellular trafficking [2, 4].

Moreover, most LSDs present with different clinical variants and are also classified based on the patients' age at symptom onset: infantile, juvenile and adult forms are typically identified. The most severe infantile forms frequently present with brain pathology: affected individuals generally appear normal at birth but symptoms appear soon after birth. Neuropathology is progressive and ultimately leads to death at an early age. In adult forms, instead, disability results mainly from peripheral symptoms and the progression is slower. Juvenile forms are intermediate between infantile and adult forms.

1.1.1 Lysosomes and lysosomal hydrolases

Lysosomes are the main degradative organelles in all cells: being at the crossroad of multiple routes within the endosomal-autophagic-lysosomal system, they play a central role in the clearance of both endogenous and extracellular substrates. The catabolic process is performed through the concerted action of approximately 60 soluble enzymes contained in the lysosomes and called lysosomal acid hydrolases. They belong to different protein family, such as sulfatases, glycosidases, nucleases, phosphatases, lipases and peptidases. These enzymes catalyze the hydrolytic cleavage of specific chemical bonds in

their substrates and they reach the maximum activity at the acidic pH of the internal compartment of the lysosomes, that is maintained between 4.5 and 5 by proton-pumping ATPases located in the lysosomal membrane [6, 7].

Lysosomal hydrolases, as proteins of the secretory pathway, are synthesized on the surface of the Rough Endoplasmic Reticulum (RER) and are co-translationally glycosylated on asparagine residues; next, they move to the *cis* Golgi network, where they are recognized by phosphotranspherases that covalently modify them by adding a phosphate group on some of their mannose residues. The resulting mannose-6-phosphate (M6P) groups act as targeting signals: in the *trans* Golgi network they are selectively recognized and bound by M6P receptors (MPRs), and enzyme-receptor complexes are gathered into clathrin-coated vescicles that bud off from the Golgi and fuse with late endosomes. Once the complexes have been delivered to the endosomes, the acidic pH of the organelles causes the dissociation of the hydrolases from the receptors and their release into the lumen as soluble active enzymes; empty receptors are recycled to the Golgi apparatus (Fig.1)

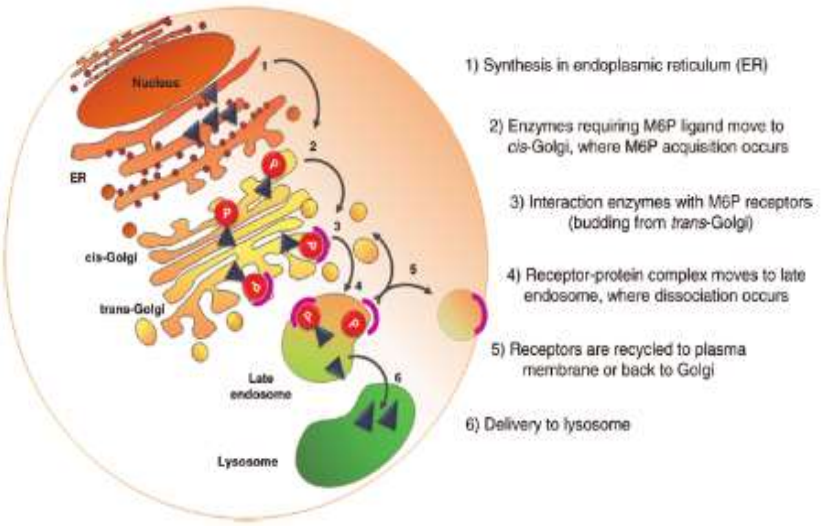

Fig.1. Simplified scheme of M6P-dependent enzymes sorting to the lysosome [5].

Some hydrolases, although M6P-tagged, escape binding to MPRs and are directed by default to cell surface and secreted; anyway, since some MPRs are localized even at the plasma membrane, the enzymes can be recaptured and they can reach the lysosomes by receptor-mediated endocytosis [8].

In addition, specific enzymes do not depend on MPR for lysosomal delivery, such as ß-glucocerebrosidase, which is transported to lysosomes by lysosomal integral membrane protein 2 (LIMP-2) [9].

Substrates are transported to lysosomes through different routes. Specialized endocytic mechanisms (phagocytosis, macropinocytosis, clathrin-mediated endocytosis, caveolin-mediated endocytosis, and clathrin- and caveolin-independent endocytosis) are preferentially engaged according to the nature of the molecules. Intracellular materials are transported to the lysosomal compartment mainly through autophagy, a process by which cells capture and convey their own

cytoplasmic components and organelles to lysosomal degradation and recycling [3].

Recent studies have expanded our perspective on lysosomal function highlighting that lysosome are not only catabolic organelles, but are also involved in fundamental cellular functions such as signaling, vesicle trafficking, nutrient sensing and cellular growth. To give an example, it has become evident that the lysosome plays an important part in nutrient sensing and in signaling pathways involved in cell metabolism and growth. The recent discovery that the mammalian target of rapamycin complex 1 (mTORC1) kinase complex, the master controller of cell growth, exerts its function on the lysosomal surface suggests that cell growth and cell catabolism are co-regulated[10, 11] . Recent studies have shown that the level of amino acids in the lysosomal lumen controls mTORC1 localization on the lysosomal surface. During starvation, mTORC1 inhibition potently activates autophagy.

Lysosomal function requires the concerted action of hydrolases, acidification machinery, and membrane proteins. It has been recently discovered that genes involved in lysosomal function belong to a gene network—the coordinated lysosomal expression and regulation (CLEAR) network—and are transcriptionally regulated by the lysosomal master gene TFEB [12]. TFEB positively regulates the expression of lysosomal genes, controls the number of lysosomes, and promotes degradation of lysosomal substrates. TFEB-mediated regulation allows lysosomal function to adapt to different physiological and pathological conditions (e.g. starvation or storage). Interestingly, phosphorylation of TFEB by mTORC1 negatively regulates its activity

by retaining it in the cytoplasm, thus blocking its nuclear translocation. During starvation, mTORC1 inhibition allows TFEB to translocate to the nucleus and perform its transcriptional activity. This is the first example of a lysosome-to-nucleus signaling mechanism [13].

1.1.2 Etiopathogenesis and clinical features of LSDs

Degradation of substrates occurring in the lysosomes is a stepwise activity that requires the sequential action of a series of lysosomal hydrolases, each one catalyzing a step in the catabolic pathway of specific macromolecules. If a step in the process fails, further degradation is impossible and partially degraded substrates accumulate [14]. For this reason, mutations in genes that encode lysosomal hydrolases, or in proteins that are necessary for their post-translational modification, targeting and transport to the lysosome, often result in LSDs [15]. The main hypothesis concerning the etiopathogenesis of LSDs consists in that the primary enzyme deficiency causes the intralysosomal accumulation of substrates normally degraded by the lacking enzyme, leading to lysosomal engulfment; this affects cell architecture and cell function, sometimes leading to cell death. In the last few years, the numerous and interconnected cellular pathways perturbed in LSDs as a result of the primary lysosomal defect are being identified [16-18]. The most notable and most studied defective mechanisms are:

- autophagy block;
- defective proteins and organelles turnover;
- biochemical injury due to toxic metabolites accumulation;
- derangements in pH regulation, calcium and iron homeostasis;

- synaptic release impairment;
- abnormalities in endoplasmic reticulum stress responses;
- energy failure;
- inflammatory and apoptotic response.

The resultant clinical phenotype reflects the amount of residual enzyme activity and the pattern of cell types involved: as lysosomes are ubiquitous organelles and their role is crucial in almost all cell types, however, LSDs are typically multi-systemic diseases, which means that many tissues and organ systems are affected in each of them.

Even if LSDs are heterogeneous in terms of age of onset, clinical features and rate of disease progression, most are characterized by pediatric onset, progressive course, significant morbidity with abnormalities of the nervous system, viscera, bone and cartilage and reduced lifespan -usually fatal within the first two decades of life- as a consequence of cardio-pulmonary and nervous system involvement [19].

1.2 Mucopolysaccharidoses

Mucopolysaccharidoses (MPSs) represent a prominent subgroup among the lysosomal storage diseases. They result from a deficiency in the activity of lysosomal enzymes required for the catabolism of glycosaminoglycans (GAGs), once known as mucopolysaccharides, which are long unbranched polysaccharides, ground substance of all connective tissues. Thus, MPSs are characterized by intralysosomal storage of partially degraded GAGs, which results in cell, tissue and

organ dysfunction, increased GAGs accumulation in the extracellular spaces and GAGs urine excretion [20].

The stepwise degradation of GAGs requires eleven enzymes: four exoglycosidases, five sulphatases, one transferase and one endoglycosidase [21]. Deficiency of each one of these enzymes has been associated with one of the MPSs identified until now. These diseases initially took the name from the scientists who described them for the first time, but from the 1970s until 2006, with the identification of the enzymes involved in the catabolism of GAGs, they have been classified on the basis of the specific enzyme defective in each disease. To date, seven types of MPSs are recognized: MPS type I, II, III, IV, VI, VII, IX. MPS type III phenotype can be caused by defects in four different enzymes and MPS type IV phenotype by defects in two different enzymes, so this two MPSs are divided into four and two subgroups, respectively: MPS type III A, B, C or D and MPS type IV A or B. As a result, eleven different MPSs are currently known: their name can be found in Table 2 together with the genetic defect that characterizes each one of them [22].

All MPSs show autosomal recessive pattern of inheritance except for MPS type II, which is X-linked. MPSs are rare diseases: data on the incidence of each MPS type are available for only a few countries and they are extremely variable due to the rarity and the difficulty in diagnosis; the overall incidence of MPSs as a group, anyway, is estimated to be higher than 1 in 25000 live births [21].

MPS	Name	Increased GAGs	Inheritance	Enzyme deficiency
I	Hurler, Hurler-Scheie or Scheie	HS + DS	autosomal recessive	α-duronidase
II	Hunter	HS + DS	X-linked recessive	Iduronate sulfatase
III A	Sanfilippo A	HS	autosomal recessive	Heparan-N-sulfatase
III B	Sanfilippo B	HS	autosomal recessive	α-N-acetylglucosaminidase
III C	Sanfilippo C	HS	autosomal recessive	AcetylCoA α- glucosamine acetyltransferase
III D	Sanfilippo D	HS	autosomal recessive	N-acetylglucosamine 6-sulfatase
IV A	Morquio A	KS	autosomal recessive	Galactosamine-6-sulfate sulfatase
IV B	Morquio B	KS	autosomal recessive	α-galactosidase
(V)	Scheie syndrome, initially proposed as type V, was recognized to be the attenuated end of the MPS I spectrum			
VI	Maroteaus-Lamy	DS	autosomal recessive	N-acetylgalactamine 4-sulfatase
VII	Sly	HS + DS	autosomal recessive	α-glucuronidase
(VIII)	An enzyme defect was found and proposed as MPS VIII, but shortly thereafter recognized as a laboratory pitfall			
IX	Natowicz	Hyaluronan	autosomal recessive	Hyaluronidase 1

Table 2. List of Mucopolysaccharidoses (MPSs) providing information about name, increased GAG(s), inheritance and enzyme deficiency relative to each disease; HS= heparan sulphate, DS= dermatan sulphate, KS= keratan sulphate (adapted from. [22]).

1.2.1 Glycosaminoglycans and their physiological role

Glycosaminoglycans (GAGs) are organic macromolecules consisting of long unbranched polysaccharides made up of a succession of 50-25000 disaccharide units; one component of the disaccharide unit is always an amino sugar (N-acetylglucosamine or Nacetylgalactosamine), from which the name "glycosaminoglycans", while the other is an uronic acid (glucuronic acid or iduronic acid) - except for the GAG keratin sulphate, in which the second component of the disaccharide is D-galactose.

GAGs often exhibit a high rate of sulphation, that can occur in various degree and on different sugar positions, and gives to these macromolecules a clear negative electric charge, rendering them highly water-attractive [23].

Specific GAGs have different names depending on their chemical characteristics such as the sugar constituents of their disaccharide units and the geometry of the glycosidic linkage between them. On this basis, the following GAGs are identified (Table 3) [21]:

- hyaluronate;
- chondroitin sulphate (CS);
- heparan sulphate (HS);
- heparin;
- dermatan sulphate (DS);
- keratan sulphate (KS).

GAG	LOCALIZATION	COMMENTS
Hyaluronate	synovial fluid, articular cartilage, skin, vitreous humor, ECM of loose connective tissue	large polymers, molecular weight can reach 1 million Daltons; high shock absorbing character
Chondroitin sulfate	cartilage, bone, heart valves	most abundant GAG; usually associated with protein to form proteoglycans; the chondroitin sulfate proteoglycans form a family of molecules called lecticans and includes aggrecan, versican, brevican, and neurcan; major component of the ECM; loss of chondroitin sulfate from cartilage is a major cause of osteoarthritis
Heparan sulfate	basement membranes, components of cell surfaces	found associated with protein forming heparan sulfate proteoglycans (HSPG); major HSPG forms are the syndecans and GPI-linked glypicans; HSPG binds numerous ligands such as fibroblast growth factors (FGFs), vascular endothelial growth factor (VEGF), and heptocyte growth factor (HGF)
Heparin	component of intracellular granules of mast cells, lining the arteries of the lungs, liver and skin	more sulfated than heparan sulfates; clinically useful as an injectable anticoagulant although the precise role in vivo is likey defense against invading bacteria and foreign substances
Dermatan sulfate	skin, blood vessels, heart valves, tendons, lung	may function in coagulation, wound repair, fibrosis, and infection; excess accumulation in the mitral valve can result in mitral valve prolapse
Keratan sulfate	cornea, bone, cartilage	usually associated with protein forming proteoglycans; keratan sulfate proteoglycans include lumican, keratocan, fibromodulin, aggrecan, osteoadherin, and prolargin

Table 3. List of glycosaminoglycans (GAGs) with information about their tissue distribution and their physiological role (modified from themedicalbiochemistrypage.org).

The majority of GAGs are covalently linked to core proteins on some serine residues, forming large complexes known as proteoglycans: these macromolecules have a brush-like structure in which GAGs extend perpendicularly from the protein core, and their molecular weight is huge (30 to 500 kilodaltons) [24]. Alone or as components of proteoglycans, GAGs are main constituents of the extracellular matrix of connective tissues: they are abundant in skin, cartilage, bone, tendons, blood vessels and in the stroma of all organs. Their mechanical

role in these tissues depends on their capacity to retain water and on their elastic properties, thanks to which they form a jelly-structure having unique lubrication and shock absorbing capacity. This role is especially noticeable in joint cartilage. GAGs are also designed to guarantee the maintenance of a hydrated organized extracellular space in which nutrients and signaling molecules can move from cell to cell. Therefore, they fulfill a variety of physiological functions in modulating processes such as [24, 25] cell adhesion;

- cell motility;
- growth factors and cytokines signaling;
- cell response to damage such as wounding and infection;
- embryogenesis;
- neurogenesis and neuronal regeneration;
- bone formation and remodeling.

1.2.2 Clinical features of MPSs: implications of GAGs accumulation

Like the other macromolecules in the body, GAGs are continuously renewed, in part in the lysosomes after uptake through endocytosis and in part extracellularly by secreted enzymes. The lack of GAGs degradation due to lysosomal enzyme deficiency observed in MPSs leads to GAGs storage with loss of cellular function, tissue damage and organ dysfunction, determining the clinical symptoms observed in patients. Since GAGs role is prominent in cartilaginous tissue, MPS patients typically develop a series of bone and joint abnormalities; but GAGs accumulation affects all connective tissues, so MPSs definitely have the characteristics of multisystemic diseases [24, 26, 27] MPSs, as

LSDs, are usually characterized by a chronic and progressive course, with age of onset and velocity of progression depending on the severity of the defect. Signs and symptoms suggestive of MPSs are [28]:

- common bone and joint features:
  - early joint involvement with joint stiffness and contractures;
  - radiological evidence of dysostosis multiplex: spinal deformity, claw hand and others;
- other common clinical signs:
  - short stature;
  - mental retardation;
  - coarsening of facial features over time;
  - corneal clouding;
  - deafness;
  - frequent respiratory infections, chronic nasal congestion, noisy breathing;
  - heart murmur;
  - carpal tunnel syndrome, trigger fingers;
  - abdominal protuberance due to liver and spleen enlargement;
  - recurrent inguinal or umbilical hernia.

The exact molecular bases for the skeletal and connective tissue anomalies common in all MPSs are still under investigation. Studies in animal models have provided evidence that these abnormalities are not simply a consequence of primary GAGs accumulation in both the lysosomal compartment and the extracellular matrix, because GAGs are not an inert storage material: they are indeed biologically active

molecules involved in many critical cellular and tissue pathways. For this reason, the defect in GAGs turnover gives rise to a complex and multistep pathogenic cascade [29].

1.3 Mucopolysaccharidosis type I

Mucopolysaccharidosis type I (MPS type I or MPS I) is an autosomal recessive disease included within the group of Mucopolysaccharidoses; it is one of the most frequent lysosomal storage disorders.

MPS I is due to a deficiency in α-L-iduronidase (IDUA) enzyme which is involved in the degradation of both the GAGs heparan sulphate and dermatan sulphate. As a consequence of low or absent IDUA activity, these GAGs accumulate in the lysosomal compartment, in the extracellular spaces and from there into biological fluids (plasma and urine), in which they are commonly dosed for the diagnosis of this disorder [30, 31].

The study of this disease started about one hundred years ago [22, 32]: MPS I was one of the first MPSs described, in 1919, by the German pediatrician Gertrude Hurler, who reported the case of two unrelated boys displaying visceromegaly and bone abnormalities [33]; the disease was named Hurler syndrome after her. Another historical denomination of this disease, coined by Ellis, Sheldon and Capon, was "Gargoylism", because the coarse facial features of affected children reminded these known grotesque figures of the Gothic cathedrals [34]:

- in 1962, Harold Scheie described an attenuated phenotype of Hurler disease; hence, this second disorder was called Scheie syndrome [35].

- in 1965, McKusick, re-classified all already known MPSs, by calling them Hurler syndrome “Mucopolysaccharidosis type I” and Scheie syndrome “Mucopolysaccharidosis type V” [36].
- in 1970, Wiesmann and Neufeld showed that Hurler and Scheie syndromes resulted from the deficiency of the same enzyme [37]. so, in 1972, McKusick reclassified MPS I and MPS V as MPS I clinical subtypes I-H and I-S respectively. The clinically intermediate phenotype displayed by some patients was called MPS I-H/S (Hurler/Scheie syndrome) [38].

So, the same gene defect in MPS type I can result in a wide range of phenotypic expression with three recognized clinical entities: Hurler syndrome (MPS I-H; OMIM (Online Mendelian Inheritance in Man) # 607014), Hurler/Scheie syndrome (MPS I-H/S; OMIM # 607015) and Scheie syndrome (MPS I-S; OMIM # 607016). Hurler and Scheie syndromes represent the severe and mild ends of the MPS I clinical spectrum respectively, and Hurler/Scheie syndrome is intermediate in terms of phenotypic expression (Table 4) [20].

However, it is increasingly being recognized that MPS I, with significant variability concerning age of presentation, symptoms and rate of disease progression, is often being classified into only two groups: “severe” MPS I-H and “attenuated” MPS I-H/S and MPS I-S. The majority of patients fill into the severe group, the best described and more precisely defined one; cases of attenuated MPS type I, instead, are very various in term of age of onset, clinical signs and disease course [39].

Pathology	Subtype	Enzyme deficiency	Affected GAG	Clinical manifestations
MPS I	Hurler (H)	α-L-iduronidase	Dermatan and heparan sulfate	Corneal clouding; dysostosis multiplex; organomegaly; heart disease; mental retardation; death in childhood.
	Hurler -Scheie (H/S)	α-L-iduronidase	Dermatan and heparan sulfate	Intermediate phenotype, between MPS IH and MPS IS.
	Scheie (S)	α-L-iduronidase	Dermatan and heparan sulfate	Corneal clouding; stiff joints; normal intelligence and life span.

Table 4. Summary of the three subtypes of MPS I providing information about enzyme deficiency, affected GAGs and clinical manifestations (adapted from [20]).

MPS I is the most diagnosed worldwide MPS type. The overall prevalence of this disease is 1:100,000 live births; regarding the prevalence of the three MPS type I sub-syndromes, one can assert that [40]: MPS I-H is far the most common subtype, with a prevalence of 7.6: 10,000;

- MPS I-H/S has an intermediate recurrence of 2.4: 10,000;
- MPS I-S is the rarest, with 0.7: 10,000 affected.

1.3.1. Molecular bases and phenotype determination of MPS I

The IDUA enzyme is an ubiquitarious lysosomal acid hydrolase that catalyzes the hydrolysis of unsulphated α-Liduronosidic linkages, removing the terminal α-L-iduronic acid residues of the glycosaminoglycans dermatan sulphate and heparan sulphate. Its activity is indispensable for GAGs turnover [37]. IDUA is a monomeric soluble protein with a molecular mass of 82 kDa; its primary structure consists of 653 aminoacids [36].

Aminoacidic sequence data from purified human liver IDUA allowed Scott et al. in 1990 to isolate a genomic and cDNA clone for IDUA and consequently to determine, by in situ hybridization to human metaphase chromosomes and Southern blot analysis of mouse-human cell hybrids, that the human *IDUA* gene maps to 4p16.3, from base pair 980784 to base pair 998316 (Fig. 2) [41].

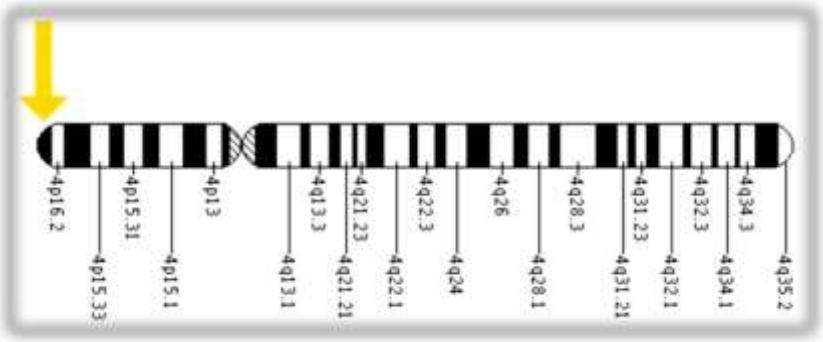

Fig. 2. Location of the human *IDUA* gene on the short arm of chromosome 4 (from ghr.nlm.nih.gov).

In 1992, Scott and collaborators cloned and purified the gene that encodes IDUA enzyme: they demonstrated that it spans approximately 19 kb and it contains 14 exons, which length varies from 77 to 217 bp; the first two exons are separated by an intron of 566 bp, then an intron of approximately 13 kb follows, and the last 12 exons are clustered within 4.5 kb (Fig. 2) [42].

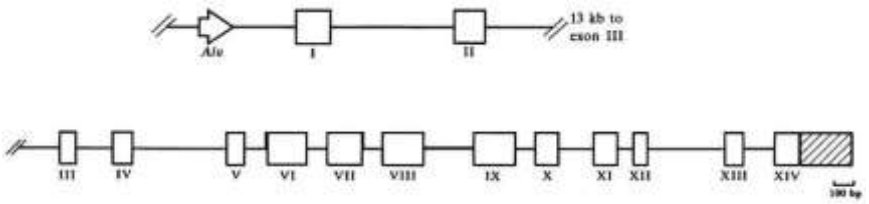

Fig. 3. Diagrammatic representation of *IDUA* gene (adapted from [32]).

To date, the Human Genome Mutation Database (HGMD) accounts for 207 possible mutations in *IDUA* gene, the majority of which are nonsense mutations, missense mutations, small insertions or deletions, splice site mutations. Only certain mutations allow the prediction of phenotype. In general, genotype-phenotype correlation and prediction of patient's clinical phenotype via genetic analysis in MPS type I is difficult, due to:

- the high degree of genotypic heterogeneity: large number of private single mutations, great prevalence of novel mutations and lack of recurrent mutations; moreover, frequency of MPS I alleles varies very widely among different ethnic populations, as documented below;
- the wide clinical variability in the MPS I patient population.

The most characterized and recurrent mutations are:

- W402X: it introduces a stop codon at position 402; first described by Scott et al. in 1992 in a study of 64 MPS type I patients, it is associated with an extremely severe clinical phenotype in homozygotes [43];
- Q70X: it introduces a stop codon at position 70 and it is associated with an extremely severe clinical phenotype in homozygotes [44];

- P533R: it exchanges the proline at position 533 to an arginine and it is associated with variable clinical phenotypes in homozygotes [44].

Patients who are compound heterozygotes, having one allele carrying a severe mutation (W402X, Q70X, P533R), show a wide range of clinical phenotypes. Alleles that cause the milder phenotypes, Hurler/Scheie and Scheie syndromes, are often missense mutations, as they are most likely to allow for some residual enzyme activity. In particular, R89Q mutation has been found in numerous mild patients, even in combination with a nonsense mutation [45] W402X and Q70X are the most common mutations among Caucasian, while they are rare among Japanese, Korean and Moroccan patients: they are present in 60-70% of alleles in Northern European patients. P533R mutation, instead, has a low incidence in European countries and a high recurrence among North Africans [39, 45, 46]. The most recurrent mutations in Italian patients are Q70X, P533R, G51D and W402X, which together represent 53% of all alleles [47].

A combination of differences in environmental and genetic backgrounds is postulated to explain the differences in clinical phenotype often observed even between patients with the same pathogenic mutation [48].

As little as 0.4% of normal residual activity is sufficient to produce a mild phenotype [49]. All forms of MPS I have nearly undetectable enzyme activity with currently available clinical and laboratory testing techniques, which are not able to detect small differences in residual enzyme activity. For this reason, residual enzyme activity cannot be used to predict disease phenotype [39].

1.3.2 Clinical manifestations of MPS type I

The lack of degradation of the GAGs heparan sulphate and dermatan sulphate in MPS I patients results in progressive accumulation of these components of proteoglycans within the lysosomes and in the extracellular matrix; subsequent abnormalities in cell function as well as in structural support to the extracellular matrix cause progressive multi-organ dysfunction and damage.

MPS I, with significant variability in age of onset, presenting symptoms, clinical signs and rate of disease progression, is characterized by marked clinical heterogeneity; however, this gradual multisystemic deterioration is typical of all MPS type I subtypes (Table. 5).

	"Severe" MPS I, MPS IH	"Intermediate" MPS I, MPS IHS	"Attenuated" MPS I, MPS IS
General	Early (<12 months) onset, rapid disease progression, hepatosplenomegaly, hernias (inguinal, umbilical, and hiatal), and death in first decade if untreated	Intermediate onset, hepatomegaly, and hernias (inguinal, umbilical, and hiatal)	Childhood onset, hernias (inguinal, umbilical, and hiatal), and normal life expectancy
Cognition	Normal early development, developmental delay/plateau, and neurocognitive decline	Learning disability possible and attention deficit possible	Typically no symptoms
Neurologic	Communicating hydrocephalus	Cervical spinal cord compression and cervical instability	Cervical spinal cord compression and cervical instability
Ophthalmologic	Corneal clouding and open-angle glaucoma	Corneal clouding and open-angle glaucoma	Corneal clouding, open-angle glaucoma, and retinal degeneration
Otolaryngological	Chronic recurrent rhinitis, persistent nasal discharge, obstructive sleep apnea, recurrent acute otitis media, and mixed hearing loss	Chronic recurrent rhinitis, persistent nasal discharge, obstructive sleep apnea, recurrent acute otitis media, and mixed hearing loss	
Cardiac	Valvular dysplasia and insufficiency, cardiomyopathy Cor pulmonale (especially with sleep apnea), myocardial infarction	Valvular dysplasia and insufficiency Cor pulmonale (especially with sleep apnea)	Valvular dysplasia and insufficiency
Orthopedic	Vertebral dysplasia, Kyphosis/lumbar gibbus, hip dysplasia/dislocation, global restriction of joint mobility, carpal tunnel syndrome, short stature, and osteopenia/osteoporosis	Vertebral dysplasia, kyphosis/lumbar gibbus, hip dysplasia/dislocation, global restriction of joint mobility, Carpal tunnel syndrome, short stature, and osteopenia/osteoporosis	Lumbar spondylolisthesis, lumbar spinal compression, joint stiffness, Carpal tunnel syndrome, milder short stature, and osteopenia/osteoporosis

Table 5. Clinical signs of the three subtypes of MPS type I [49].

General considerations

All MPS I patients appear normal at birth. Early growth is often excessive, with height, weight and head circumference at or above the 90% for age in the first two years of life. Hurler patients develop the characteristic coarse facies, the first skeletaldeformities, movement difficulties and respiratory infections before the first year of life; length is often normal until 2 years of age, then growth starts to delay. First symptoms of attenuated forms of MPS type I, instead, usually occur between 3 and 8 years of life; the most frequently reported signs at clinical presentation are movement difficulties, corneal clouding, recurrent ENT (ear-nose-throat) symptoms and umbilical hernia.

Without appropriate treatment, Hurler patients' life expectancy is severely limited: the median survival is less than 5 years, with only rare survivors beyond 10 years; death usually occurs for cardiac and respiratory complications; in not treated patients with the intermediate MPS I-H/S phenotype, death frequently occurs for the same reasons during the second or third decade of life; MPS I-S, instead, allows a near-normal life expectancy.

Cognitive development

One of the main clinical signs of Hurler syndrome is progressive cognitive impairment: early development seems to be normal, but between the first and the second year of life development delay becomes obvious, patients reach a cognitive plateau and then they manifest a serious and progressive neurocognitive decline; at the time of death, they are usually severely mentally disabled. Hurler patients develop minimal language skills because of their enlarged tongue,

hearing loss and cognitive impairment; their behavior is placid and pleasant and they do develop some social skills. Cognitive development is only slightly impaired or normal in attenuated forms of MPS type I.

Neurologic manifestations

In the severe form of the disease, communicating hydrocephalus and chronic increases in intracranial pressure are frequent. In the attenuated forms, communicating hydrocephalus is less common, but spinal cord compression, cervical instability due to odontoid dysplasia and carpal tunnel syndrome are often observed.

Eear, nose and throat manifestations

Chronic recurrent rhinitis and ear infections affect almost all MPS type I patients, often requiring tonsillectomy and adenoidectomy or even T-tube placement in order to facilitate breathing. Obstructive sleep apnea is typical. In the severe form, conductive and neurosensory deafness is common; hearing loss can also occur due to ear infections or defective ossification of middle ear bones, even in attenuated patients.

Ophthalmologic manifestations

In all MPS I patients, some degree of corneal clouding is observed; as a result, loss of vision is common. Open-angle glaucoma is another frequent clinical sign.

Respiratory and pulmonary manifestations

The risk of severe respiratory insufficiency due to obstructive sleep apnea or restrictive lung disease is high, particularly in the severe form

of the disease. Obstructive sleep apnea can result from enlarged tongue, narrowed trachea, redundant airway tissue; restrictive lung disease from skeletal abnormalities of the chest and spine and hepatosplenomegaly can occur.

Cardiac manifestations

Heart is one of the most compromised organs in MPS type I. The typical cardiac manifestation of the disease is valvular dysplasia - caused by anomalies in the cartilage structure of the heart valves - with mitral and aortic regurgitation. Arhythmia, cardiomyopathy, congestive heart failure and coronary artery disease are common, too. A frequent cause of death in Hurler patients is upper respiratory infection due to myocardial infarction secondary to coronary artery disease.

Abdominal manifestations

Organomegaly for mucopolysaccharides accumulation, in particular liver and spleen enlargement, is really frequent among patients and it is the cause of abdominal protuberance. Recurrent inguinal and umbilical hernias, resulting from impaired elastogenesis, are also common.

Skeletal manifestations and joint disease

Skeletal complications represent without of doubts the hallmark feature of not only MPS I, but also all the other Mucopolysaccharidoses. The term “dysostosis multiplex” has been coined and used to sum up the spectrum of bone abnormalities that characterizes these disorders, in which most bones are involved. Faulty GAGs metabolism alters both endochondral and intramembranous ossification processes, and GAGs

infiltrations into tendons, ligaments and joint capsules impairs mobility and function of these tissues.

All MPS I patients develop bone and joint disease in a variable but progressive form: in MPS I-H the gradual worsening of this status leads to severe joint stiffening and arthropathy, and ultimately to significant movement impairment and disability. The following defects belong to the framework of dysostosis multiplex:

- dorsal gibbus, a deformity of the lumbar spine that is the first clinical sign of bone involvement in patients and becomes apparent at 6-24 months of age; other spinal defects are flattened and beaked vertebrae, scoliosis and kyphosis;
- macrocephaly, J-shaped sella turcica and platyspondyly, as well as atlantooccipital instability;
- dental abnormalities;
- narrow pelvis, flared iliac wings, hips dysplasia or subluxation;
- thick ribs and short thick clavicles;
- metaphyseal and diaphyseal alterations, evident in long bones, which irregular development causes valgus and varus deformities and short stature; genu valgum is especially frequent in patients;
- bullet-shaped phalanges, that produce the typical claw hands deformity and trigger digits, with impairment of hand function;
- osteopenia, osteoporosis, microfractures, causing generalized pain.

Examples of some of the clinical sign illustrated above are reported in Figure 4 and Figure 5, respectively showing the main phenotypic manifestations and the characteristic bone abnormalities of MPS type I.

Fig. 4. Common phenotypic manifestations of Hurler syndrome. A) Coarse facial features. **B)** Hirsutism, corneal clouding. **C)** Claw hands. **D)** Macrocephaly, dorsal gibbus, prominent abdomen. **E)** Umbilical hernia. **F)** Joint stiffness, genu valgum. **G)** Protruding abdomen due to organomegaly (images come from mps1disease.com).

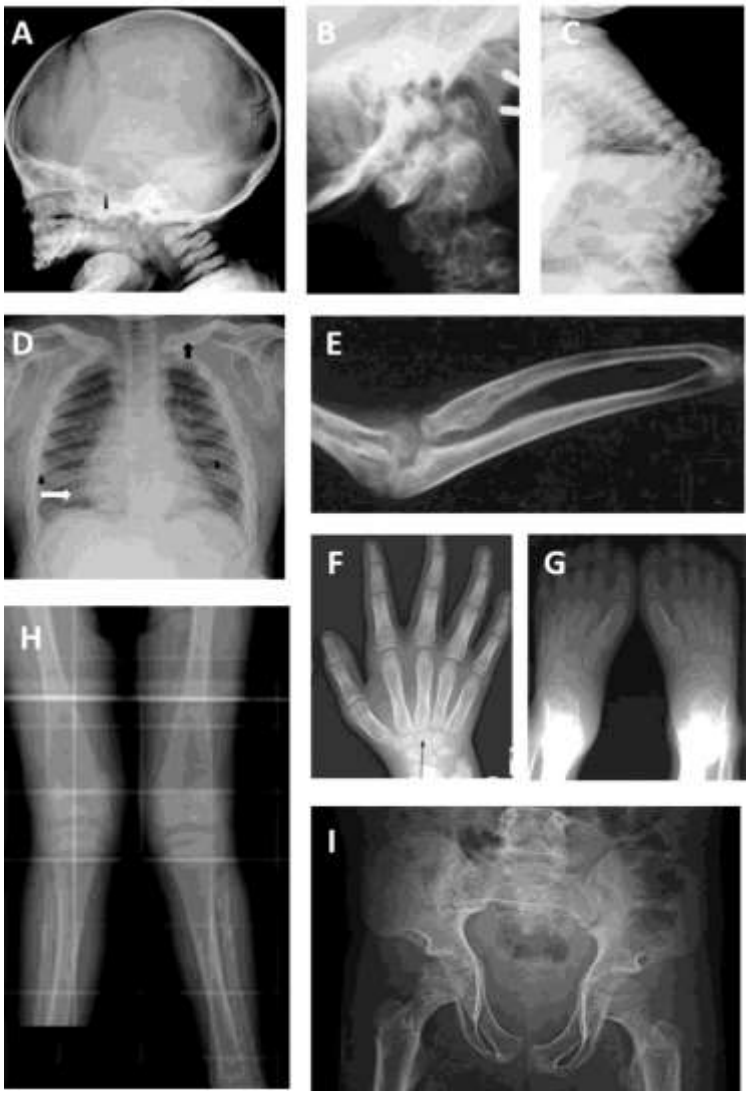

Fig. 5. Common skeletal manifestations of Hurler syndrome (dysostosis multiplex). A) Macrocephaly, J-shaped sella turcica (arrowhead). **B)** Atlanto-occipital instability. **C)** Dorsal gibbus. **D)** Cardiomegaly (white arrow), thick ribs (arrowheads), short thick clavicles (black arrow) and scoliosis. **E)** Metaphyseal and diaphyseal alterations. **F)** Bullet-shaped phalanges. **G)** Bilateral calcaneovalgus deformities of feet. **H)** Genu valgum. **I)** Narrow pelvis and flared iliac wings [50].

1.3.3 Insights of pathological bone mechanisms in MPS patients

The cellular and molecular mechanisms underlying the skeletal disease in MPS I remain largely unknown also because an extremely limited number of papers in this field has been published. Studies in the MPS I mouse model revealed aberrant bone remodelling, as well as growth plate development and maturation with abnormalities in the early cortical bone structure. In young mice, the growth plate appeared thickened with a high number of chondrocytes, and a disorganized structure was observed in the hypertrophic zone. Arrangement of the primary trabecular bone was abnormal and an increased presence of cartilage within the woven bone was observed, suggesting difficulties in cartilage resorption during endochondral ossification. Wilson et al. have recently demonstrated that high concentrations of GAGs in MPS I may inhibit the collagenolytic activity of cathepsin K, a lysosomal cysteine protease highly expressed by osteoclasts and responsible for a significant part of total bone resorption [51]. These studies suggest that an impairment of cathepsin K activity may contribute to the deranged bone remodelling in MPS I. In another study, Simonaro et al. reported that GAGs storage in MPSs led to elevated expression of numerous inflammatory molecules, such as Toll-like receptor 4 (TLR4). As a part of this inflammatory cascade, tumor necrosis factor (TNF-α) was released, leading to the up-regulation of receptor activator of nuclear factor-kb ligand (RANKL), which consequently enhanced osteoclasts formation. In turn, this caused an altered bone remodelling. Moreover, GAGs accumulation led to apoptosis of cartilage cells, and synovial hyperplasia, resulting in poorly organized and metabolically abnormal

connective tissue matrices [52]. In addition, they reported that treatment of MPS VI rats with an anti-TNF-α drug dramatically reduced the inflammation in the joints, which was associated with improved joint pathology [53].

As these studies highlighted, inflammatory state and osteoclastogenesis may play an essential role in MPSs bone disease. Thus, the RANKL/OPG/RANK pathway attracted many scientists because of its role in normal and aberrant bone formation.

1.3.3.1 The RANKL/OPG/RANK pathway

Bone is a rigid organ. Yet it is regulated by a highly dynamic remodelling process that is carried out by bone degrading osteoclasts, bone forming osteoblasts, and mechanical-sensing osteocytes. The coordinated action of osteoclasts and osteoblasts is critical for normal bone remodelling. When the balance between bone formation and degradation is lost, diseases occur.

Osteoclasts originate from hematopoietic stem cells (HSCs) and they are the only cell type that can remove bone, which is an important activity during both skeletal development and skeletal maintenance in adulthood [54, 55].

The fusion of myeloid precursors gives rise to multinucleated specialized macrophages in bone, which represent osteoclast progenitors [56, 57]. Macrophage colony-stimulating factor (M-CSF) and RANKL are two major proteins that trigger precursor proliferation and osteoclast differentiation, respectively. M-CSF receptor signalling directs myeloid progenitors to monocyte-macrophage lineage, and the consequent expression of RANKL receptor in these cells signify them

as osteoclast precursors [58-60]. Once these events occurred, osteoclasts differentiate.

Osteoblasts, instead, are derived from mesenchymal stem cells (MSCs) via a process that requires the sequential action of several transcription factor, including runt-related transcription factor-2 (Runx2), osterix (SP7), and activating transcription factor-4 (ATF4). Osteoblasts secrete bone matrix proteins, type I collagen, and other noncollagen proteins such as osteocalcin (OTC) and osteopontin (OPN) [61].

During the process of bone formation, matrix-synthesizing osteoblasts have at least three potential fates: (1) some of them become embedded within the bone matrix and are thereafter referred to as osteocytes, which continue to live and function within the mineralized tissue; (2) at the end of the remodelling cycle, some osteoblasts become flattened and then remain as quiescent lining cells at the bone surface; and (3) some matrix-synthesizing osteoblasts die by apoptosis [62]. In the bone microenvironment, the osteoblast lineage functionally regulates the osteoclast lineage [63]. In fact, osteocytes and osteoblasts produce RANKL and M-CSF to promote osteoclast differentiation; at the same time, they also secrete a decoy RANKL receptor, osteoprotegerin (OPG), to inhibit osteoclast differentiation [64, 65]. Thus, the RANKL to OPG ratio has been shown to critically reflect bone metabolic activity in various bone-remodelling conditions [66, 67]. The ablation of mature osteoblasts is sufficient to abrogate osteoclastogenesis *in vivo*. Mice with a disruption of RANK or RANKL exhibit severe osteopetrosis accompanied by a defect in tooth eruption due to a complete absence of osteoclasts. In contrast, mice lacking OPG exhibit severe osteoporosis, resulting from both an increased number and enhanced activity of

osteoclasts [68, 69]. Ultimately, it is clear that the molecular triad RANKL/OPG/RANK is the key regulator not only for normal but also pathological bone metabolism [70, 71]. Alteration of this pathway and, as a consequence, of the balance between osteoblasts and osteoclasts is the cause of different bone pathology such as familial expansile osteolysis, autosomal recessive osteopetrosis and Juvenile Paget's disease [68] Recently, our laboratory was the first to demonstrate that Hurler patients show an altered osteoclastogenesis, possibly due to the imbalance in the RANKL/OPG ratio. In particular, MPS IH-MSCs and osteoblasts displayed an increased capacity to support osteoclastogenesis because of a higher expression level of RANKL, compare to HD. Our results supported the hypothesis that aberrant osteoclastogenesis may be one of the aspects involved in Hurler bone disease, and that the abnormal ability of MPS IH-MSCs and osteoblasts to support osteoclastogenesis may contribute toward an explanation of the aspects of the skeletal phenotype seen in this disease [72].

It has been reported that a number of proresorptive cytokines, such as TNF-α and IL-1, modulate the RANKL/OPG/RANK system primarily by stimulating M-CSF production (thereby increasing the pool of preosteoclastic cells) and by directly increasing RANKL expression. In addition, a number of other cytokines and hormones, such as TGF-ß (increased OPG production), PTH (increased RANKL/decreased OPG production), 1,25-dihydroxyvitamin D3 (increased RANKL production), glucocorticoids (increased RANKL/decreased OPG production), and estrogens (increased OPG production) exert their effects on osteoclastogenesis by regulating osteoblastic/stromal cell production of OPG and RANKL [73]. RANKL, RANK and OPG

belong to the tumor necrosis factor (TNF) protein and TNF receptor (TNFR) superfamily. RANKL is a transmembrane protein and it is released from the cell surface as a soluble molecule following proteolytic cleavage by matrix metalloproteinases (MMPs) such as MMP-14. Both the soluble and the membrane-bound RANKL forms function as agonist ligands for RANK. However, the membrane-bound RANKL functions more efficiently than soluble RANKL [74-76]. Osteoblasts and MSCs are thought to be the major cell types that express RANKL in support of osteoclastogenesis [69, 77]. However, because RANKL is expressed by several different cell types in both bone and bone marrow, including osteoblasts, osteocytes, and BM-MSCs, the actual major source of RANKL *in vivo* is as yet unclear. The T cell is also an important source of RANKL in the bone. Activation of T cells *in vitro* and *in vivo* leads to increased osteoclastogenesis and bone resorption, suggesting that acute and chronic inflammatory states, and certain leukaemias, contribute to pathologic bone loss.

RANK receptor is a transmembrane molecule expressed on osteoclast progenitor cells and mature osteoclasts. This receptor lacks intrinsic enzymatic activity in its intracellular domain, and transduces signals by recruiting adaptor molecules such as the TNF receptor-associated factor (TRAF) family of proteins [69]. By a yet unknown mechanism, RANKL binding to RANK induces the trimerization of RANK and TRAF6, which leads to the activation of nuclear factor-kB(NF-kB) and the mitogen-activated kinases (MAPKs) [78].

In contrast to all other TNF receptor superfamily members, OPG lacks transmembrane and cytoplasmic domains and is secreted as a soluble protein. OPG mRNA was found to be expressed in a number of tissues,

including lung, heart, kidney, liver, stomach, intestine, brain and spinal cord, thyroid gland, and bone. Because the major biologic action of OPG described to date has been to inhibit osteoclast differentiation and activity, the potential role of OPG in these other tissues remains to be established [73].

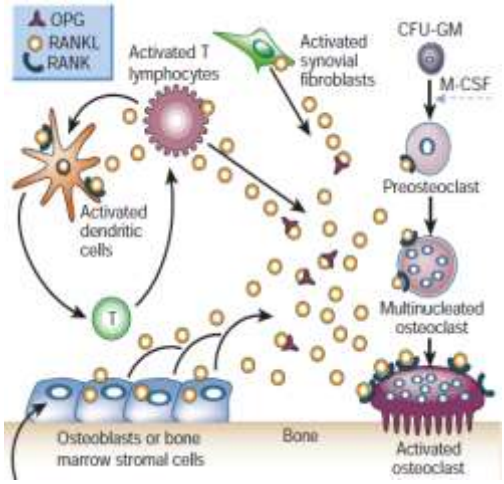

Fig. 6. RANKL expression is induced in osteoblasts, activated T cells, synovial fibroblasts and bone marrow stromal cells (MSCs), and subsequently binds to its specific membrane-bound receptor RANK, thereby triggering a network of TRAF mediated kinase cascades that promote osteoclast differentiation, activation and survival. Conversely, OPG expression is induced by factors that block bone catabolism and promote anabolic effects. OPG binds and neutralizes RANKL, leading to a block in osteoclastogenesis and decreased survival of pre-existing osteoclasts [58]

1.3.4 Diagnosis of MPS type I

Diagnostic confirmation and management of individuals with LSDs are challenging because, even if these diseases are usually caused by a single enzyme deficiency, they give rise to a spectrum of manifestations that depends not only on the amount of residual enzyme activity, but also on a series of modifiers, most of which are currently unknown. Age of onset, severity of symptoms, affected organs and life expectancy can

vary markedly even within individuals having the same disease; even though some known mutations are associated with certain phenotypes and outcomes, genotype phenotype correlation is typically not strong. All these factors together limit current diagnostic evaluation and decision making capacity [49].

Interesting information about MPS type I current diagnostic trends can be found in the MPS I Registry, an international observational database that was created in 2003 with the purpose of characterizing the natural history, long-term follow-up and treatment outcomes of this disease. As D'Aco and collaborators. assessed in 2012 using data from the Registry, the suspect of MPS type I typically derives from clinical signs and symptoms that indicate an already advanced state of the disease: changes in facial features, limited joint movement, skeletal deformities, large head circumference and frequent respiratory infections; the age of symptoms onset varies widely between MPS I-H, MPS I-H/S and MPS I-S (Table 6; [79].

MPS type I diagnosis confirmation relies on [80-82]:

- biochemical markers:
  - ✓ primary storage material (DS and HS) in biological fluids such as urine, serum or plasma and liquor; in particular, measurement of urinary GAGs level is a sensitive test, though non-specific;
  - ✓ IDUA activity deficit in leukocytes, cultured fibroblasts or plasma;
- molecular analysis: definition of the mutation by sequencing of the *IDUA* gene.

There is a considerable delay between MPS type I age of onset and age of diagnosis, especially for the attenuated forms of the disease, and further time passes between diagnosis confirmation and treatment decision and initiation (Table 6; [79]). This limits the effectiveness of the currently available therapeutic options for the disease -enzyme replacement therapy and hematopoietic stem cell transplantation- which successful outcome depends on patients' age at treatment start (see **1.3.5 Treatment of MPS type I** section for further information). Indeed, by the time therapy is begun, the substantial progression in the storage of GAGs has often caused irreversible damages.

Baseline characteristics	Hurler	Hurler–Scheie	Scheie
Median age of symptom onset (range) [total number]	0.5 (0–6.5) [485]	1.9 (0–12.4) [187]	5.4 (0–33.8) [87]
Median age of diagnosis (range) [total number]	0.8 (0–23.8) [508]	3.8 (0–38.7) [209]	9.4 (0–54.1) [97]
Median age of first treatment (range) [total number]	1.4 (0.1–31.2) [438]	8.6 (0.3–47.2) [197]	17.1 (3.1–62.9) [85]

Table 6. Chronology of symptoms onset, diagnosis and treatment initiation of the three subtypes of MPS type I; data are expressed in years (adapted from [79]).

As early diagnosis and treatment can significantly prevent disease severity, associated disabilities and death, MPS type I, like LSDs in general, has been recognized as an ideal candidate for newborn screening (NBS) programs. NBS is a preventive public health program for perinatal identification of congenital disorders that can affect newborns long-term health; these disorders are selected for NBS on the basis of their prevalence, treatment availability, outcome and overall cost effectiveness. NBS for MPS type I and other MPSs can be realized by measurement of GAGs content or enzyme activity in neonatal dried blood spots (DBSs) on filter paper [49, 83, 84]. From the early 2000s, sensitivity, specificity and cost effectiveness of these assays have been

improved with the introduction of high-throughput tandem mass spectrometry or digital microfluidics techniques [15, 60].

Prenatal diagnosis is also available, based on either enzyme activity measurement in amniotic fluid cells, chorionic villi or cord blood, or molecular genetic testing in families where the mutations has already been identified [22, 80, 85, 86].

1.3.5 Treatment of MPS type I

During the last decades, the outlook for MPS patients has significantly improved, because of the better understanding of disease pathogenesis and natural history and the advancing availability of both supportive and disease-specific therapies.

It is unanimously recognized that, given the progressive nature of these disorders, early diagnosis and, most of all, early treatment is of major importance. Disease progression is accompanied by worsening organ damage, a secondary effect of GAGs metabolism deregulation and GAGs accumulation, which is often irreversible; hence, response to any treatment depends on the severity of the disease phenotype and on the degree of disease progression at treatment initiation [87].

Because MPSs usually present a broad and complex spectrum of disease manifestations, diagnosis, treatment choice and fulfilment and patients follow-up require a multidisciplinary approach, involving specialists such as geneticists, neurologists, cardiologists, ophthalmologists, otolaryngologists, orthopaedic surgeons, physical and speech therapists and other professional figures.

Before the advent of MPS-specific therapies, and still nowadays beside them, supportive symptom-based interventions were performed to

improve patient's lifespan and quality of life and to solve or reduce some secondary complications of the disorders (Table 7) [27, 79, 87]. They mainly consist in:

- surgical interventions such as ventriculoperitoneal shunt for communicating hydrocephalus, corneal transplant for corneal clouding, tonsillectomy and adenoidectomy up to tracheostomy for airway obstruction, cardiac valve replacement for valve regurgitation, median nerve release for carpal tunnel syndrome, hernia repair;
- spinal fusion for spinal cord compression and other orthopaedic procedures to correct skeletal defects;
- physical therapy to minimize joint contractures and stiffness;
- speech therapy and behavioural therapy to ameliorate developmental skills;
- medications for generalized pain and gastrointestinal disturbances.

Symptoms	Management/treatment
Bone	Orthopaedic surgery to correct spinal deformities, acetabular hip dysplasia, genu valgum
Cardiac valve disease	Valvular replacement Catheter balloon valvuloplasty
Carpal tunnel and trigger finger	Neurosurgical decompression surgery
Corneal clouding	Corneal transplant Corrective lenses
Deafness	Hearing aids Myringotomy with placement of ventilating tubes
Endocrine function	Human growth hormone (effects unproven)
Joints	Physical therapy for strength and stiffness Hydrotherapy for stiffness and pain Splints to position joints and prevent flexion deformities
Language problems	Hearing aids and speech therapy
Learning disabilities	Standard interventions considering the patient's auditory, visual and motor issues
Hydrocephalus	Ventriculoperitoneal shunt
Spinal cord compression	Decompression surgery
Obstructive sleep apnoea/ airway obstruction/ respiratory involvement	Tonsillectomy Adenoidectomy Continuous positive pressure ventilation (CPAP and BiPAP) with oxygen enrichment Tracheotomy Asthma medications Antibiotics Nasal decongestants or isotonic or hypertonic saline solution
Otitis media	Myringotomy with placement of ventilating tubes
Umbilical and inguinal hernias	Hernia repair surgery

Table 7. Symptom-based treatments for MPSs disorders (adapted from [87]).

Anyway, the advance in scientific research allowed the comprehension of the physiopathological mechanism at the basis of MPSs; thus, disease-specific treatments were developed, aimed at solving the deficit through the supply of the missing enzyme to the body.

In 1968, Fratantoni and Neufeld first demonstrated that fibroblasts from patients with Hurler syndrome and Hunter syndrome (Mucopolysaccharidosis type I and II, both caused by a genetic defect that makes cells unable to catabolize glycosaminoglycans, due to the deficiency of α-L-iduronidase and iduronate sulphatase activity respectively), when cultured together, could compensate each other's defect: both cell types acquired the ability to degrade GAGs [88]. The mechanism by which cells complemented each other's defect consisted

in the exchange of the necessary “factors”, actually the defective enzymes, through the culture medium. This phenomenon was called “cross-correction”, that is the process by which the proximity of normal cells leads to the correction of the biochemical consequences of enzymatic deficiency within surrounding cells [89]. Cross-correction of the defect in MPS cells is possible because, as described in **1.1.1. Lysosomes and lysosomal hydrolases** section, a minority of the M6P-tagged lysosomal hydrolases escapes lysosomal targeting and is secreted in the extracellular space: thus, the enzymes can be recognized for their M6P-tag by surface M6P receptors (MPRs) of neighbouring cells and endocytosed; in this way, an enzyme defective cell can be able to capture exogenous enzymes and partially restore its ability to degrade GAGs (Fig. 7) [7].

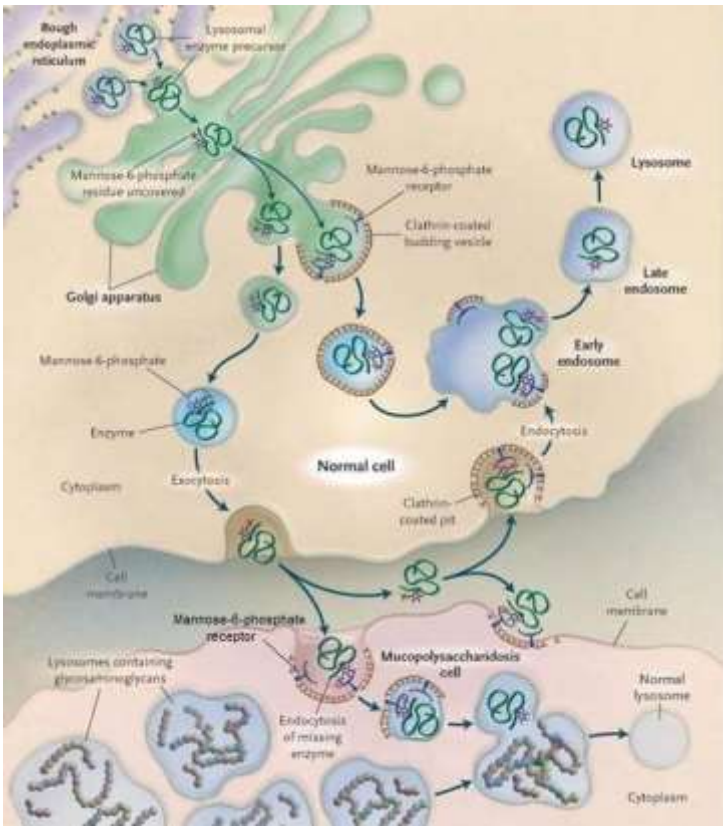

Fig. 7. Lysosomal enzymes trafficking and cross-correction: lysosomal enzymes acquire the M6P-tag in the Golgi and are targeted to the lysosomes; some of them are instead secreted into the extracellular space and can undergo receptor-mediated endocytosis, enter defective cells lysosomes and restore their potential to degrade GAGs [81].

The mechanism of cross-correction forms the basis of the first developed therapeutic approaches that are now extensively employed for the treatment of MPS type I and other LDSs:

- enzyme replacement therapy;
- hematopoietic stem cell transplantation.

Enzyme replacement therapy

Enzyme replacement therapy (ERT) is a treatment that consists in the periodic intravenous administration of an enzyme that is deficient in the patient.

As long ago as 1966, De Duve and Wattiaux suggested the possibility of treating LSDs by replacement of the faulty enzyme by supplying the normal one [90]; two years later, the proof of principle of ERT was demonstrated *in vitro* in cell cultures by Fratantoni and Neufeld [88] and in 1971 it was confirmed *in vivo* by experiments in which Hurler and Hunter patients were treated with administration of human plasma from healthy individuals –thus containing a quote of secreted lysosomal enzymes– obtaining a transient recovery of enzyme activity (67).

The effectiveness of ERT relies on the biodistribution of the therapeutic enzyme, that can spread throughout the body via blood circulation; the enzyme can fulfill its function in the extracellular fluids and spaces or it can be taken up by cells through receptor-mediated endocytosis and restore lysosomal function (Fig. 8) (7, 68).

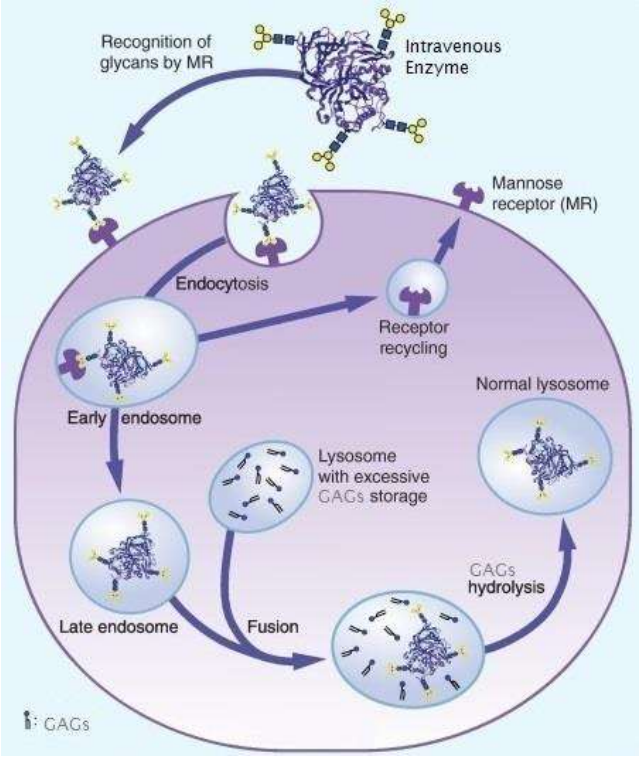

Fig. 8. Uptake of intravenously administered recombinant enzyme; late endosomal and lysosomal fusion delivers the therapeutic enzyme to the lysosome, which subsequently restores GAGs to normal levels (modified from [91]).

MPS type I was the first MPS treated with ERT. In 1971, Barton and Neufeld first purified from human urine the IDUA protein responsible for the correction of Hurler syndrome deficit [92], but the enzyme became available for a potential clinical use only in 1994, when Kakkis et al. produced and purified a polymorphic variant of the human alpha-L-iduronidase by recombinant DNA technology in the Chinese hamster ovary (CHO) cell line; recombinant IDUA was efficiently endocytosed by Hurler fibroblasts though a M6P-dependent mechanism and it was corrective for abnormal GAGs accumulation [93].

Preclinical studies in the canine model of MPS type I showed that repetitive intravenous administration of recombinant human α-L-iduronidase over months resulted in enzyme uptake by the organs, reduction of GAGs accumulation in numerous tissues, except for brain, cartilage, heart valves and cornea, and decrease of GAGs excretion in the urine; the animals developed antibodies against IDUA, but clinical symptoms of the immune response could be prevented by premedication with antihistamines or slow infusion of the enzyme [94, 95].

On this basis, in 1997, the first clinical trial for the use of ERT in MPS type I patients began; Table 8 reports a list of the trials completed so far, which references are indicated in the caption.

In 2003, after the phase I/II trial, recombinant human α-L-iduronidase (laronidase, Aldurazyme®, Genzyme/Biomarin) was approved for the treatment of MPS type I patients in the United States and in Europe by FDA (Food and Drug Administration) and EMEA (European Medicine Agency), respectively. The purified enzyme is available in vials containing 5 mL of drug solution at a concentration of 0.58 mg/mL. The recommended dose is 0.58 mg/kg body weight; the required dose is dispersed in 100-250 mL of isotonic saline, depending on patient's weight, and infused over 2-4 hours, once a week.

	Phase 1/2 and extension	Phase 3 and extension	Under 5 years	Dosing trial
Study type	Open label	Randomized, double-blind, placebo-controlled with open-label, 3.5-year extension	Open label	Randomized, open-label, dose-optimization
Participants (n)	10 → 5	45 → 40	20	33
Phenotype distribution	80% Hurler-Scheie 10% Hurler 10% Scheie	84% Hurler-Scheie 16% Scheie	20% Hurler-Scheie 80% Hurler	49% Hurler-Scheie 30% Hurler 21% Scheie
Mean age at baseline, years	12.4 (range 5-22)	15.7 (range 6.3-43.3)	2.9 (range 0.8-5.1)	8.9 (range 1.4-20.7)
Dose	0.58 mg/kg (100 U)/kg/week	0.58 mg/kg (100 U)/kg/week	0.58 mg/kg (100 U)/kg/week	0.58 mg/kg (100 U)/kg/week 1.2 mg (200 U)/kg/week 1.2 mg (200 U)/kg/every 2 weeks 1.8 mg (300 U)/kg/every 2 weeks
Duration of study	1 year with 5-year extension	6 months with 3.5-year extension	1 year	6 months
Trial purpose/ end points	Safety Overall efficacy	Change in per cent predicted FVC Distance walked in 6-min walk test	Safety Global assessment of clinical status	Safety Dosing Urinary GAG Hepatomegaly
Other clinical measures evaluated	Urinary GAG Hepatomegaly Growth Shoulder flexion Apnoea/ hypopnoea NYHA class	Urinary GAG Hepatomegaly Joint flexion Apnoea/hypopnoea index Visual acuity Quality of life Left ventricular hypertrophy Valvular disease Growth	Urinary GAG Hepatomegaly LVF Apnoea/hypopnoea Growth Cognition	6-min walk test

Table 8. Information about clinical trials of ERT with laronidase for MPS type I (adapted from [87]): phase I/II and extension ([94, 96]), phase III and extension ([97, 98]), trial on patients under 5 years ([99]), dose-optimization trial ([100]).

The overall results of the clinical employment of laronidase in treating MPS type I are encouraging, since many aspects of the disease are stabilized or reversed during long-term therapy [96-98, 101-104]; indeed, ERT induces:

- decrease in urinary GAGs excretion;
- reduction in lysosomal storage of GAGs;
- significant decrease in hepatosplenomegaly;
- significant increase in the range of motion of shoulder and elbow;
- decrease in sleep apnea and hypopnea episodes;
- significant improvement in the ability to perform physical tasks and daily activities;

- increase in the rate of growth in height and weight in prepuberal patients.

Some adverse effects of laronidase are infusion reactions such as flushing, fever and headache or allergic reactions such as urticarial, rash, nausea, edema; they are limited and easily manageable by reduction of infusion rate and antihistamine and antipyretic medication; moreover, they usually decline after the first few months of treatment.

However, current ERT for MPS type I undoubtedly has some limits. Laronidase treatment has no effects on the following disease manifestations, which remained stable or worsened during the treatment period in clinical trials:

- neurological symptoms: the intravenously infused enzyme is not expected to cross the blood-brain barrier in appreciable amounts at the administered dosage level; for this reason, laronidase treatment is recommended only for the attenuated forms MPS type I, the ones with null or limited neurological involvement [105]; attempting to overcome this problem, intrathecal, intranasal or brain-targeted ERT approaches are under development in animal models [106-109];

- dysostosis multiplex: the enzyme can hardly spread to organs that have a poor vascular supply, such as bone [28], and the correction of GAGs storage in the growth plate and in the articular cartilage is challenging, also because the therapeutic enzyme diffuses slowly through the molecular structure of the matrix [24];
- corneal clouding;

- valvular disease.

Furthermore, in nearly all (>90%) patients undergoing ERT, immune reactions with the development of IgG antibodies anti-IDUA are detected; this does not seem to affect the clinical efficacy of the therapy, but the long-term impacts of the phenomenon are still unknown and under investigation [110, 111].

Finally, ERT is a chronic treatment: the need for weekly infusions over a lifetime leads to compliance problems and impairs patients' and families' quality of life; patients' families and/or the sanitary system are charged for the high costs of individuals undergoing ERT: laronidase-based therapy costs between 250000 and 1000000 dollars per year per adult [15].

Hematopoietic stem cell transplantation

Hematopoietic stem cell transplantation (HSCT) consists in the intravenous infusion of autologous or allogeneic hematopoietic stem cells (HSCs) with the aim of re-establishing hematopoietic function in patients whose bone marrow is damaged or defective. This procedure is usually performed to treat malignant diseases such as leukemia or lymphoma or to correct non-malignant diseases like hemoglobinopathies, inborn errors of metabolism and others.

The currently used sources of HSCs cells are [112]:

- bone marrow (BM), the traditional font of HSCs; BM-HSCT is simply and historically called bone marrow transplantation (BMT);
- mobilized peripheral blood;

- umbilical cord blood (UCB), the more recently recognized source, that provides cells for umbilical cord blood transplantation (UCBT).

HSCT can be autologous, which means that the subject is transplanted with his own stem cells, or allogenic, when stem cells come from a donor source other than the patient. In the context of non-malignant congenital disorders such as LSDs, allogenic HSCT is typically performed, to replace the enzyme-defective host cells with normal ones coming from a healthy donor; yet, gene correction of patient's stem cells, aimed at allowing the treatment of these disorders with autologous HSCT, is a promising and emerging possibility [113, 114].

In an allogenic HSCT, one of the most important factors to consider is the degree of HLA match between the donor and the recipient: well-matched transplants decrease the risk of graft rejection and graft versus host disease (GVHD), two possible although undesirable outcomes of transplantation. The use of sibling donors, who are often carriers of the disease and thus deliver approximately 50% of the normal enzyme compared to non-carrier donors, may yield mediocre results.

Patients undergoing HSCT are subjected to a conditioning regimen aimed at totally or partially ablating their hematopoiesis, in order to facilitate recipient's HSCs replacement by donor's ones and to provide immunosuppression sufficient to prevent rejection of the transplanted graft; the likelihood of the latter phenomenon augments with the degree of HLA mismatch between donor and recipient [115]. Conditioning regimens can be:

- myeloablative, designed to kill all recipient bone marrow cells; radiation containing myeloablative conditioning is realized by

high-dose total body irradiation, whereas non-radiation-containing is obtained with the administration of various combinations of chemotherapeutic agents such as busulfan, cyclophosphamide and others;

- non myeloablative: immunosuppressive but not myeloablative; it is realized administering doses of chemotherapeutic drugs and radiations lower than those of myeloablative regimens.

The goal of HSCT as a therapy for LSDs is to obtain the repopulation of patient's hematopoietic compartment by metabolically correct donor cells, that can represent a source of functional enzyme for the recipient organism [116]. The rationale for the potential usefulness of HSCT in the treatment of MPSs relates on the demonstration of the cross-correction phenomenon by Fratantoni and Neufeld [88]; a few years later, in 1971, a restoration of deficient enzyme activity was obtained *in vivo* administering human lymphocytes to a child with Mucopolysaccharidosis type II [117].

The effective cross-correction by HSCT in a MPS patient relies on the migration, homing and engraftment of donor-derived cells to affected organs: donor's hematopoietic cells can settle in non-hematological organs and specialize, becoming microglial cells in the brain, macrophages in the lungs and in other organs, Kupffer cells in the liver, thus living in close proximity to recipient's enzyme-deficient cells of these organs and releasing M6P-alpha-L-iduronidase moieties; the latters can be taken up by surrounding cells, which corrects aberrant intracellular GAGs storage (Fig. 9) [89]. Furthermore, the secreted enzyme can also act in the extracellular spaces, removing GAGs

deposits from the extracellular matrix, and it can reach distant organs through blood and lymph circulation.

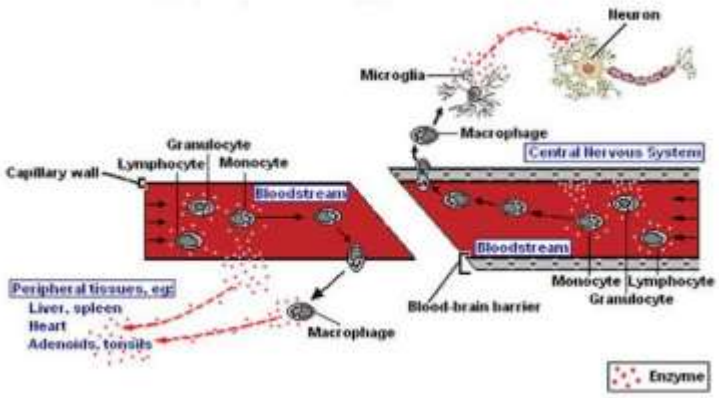

Fig. 9. Enzyme delivery to peripheral tissues and central nervous system (CNS) after HSCT. From bloodstream, the enzyme reaches the tissues either by diffusion of plasma enzyme, secreted by donor leukocytes, or by leukocytes leaving the circulation and entering the tissues; in the CNS, enzyme is delivered by the latter mechanism only, because the blood brain barrier does not permit diffusion of the plasma-derived enzyme [118].

2.Stem cells

2.1 General characteristics

The development of an organism from the zygote and, consequently, the cell turnover in adult tissues, are possible thanks to the existence of stem cells.

A stem cell is defined as a cell type which has the property to self-renew while maintaining the capacity to differentiate into diverse cell types. Stem cells are therefore different from progenitor cells which can differentiate into mature cell types but are incapable of self-renewing,

or somatic cells which are capable of proliferating but unable to differentiate [119].

Stem cells present two different mechanisms of cell division (**Fig.10**):

- Asymmetric cell division:

  A stem cell originates two daughter cells which are morphologically equal but functionally different. Indeed, one cell remains a stem cell, holding its characteristic of self-renewal and undifferentiated state, while the other become a progenitor cell, which has by definition, a limitative proliferative capacity and will originate cells of a particular organ.

- Symmetric cell division:

  A stem cell originates two daughter cells which are identical and present a finite probability of being either stem cells or committed progenitors.

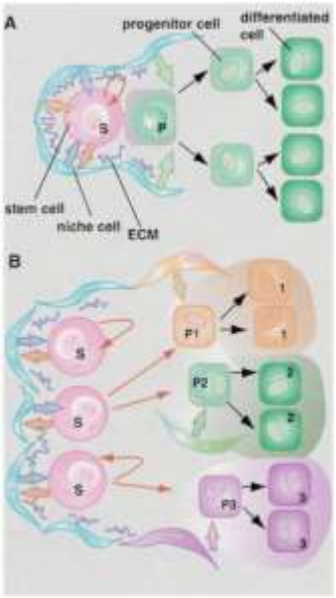

Fig. 10. Alternative models for stem cell division [120].

They can be divided in two main groups in accordance with their origin and their capacity of differentiation.

Classification by DIFFERENTIATION CAPACITY

- ✓ Totipotent
- ✓ Pluripotent
- ✓ Multipotent
- ✓ Unipotent

Totipotent stem cells are cells capable of originating cell types of an entire organism, including the extra-embryonic tissues. Embryos at one and two cell stages and germ cells (GCs) are the only cells that hold this characteristic.

Pluripotent stem cells can differentiate into the derivatives of the three germ layers and GCs but not into extra-embryonic tissues. This category is represented by embryonic stem cells (ESCs) which are present in the inner cells mass (ICM) of the blastocyst.

Multipotent stem cells are able to originate all cell types of an interest organ. The most prominent example remains hematopoietic stem cells (HSCs), which are capable of reconstitute an entire hematopoietic system.

Unipotent stem cells, finally, are those cells that generate cells only of a specific lineage.

Classification by their ORIGIN

- ✓ Embryonic stem cells (ESCs)
- ✓ Fetal stem cells
- ✓ Stem cells of extra-embryonic tissues
- ✓ Adult stem cells

Embryonic stem cells: they are pluripotent stem cells derived from the ICM of embryos at the blastocyst stage. The blastocyst is originated from the morula (embryo at 16 blastomeres) following a cavitation process that leads to the formation of a hollow structure. It consists of three main parts: the *trophoblast*, outer cell layer from which the chorion and the umbilical cord will be formed; *blastocoele*, i.e. the cavity inside the blastocyst; the *inner cell mass* (ICM), the group of about thirty cells placed at one end of the cavity that will originate the embryo. Embryonic stem cells are derived from the ICM of the blastocyst as a consequence of destruction of the trophoblast. (Fig. 11). As mention before, since they are pluripotent, they are undifferentiated cells with high proliferation and differentiation capacity.

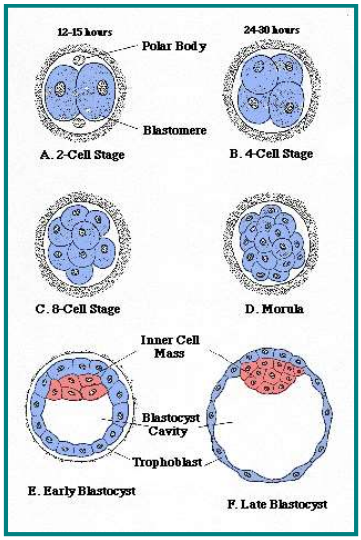

Fig. 11. Schematic representation of blastocyst formation.

Fetal stem cells: they are found in later stages of the embryo and in fetus and are responsible for the growth of tissues in utero. They are halfway as proliferative capacity between embryonic and adult stem cells.

Stem cells of extra-embryonic tissues: cells with characteristics ranging from multipotency to unipotency. They can be found in extra-embryonic tissue such as the umbilical cord, the placenta and the amniotic fluid. It was shown that the blood of the umbilical cord and of the placenta is rich in stem cells and immature hematopoietic progenitor cells. The cord blood stem cells are able to give rise to different cell types and their differentiative capacity can be compared to those of hematopoietic stem cells isolated (HSC) from bone marrow (BM) [121].

Several studies indicate that they are able to generate blood cells and are then used to cure various diseases such as leukemia, serious forms of anemia and hereditary immunodeficiencies. These cells are readily

available in that, after birth, the umbilical cord and placenta are normally eliminated [122].

Adult stem cells: They are undifferentiated cells sited in the tissues of an adult organism whose purpose is to maintain and repair their organ of origin. Adult stem cells reside in a particular micro-environments called "niches" in which they remain quiescent until a particular external stimulus, such as a tissue damage, induce them to proliferate. In this case, they moved out from the niche and differentiate in the specific cell type of the belonging tissue. The niche also contains other cells whose purpose is to organise the extra-cellular matrix and to secrete specific factors that guarantee the maintenance of self-renewal and differentiation capacity of the stem cells.

Adult stem cells have the ability of self-renewal and differentiation, although more limited than ESCs. Previously it was believed, instead, that their differentiation capacity was limited and they could give rise only to specific cells of the belonging tissue, proving to be exclusively unipotent. However, several experiments have shown that some types of adult stem cells are multipotent, i.e. able to differentiate into different cell types.

In the sixties, two populations of adult stem cells within the BM were discovered: HSCs and mesenchymal stem cells (Mesenchymal Stem Cells or MSCs). HSCs give rise to blood cells, while MSCs are stromal cells which differentiate into different cell types of the mesoderm lineage such as adipocytes, chondrocytes, osteocytes and other cells of the connective tissue [123, 124]. Moreover, it has been demonstrated that HSCs can be differentiated into neuronal cells, skeletal muscle

cells, cardiac cells and liver cells [125-127]; neuronal stem cells, instead, can give rise to blood cells and skeletal muscle cells [128, 129]. Unexpected was the discovery of adult stem cells in organs where it was thought there was no regenerative capacity, such as the heart and brain [130, 131]. It is already known that almost all the organs of our body contain adult stem cells. For instance, the brain, the liver, the bone marrow, the blood vessels, the muscles, the skeleton and skin.

2.2 Induced Pluripotent Stem Cells

Induced pluripotent stem cells (iPSCs) represent a new category of stem cells. In 2000 Yamanaka and colleagues made a breakthrough discovery that added another dimension to the stem cells field. This group found a combination of defined transcription factors (Oct4, Sox2, Klf4 and cMyc) that when introduced into murine fibroblasts by retroviruses, would induce reprogramming of the cell to a pluripotent state, resembling ESCs. These cells were named iPSCs [132].

This remarkable discovery not only changed the way of thinking research in the biomedical field, but also reformed our concept of cell plasticity and cell fate.

2.2.1 The history

It was long thought that a committed cell had reached a terminal differentiated state and that its state could not be modify any longer. It seemed obvious that a differentiated cell had lost chromosomes or permanently had inactivated genes that it no longer needed [133].

Several studies, however, had started to suggest that a committed cells of an embryo was “plastic” and that still retrained the possibility to revert or change its phenotype. Three approaches to nuclear reprogramming have shown conclusively that cell fate could be reversed, even to an embryonic state: nuclear transfer, cell fusion and transcription-factor transduction. These studies pointed out that a highly specialized somatic cells conserve all the genetic information that is needed for them to revert to ESCs and that genes of the somatic cells have not been permanently inactivated. Moreover, cellular state is dynamically controlled and subjected to change when they are explanted or exposed to a different microenvironment in the cell at any given time.

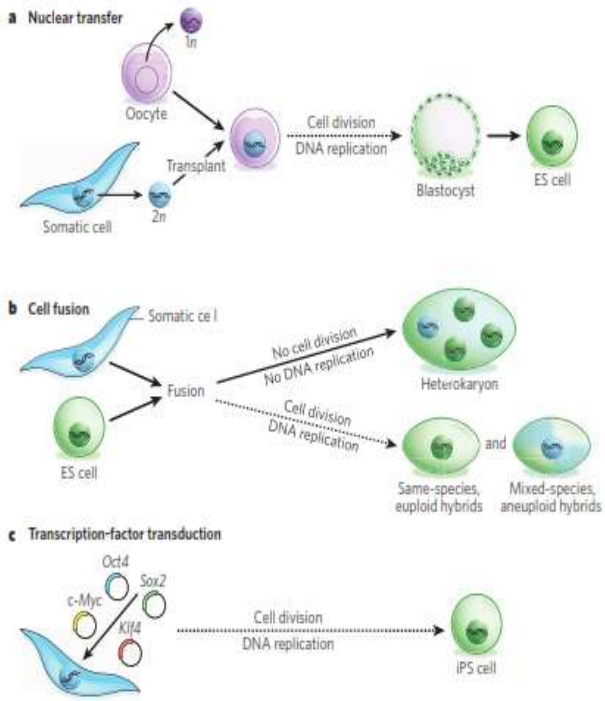

Fig. 12. Three approaches to nuclear reprogramming to pluripotency. [134]

Nuclear Transfer

When a nucleus from a differentiated somatic cell is transplanted into an enucleated oocyte, nuclear reprogramming occurred, leading to the generation of an entire individual, which is a genetically identical clone of the original somatic cell. Such experiment, also known as cloning (Fig. 12a), have definitively demonstrated that all genes required to create an entire organism are present in the nucleus of the specialized cell and that can be activated on exposure to reprogramming factors present in the oocyte. These experiments provided the first evidences that cell specialization involved a change in gene expression and not in gene content, and the process of differentiation can be fully reversed.

Briggs and King were the first to demonstrate that transfer from nuclei from early blastocysts into enucleated oocyte resulted in clones, in this case of swimming tadpoles. It was 1952 [135]. Anyhow, they had difficulties reproducing this result with cells from a more specialized tissue, which often gave rise to abnormal tissue.

A decade after, Gurdon reproduce the same experiments with a different frog species and succeeded in transferring nuclei from highly specialized tadpole intestinal cells into ultraviolet-light-irradiated oocytes, obtaining not only tadpoles but also normal adult frogs [136, 137]. The finding that differentiation might be reversible received immediate success and curiosity but also some concerns due to the low frequency (~1%) and to the impossibility to replicate the experiments in other species.

These obstacles were overcome three decades after. In 1997 Wilmut and colleagues were the first to clone a mammal, “Dolly the sheep”, made by adopting the nuclear transfer technique [138]. A year later,

Wakayama and collaborators succeed in cloning mice. These results were possible because of improvements in the somatic-cell nuclear transfer (SCNT) technique. Indeed, this process was soon replicated in many different laboratories. In addition to sheep and mice, a wide range of species have now been successfully cloned using SCNT, ranging from domesticated animals such as dogs and goats, and their hybrids such as mules, to wild animals such as African wildcats and wolves. A low efficiency of nuclear cloning (1–2%) is still typical of mice, which are the most widely used experimental animal model. It is notable that nuclear-transfer-derived ES cells cells (ntES cells) can be generated with much higher efficiencies (~20%) from blastocysts formed by SCNT [139].

Some concerns still remain about SCNT fidelity for generating cloned organisms or cells without phenotypic defects. Common abnormalities include aberrant gene expression in embryos, telomere elongation, obesity in adults, impaired immune systems and, often, increased cancer susceptibility and premature death. The developmental defects in cloned animals are presumed to result, in part, from problems with the fidelity of genomic reprogramming, owing to a failure to erase "epigenetic memory" completely.

Cell fusion

Cell fusion involves fusing two or more cell types to form a single entity. This allows the impact of one genome on another to be studied and, in this way, the existence of *cis* and *trans*-acting repressors and tumour-suppressor proteins was uncovered in the late 1960s (Fig. 12b). These experiments helped to make a step forward the comprehension

of cellular reprogramming by showing that the differentiated state is not fixed and irreversible, but it is dictated by the balance of regulators and requires continuous control.

Cell fusion can originate heterokaryons or hybrids. Heterokaryons do not proliferate and therefore contain multiple distinct nuclei, whereas hybrids proliferate, causing the nuclei of the original cells to fuse.

In 1983, the first definitive evidence that previously silent genes could be activated in mammalian cells was obtained by Blau and colleagues, by producing heterokaryons. If the cell types are from different species, their gene products can be distinguished, and nuclear reprogramming can be assessed [140]. The relative ratio of the nuclei, or the gene dosage, contributed by the two cell types dictate the direction of reprogramming [141, 142]. These experiment were confirmed by other laboratories and the technique was applicable to different cell types.

Tada, Surani and colleagues were the pioneers of studying nuclear reprogramming of somatic cells in proliferative hybrids. They fused female embryonic germ cells, which are pluripotent stem cells derived from primordial germ cells, with thymocytes from adult mice. They then investigated which sequences of DNA had been demethylated, and whether certain imprinted and non-imprinted genes from the somatic genome had been activated. Furthermore, they showed that their fused tetraploid cells were pluripotent: the cells could contribute to the three germ layers in chimaeric embryos [143]. Tada and colleagues then showed that somatic cells can acquire a pluripotent state after being fused with ES cells [144]. Important key regulatory genes of pluripotency started to be discovered. As an example, Smith and colleagues demonstrated that, in mice, overexpression of Nanog, which

encodes a pluripotency transcription factor, substantially enhanced fusion-based nuclear reprogramming [145]. Results from two laboratories using mixed-species heterokaryons have shown that pluripotency genes, such as Oct4 and Nanog, were activated and their promoters demethylated within 1 day of fusion of mouse ES cells with human B cells or with human fibroblasts [146, 147].

Transcription-factor transduction

The fate of a cell can be altered by forced expression of tissues specific transcription factors.

Gehring and colleagues were the first to show this in 1987: in *D. melanogaster* larvae, ectopic overexpression of a homeotic gene, Antennapedia, under the control of a heat-shock gene promoter led to a change in body plan, with an additional set of legs being formed instead of antennae.[148]. Almost a decade later, even more striking was the finding by Gehring that ectopic expression of *eyeless*, a master control gene for eye morphogenesis, led to the development of functional eyes on the legs, wings and antennae of *D. melanogaster* [149]. Weintraub and colleagues identified the first tissue-specific master regulatory transcription factor in mice in 1987. They found that it was possible to induce a phenotypic conversion to the myogenic lineage by expressing a single muscle helix–loop–helix protein MYOD [150]. More surprisingly, it was discovered that pluripotency could be regained by numerous differentiated somatic cell types through overexpressing just four transcription-factors-encoding genes. These cells were named Induced Pluripotent Stem Cells (iPSCs) and were discovered by Yamanaka and colleagues in 2006 (Fig. 12c) [132, 151]. These cells

represent the strongest example so far of the plasticity of cells in response to a disruption in the stoichiometry of their transcriptional regulators. This discovery assured him the Nobel prize award for medicine in 2012.

Although the elegant fusion experiments by Tada, Surani and colleagues clearly showed that ES cells and embryonic germ cells contain factors that can induce reprogramming and pluripotency in somatic cells, attempts by many investigators to identify master regulators of the ES-cell state have failed. As a result, the view until about four years ago was that nuclear reprogramming to a pluripotent state was a highly complex process that might require the cooperation of up to 100 factors. Yamanaka's laboratory used retroviral vectors to introduce into embryonic and adult mouse fibroblasts DNA library of 24 genes expressed by ES cells, and these genes were then tested for their collective ability to induce pluripotency. Pluripotency was assayed by examining for activation of a reporter gene construct containing the promoter of Fbx15, a gene previously identified as being specific to ES cells. Clones in which the Fbx15 promoter was activated produced a reporter protein that rendered them resistant to the drug neomycin. These drug-resistant clones had similar morphology, growth properties and gene expression characteristics to ES cells. More importantly, after injection into mice, they were capable of forming teratomas, indicating their pluripotency. Rather than determining the contribution of each factor singly or in subgroups, factors were progressively eliminated from the pool one at a time. As a result, the authors identified four key factors that were sufficient to induce pluripotency in fibroblasts: OCT4, SOX2, KLF4 and c-MYC. Strikingly, transgenes encoding the four

factors were necessary only when iPSCs were being generated. When these cells have become established, the retroviral transgenes were silenced, and the endogenous genes encoding the four factors become activated. Hence, the self-renewal of iPSCs and maintenance of their pluripotency relied entirely on endogenous gene expression of the genes encoding OCT4, SOX2, KLF4 and c-MYC, suggesting that iPSCs have undergone almost-complete reprogramming.

Thanks to the simplicity of the technic, human iPSCs were obtain within a year [132].

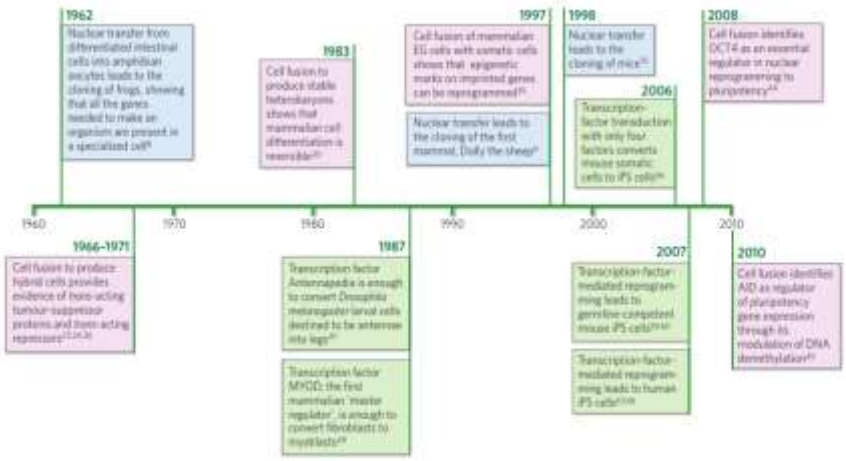

Fig. 13. Timeline of discoveries in nuclear reprogramming [134].

2.3 Comparison between iPSCs and ESCs

The debate on whether iPSCs and ESCs are equivalent cell types, generated by different methods, is still not completely solved.

iPSCs are morphologically similar to ESCs: they grow as a colony on top of a monolayer of mitotically inactivated mouse embryonic fibroblasts (iMEFs); the cells forming the colony present prominent nucleoli and scant cytoplasm. The general expression of pluripotency markers such as TRA-1-60, TRA-1-80, SSEA-3, SSEA4, Oct4, Sox2 and Nanog are the same. In addition, iPSCs pass the hallmark test of pluripotency: when injected into immunocompromised mice they form teratomas, showing their potential to differentiate *in vivo* into the three embryonic germ layers. Moreover, they also contribute to germ line transmission. iPSCs possess pluripotent differentiation potential, independently of the tissue of origin. Various reports show their differentiation into several committed functional lineages: among others, blood cells displaying hematopoietic colony activity [152, 153] motor neurons that are electrically active [154] cardiomyocytes that beat rhythmically and respond to cardioactive drugs [155] and adipocytes[156]. Many reports have claimed that, despite the fact that they both share pluripotency, iPSCs differ from ESCs by their "epigenetic memory" of somatic origin, including DNA methylation and gene expression [157-159]. However, many others have demonstrated that there are no differences between ESCs and iPSCs, even from an epigenetic point of view [160, 161]. Resolution of this argument is considered to be important for the study of developmental processes using these cell types as well as for their clinical application.

When iPSC colonies emerge, the reprogramming process is usually not complete. Thus, in early passages, iPSCs could show differences of gene expression and epigenetic status compared with ESCs that have been maintained for a longer period of time *in vitro*. Indeed, it has been demonstrated that continuous passaging of mouse iPSCs abrogates transcriptional, epigenetic and functional differences between iPSCs and ESCs, further approaching a homogeneous population [162]. Other studies demonstrated the number of cell lines analyzed might influence the conclusions regarding whether ESCs and iPSCs are equivalent. Therefore, some authors argue that mature iPSCs, which exclude incompletely reprogrammed clones, are probably indistinguishable from ESCs based on gene expression profiles and epigenetic status [163].

Nowadays, iPSCs are not only derived from fibroblasts. Different groups generated iPSCs from other somatic cells, providing evidence that is possible to reprogram cells of different origins, such as keratinocytes, MSCs, oral mucosa cells, dental pulp cells, peripheral blood and cord blood, in addition to skin fibroblasts. Similarly, iPSCs have been produced from several species: mouse, rat, monkey, pig, dog, rabbit and human.

2.4 Limitation and rapid evolution of iPSCs technology

From their discovery, there has been much anticipation regarding the potential clinical applications of iPSCs. However, first-generation of mouse iPSCs showed several unfavorable features, which restricted

their applicability. Most notably, they could have incomplete pluripotency. Recently, significant progress has been made in improving the quality of iPSCs and increasing the efficiency of generating fully reprogrammed cells. Another crucial issue with first-generation iPSCs was the use of retroviral vectors to deliver the reprogramming factors. These vectors integrate into the genome of host cells, potentially causing disruption or aberrant activation of neighboring genes. Moreover, there is also the risk of reactivation of reprogramming genes themselves. For example, reactivation of MYC sporadically induced tumor formation in iPSC-derived chimeric mice. The introduction of efficient, integration-free methods for cell reprogramming represents a turning point in solving this issue. Alternative induction methods have been developed that involve the transient expression of reprogramming factors, including adenoviruses [164-166] plasmids, transposons [167, 168], Sendai viruses [169, 170], synthetic mRNAs [171] and recombinant proteins [172]. Currently, episomal vectors, Sendai viruses and synthetic mRNAs are widely used for generating integration-free iPSCs. More recently, a report showed that a set of chemical compounds is sufficient to reprogram mouse fibroblasts to iPSCs [173]. Additionally, since 2009, xeno-free conditions have been developed to overcome the problems associated with traditional culture methods and to eliminate undefined animal components. Currently, combinations of chemically defined media and recombinant matrix proteins, such as vitronectin, matrigel or laminin, are widely used for the generation and maintenance of human iPSCs. These advancements have enabled the use of iPSCs for therapeutic purposes.

2.5 iPSCs applicability

During these recent years, iPSCs technology has already showed its potential for clinical applications and disease modelling. Some of the limitations that animal models have are due to their genomic differences in terms of genetic background and number of chromosomes. Moreover, sometimes it is difficult to obtain an animal model because of diseases restricted representation of pathophysiology. Since iPSCs retain pluripotency, they could originate all cell types with a clinical interest. Moreover, patient-specific iPSCs can be derived and used to study a particular lineage of concern, while maintaining the genetic profile of the patient. The proof of concept of iPSCs clinical applicability was provided by a sickle cell anaemia mouse model treated with iPSC-derived hematopoietic progenitors [174]. Similarly, neural cells derived from mouse iPSCs have been used successfully to cure Parkinson disease and spinal cord injury in experimental mouse models and found to be safe [175, 176]. Their therapeutic applicability is further strengthened by combining iPSC technology with genome engineering, which allows the correction of mutation in patient-derived iPSCs, as well as modification of reporter lines to facilitate differentiation towards specific cell types.

Moreover, patient specific-iPSCs hold the possibility for drug discovery and molecular pathway clarification.

In addition to their use in modelling diseases and drug screening, the most promising purpose of iPSCs is their potential application in regenerative medicine. The ultimate goal of this technology would be

the transplantation of a lineage restricted progenitor cells, derived from a patient-specific iPSCs, that does not trigger any immune response, does not promote tumor formation and that could recover the target-damaged tissue. Surprisingly, this application no longer seems an impossible dream. Recently, the first clinical trial for wet age-related macular degeneration using iPSC-derived retinal pigment epithelium has begun in Japan, with the aim of assessing the safety and effectiveness of iPSC-based therapies in humans.

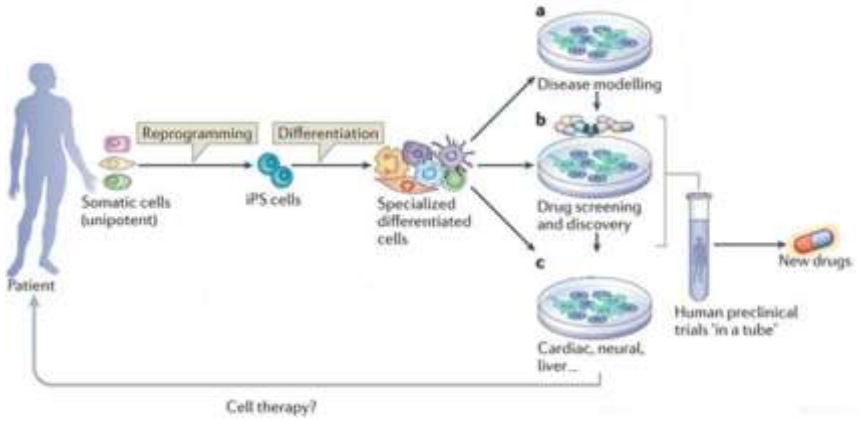

Fig. 14. Human iPS cell derivation, differentiation and applications. Adult somatic cells (unipotent) from any patient can be reprogrammed into induced pluripotent stem (iPS) cells. After inducing differentiation in vitro, human iPS cells form specialized cells that have several applications. a) Human iPS cells can be used in disease modelling to understand the molecular mechanisms underlying disease phenotypes. b) Another application of human iPS cells is in drug screening and discovery, to determine the effects of candidate drugs and new compounds and identify target pathways. c) Human iPS cells are also valuable in cardiac, neural and liver toxicity tests to assess cellular toxic responses. Drug screening and toxicity tests together represent human preclinical 'trials in a tube' that allow the introduction of 'the patient' in early stages of the drug discovery process (Modified from [177]).

3. iPSCs osteogenic differentiation

Bone disorders represent serious public health issue affecting a respectable portion of the median and elderly population. Many efforts have been made in studying MSCs derived from different tissues as a promising sources of cells for bone-skeletal regeneration. In fact, they hold the potential to differentiate into cartilage, bone and adipose tissue [178, 179]. However, MSCs possess limited proliferation capability which significantly decrease with donor age. Moreover, the invasive procedure required to harvest MSCs represents another limitation.

Due to their high proliferation and differentiation capacity, iPSCs started to become an attractive source for bone regeneration and for studying osteogenesis. This is an optimal tool for the understanding of the molecular pathway involved in this differentiation process and allow us to intervene at a more specific manner in the cure of the skeletal pathologies.

Unfortunately, there are only few protocols that attempt to differentiate human iPSCs to osteoblasts and each of them adopt different procedures. This process is still largely unknown and unexplored. Beside the lack of clear and univocal experimental procedures, there are also limited data/information to ensure the accomplishment of the differentiation. Anyhow, the investigation around MSCs were helpful to elucidate the molecules and the procedures requested for the isolation of osteoblasts from pluripotent stem cells. This paved the way toward the use of ESCs as a new cellular source, which represented a second step forward in the comprehension of *in vitro* osteogenesis.

Consequently, the differentiation of iPSCs to bone has been adapted from protocols for osteogenic differentiation of MSCs and ESCs. Therefore, the differentiation patterns and the molecular mechanism for specifically induce osteogenic differentiation from iPSCs still remain to be well define.

Nowadays, protocols for iPSCs differentiation to osteoblasts generally include an intermediate passage either to mesoderm lineage cells (i.e. MSCs) or to chondrocytes.

Most bones in the body are formed via endochondral ossification, which involves the formation of cartilage tissue from condensed mesenchymal cells and the subsequent replacement of the cartilage template by bone. In contrast, direct conversion of mesenchymal tissue into bone is called intramembranous ossification, which occurs primarily in the craniofacial skeleton.

Thus, the intent is to obtain osteogenic precursors and recapitulate the developmental pathways that occur during embryogenesis. This often implies segmenting the differentiation protocols into stages, each of which consists of defined culture conditions that enrich for intermediate cell populations before progression to the next step.

3.1 iPSCs osteogenic differentiation through intermediate mesoderm lineage generation

Most iPSCs osteogenic differentiation protocols contemplate an intermediate passage through cells of the early mesoderm lineage and/or to MSCs. The embryoid bodies (EBs) based method is widely used. EBs are spherical aggregates that are formed spontaneously from

iPSCs once detached from the feeder layer. They resemble the first stages of embryogenesis and they can naturally originate the three germ layers, if maintained in their basal medium. Since they still retain pluripotency, they can theoretically give rise to all types of cells and, through the combination of different cytokines and small molecules, you can push the differentiation toward one lineage more than another. Retinoic acid (RA) is often used during the EBs culture period, since it induces the differentiation toward mesoderm [180, 181]. Alternately, Activin A can be adopted [182]. Kim and colleagues used a combination of different molecules: EBs were treated with SB431542 (an inhibitor of transforming growth factor-beta signaling), ITS and B27 to enhance differentiation into cardiac-mesoderm and neuro-ectoderm lineages [183].

Usually, the EBs method comprises a first step of suspension culture of the aggregates of about 7-10 days, and a second incubation phase onto gelatin or fibronectin coated dishes, which allows the adhesion of the aggregates to the plate. In this period, cells outgrow from the EBs themselves.

Commonly, but not necessarily, after the enrichment of the culture with cells of the mesoderm/neuro ectoderm lineage, the heterogeneous population is more specifically differentiated toward “MSC-like” cells. This purpose is generally achieved with the culture of the cells in a “mesenchymal culture medium”, and with subsequent passaging onto tissue culture plates. This causes a shift in the morphology of the cells which become fibroblast-like, and permits the population to become even more homogeneous with the increase of the culture steps. In fact,

during this period, the non-MSC-like cells die while the MSCs-like cells adhere to the dish, as it is one of their principal characteristic.

The first steps of this monolayer culture are very delicate and important since they will determine the quality of the MSC-like cells. It is crucial to evaluate the initial cell density. Seeding at low cell density induces mitotic arrest and enlarged, flattened, irregular cell morphology. Inversely, high cell density forms clusters. In literature, cell density is controversial and ranges from 1-2 x 10^4 cells/cm^2 to 2 x 10^5 cells/cm^2 [182, 184, 185]. The EBs culture method can be associated or not with a consequent step to MSC-like cells, and so as the contrary: outgrow cells from EBs can be directly differentiate to osteoblasts in the appropriate differentiation medium. Equally, MSC-like cells can be immediately originate from iPSCs, avoiding the EBs step, and consequently induce to osteogenic lineage. Anyhow, these are rare cases and request particular precautions [180, 182, 184]. Regardless of the method of differentiation used, single cell suspension is prepared for the *in vitro* and/or the *in vivo* osteogenic differentiation.

The *in vitro* differentiation procedure does not originate a bone structure but more likely a layer of osteoblasts that produced a mineralized bone matrix as a result of the expression of osteogenic genes. The cells are seeded as monolayer at a precise concentration, which widely change between research laboratories, in an appropriate osteogenic induction medium[180-182, 184]. The basic components of the commonly used osteogenic medium are fetal bovine serum (FBS), ascorbic acid, b-glycerophosphate, and dexamethasone. Additional enhancing supplements include bone morphogenetic proteins (BMPs) or the calcium-regulating hormone vitamin D3 (VitD3)[186]. The

period of incubation varies from 2 to 3 weeks. The most common assays used to certify the accomplishment of the differentiation are staining with Alizarin Red, Alkaline Phosphatase and Von Kossa solution; q-RT-PCR analysis for key osteogenic markers such as BMP-2, runt-related transcription factor 2 (RUNX2), collagen type 1 alpha-1 (COL1A1), osteocalcin (BGLAAP), alkaline phosphatase (ALP), bone sialoprotein 1 (SPP1) and osteonectin (SPARC) [183]. The *in vivo* osteogenic capability of osteoblast-derived cells represent a robust proof of concept of a complete *in vitro* differentiation of pluripotent stem cells. Ko et al. reported that osteoinduced iPSCs were able to originate new bone, including full restoration of bone width and robust formation of trabeculae, in a calvarial defect mouse model. Equally, osteoinduced iPSCs led to healing of segmental defects [180].

Finally, *de novo* bone formation is observed when human MSC-like cells are implanted into an ectopic or orthotopic site [187]. Usually, MSC-like cells are vehicle by scaffolds and implanted into calvarial defect of immunodeficient mice[181],[188]. Currently, proposed scaffolds include those made of inorganic materials, organic or synthetic polymers, or of mixed materials (composite scaffolds) [189].

3.2 iPSCs osteogenic differentiation through intermediate chondrocytes generation

It has been demonstrated that osteoblasts can be either originate from chondrocytes, although *in vitro* bone replacement through cartilage degradation without vasculogenesis remained unclear [187, 190].

Yamashita and collaborators demonstrated a multi-step developmental processes of chondrogenesis, and subsequent bone replacement *in vitro*, by long-term expansion of cartilaginous aggregates in static suspension culture [133, 191]. This method tries to resemble what happens during chondrogenesis in the earliest phase of skeletal development: high-density micro-mass culture of stem cells mimics the formation of pre-chondrogenic mesenchymal condensations in the embryo and promotes their differentiation to the chondrocyte lineage.

In the proposed protocol, ESCs were cultured at high density in drops, for 5 days, in chondrogenic differentiation medium. 1 x 10^5 cells per 10 µl were used. After this period, aggregates were separated from the dishes by pipetting and transferred to suspension culture Petri dishes containing chondrogenic differentiation media up to 100 days. As demonstrated and highlighted by the authors, it was extremely important for chondrogenic differentiation to maintain a spherical conformation in suspension culture of the cells. In fact, it has been previously reported that the phenotypic features of chondrocytes may change into fibroblastic cells morphologically as the culture process progresses on a two-dimensional substrate [192]. Yamashita et al. demonstrated that ESCs differentiate into compact aggregates composed of chondrocytes during early culture passaging. As the culture progressed, extra-cellular matrix (ECM) was found around the cells. After prolonged culture, by day 50-60, section of the aggregates showed the presence of hypertrophic and degraded cartilage. Cartilage was then replaced by bone-like membranous tissue. More regions of bone were observed by day 100. Primary bone formation seemed to occur via cartilage resorption. Moreover, they also assessed the

capacity of the aggregates to generate cartilage and bone *in vivo*, by their transplantation into SCID mice.

Using various chondrogenic differentiation periods *in vitro*, another group demonstrated that a cartilage matrix was required for bone formation by mouse ESC. Mouse ESC-derived EBs were seeded on ceramic particles and cultured in serum-free chondrogenic differentiation medium containing TGFβ3 for 21 days. When these cartilage tissue-engineered constructs (CTECs) were implanted subcutaneously, the cartilage matured, became hypertrophic, calcified, and was ultimately replaced by bone tissue in the course of 21 days. Moreover, when CTECs were implanted orthotopically into critical-size cranial defects in rats, efficient bone formation was observed [187].

Farrell and collaborators strengthened the hypothesis that embryonic stem cells can form bone through the endochondral ossification, thereby turning *in-vitro* created cartilage into bone *in-vivo* [193]. Usually, in these protocols, the cartilage differentiation is achieved using micro-mass culture, that is culture of iPSCs at a very high density, in the differentiation medium.

Guzzo and collaborators induced chondrogenic differentiation by culturing iPSCs in micro-mass at 2×10^5 cells/10 uL drop, in defined, serum free media [184]. On day two of micro-mass formation and for the duration of the differentiation assay, iPSCs micro-masses were treated with human recombinant BMP-2. The iPSCs can be also grown in matrigel as a micromass using chondrogenic media with BMP-2 or TGF-1 [194].

4.Scope of the thesis

The scope of the present PhD project was focused on the isolation and characterization of patient specific-iPSCs (MPS-iPSCs) to create a disease model that allowed to study the early phase of the pathology and to explore still unknown disease mechanisms involved in the genetic disorder.

The first chapter highlights the general characteristics of lysosomal storage disorders (LSDs) with particular concern to MPS IH features. It also outlines the principal characteristics and applications of iPSCs. Lastly, a brief overview of current osteogenic protocols for iPSCs is provided.

The second chapter presents our first study that focuses on the mesoderm compartment. In particular, we illustrate:

1. The standardization of an iPSCs osteogenic differentiation protocol through the intermediate generation of *bona-fide* mesenchymal stem cells (hereafter named MSC-like cells).
2. The application of the designed procedure to MPS-iPSCs to characterize patient-derived mesenchymal stem cells and osteoblasts (OBs) and evaluate their role in osteogenesis and osteoclastogenesis.

The issue of the third chapter regards the ectoderm and endoderm lineage. In particular:

1. We evaluate the potential capability of MPS-iPSCs to differentiate into hepatocyte-like cells and neurons.

References

1. Wraith, J.E., *Lysosomal disorders.* Semin Neonatol, 2002. **7**(1): p. 75-83.
2. Biffi, A., *Gene therapy for lysosomal storage disorders: a good start.* Hum Mol Genet, 2016. **25**(R1): p. R65-75.
3. Lieberman, A.P., et al., *Autophagy in lysosomal storage disorders.* Autophagy, 2012. **8**(5): p. 719-30.
4. Fletcher, J.M., *Screening for lysosomal storage disorders--a clinical perspective.* J Inherit Metab Dis, 2006. **29**(2-3): p. 405-8.
5. Filocamo, M. and A. Morrone, *Lysosomal storage disorders: molecular basis and laboratory testing.* Hum Genomics, 2011. **5**(3): p. 156-69.
6. Alberts B, B.D., Lewis J, Raff M, Roberts K, Watson JD, *Molecular Biology of the Cell.* 1994. **3rd edition**.
7. Platt, F.M., B. Boland, and A.C. van der Spoel, *The cell biology of disease: lysosomal storage disorders: the cellular impact of lysosomal dysfunction.* J Cell Biol, 2012. **199**(5): p. 723-34.
8. Coutinho, M.F., M.J. Prata, and S. Alves, *Mannose-6-phosphate pathway: a review on its role in lysosomal function and dysfunction.* Mol Genet Metab, 2012. **105**(4): p. 542-50.
9. Reczek, D., et al., *LIMP-2 is a receptor for lysosomal mannose-6-phosphate-independent targeting of beta-glucocerebrosidase.* Cell, 2007. **131**(4): p. 770-83.
10. Sancak, Y., et al., *Ragulator-Rag complex targets mTORC1 to the lysosomal surface and is necessary for its activation by amino acids.* Cell, 2010. **141**(2): p. 290-303.
11. Zoncu, R., et al., *mTORC1 senses lysosomal amino acids through an inside-out mechanism that requires the vacuolar H(+)-ATPase.* Science, 2011. **334**(6056): p. 678-83.
12. Sardiello, M., et al., *A gene network regulating lysosomal biogenesis and function.* Science, 2009. **325**(5939): p. 473-7.
13. Settembre, C., et al., *A lysosome-to-nucleus signalling mechanism senses and regulates the lysosome via mTOR and TFEB.* EMBO J, 2012. **31**(5): p. 1095-108.
14. Ellinwood, N.M., C.H. Vite, and M.E. Haskins, *Gene therapy for lysosomal storage diseases: the lessons and promise of animal models.* J Gene Med, 2004. **6**(5): p. 481-506.

15. Rohrbach, M. and J.T. Clarke, *Treatment of lysosomal storage disorders : progress with enzyme replacement therapy.* Drugs, 2007. **67**(18): p. 2697-716.
16. Batzios, S.P., D.I. Zafeiriou, and E. Papakonstantinou, *Extracellular matrix components: an intricate network of possible biomarkers for lysosomal storage disorders?* FEBS Lett, 2013. **587**(8): p. 1258-67.
17. Settembre, C., et al., *Lysosomal storage diseases as disorders of autophagy.* Autophagy, 2008. **4**(1): p. 113-4.
18. Schultz, M.L., et al., *Clarifying lysosomal storage diseases.* Trends Neurosci, 2011. **34**(8): p. 401-10.
19. Wraith, J.E., *Lysosomal disorders.* Paediatrics and Child Health, 2010. **21**(2): p. 76-79.
20. Coutinho, M.F., L. Lacerda, and S. Alves, *Glycosaminoglycan storage disorders: a review.* Biochem Res Int, 2012. **2012**: p. 471325.
21. Tomatsu, S., et al., *Newborn screening and diagnosis of mucopolysaccharidoses.* Mol Genet Metab, 2013. **110**(1-2): p. 42-53.
22. Giugliani, R., *Mucopolysacccharidoses: From understanding to treatment, a century of discoveries.* Genet Mol Biol, 2012. **35**(4 (suppl)): p. 924-31.
23. Clarke, L.A., et al., *Biomarkers for the mucopolysaccharidoses: discovery and clinical utility.* Mol Genet Metab, 2012. **106**(4): p. 395-402.
24. Oussoren, E., et al., *Bone, joint and tooth development in mucopolysaccharidoses: relevance to therapeutic options.* Biochim Biophys Acta, 2011. **1812**(11): p. 1542-56.
25. Kjellén, L., *Glycobiology: Enzyme deficiencies deciphered.* Nat Chem Biol, 2012. **8**(2): p. 137-8.
26. Morishita, K. and R.E. Petty, *Musculoskeletal manifestations of mucopolysaccharidoses.* Rheumatology (Oxford), 2011. **50 Suppl 5**: p. v19-25.
27. Muenzer, J., *The mucopolysaccharidoses: a heterogeneous group of disorders with variable pediatric presentations.* J Pediatr, 2004. **144**(5 Suppl): p. S27-34.
28. Opoka-Winiarska, V., et al., *Osteoimmunology in mucopolysaccharidoses type I, II, VI and VII. Immunological regulation of the osteoarticular system in the course of metabolic inflammation.* Osteoarthritis Cartilage, 2013. **21**(12): p. 1813-23.

29. Clarke, L.A., *Pathogenesis of skeletal and connective tissue involvement in the mucopolysaccharidoses: glycosaminoglycan storage is merely the instigator.* Rheumatology (Oxford), 2011. **50 Suppl 5**: p. v13-8.
30. Campos, D. and M. Monaga, *Mucopolysaccharidosis type I: current knowledge on its pathophysiological mechanisms.* Metab Brain Dis, 2012. **27**(2): p. 121-9.
31. Pastores, G.M., et al., *The MPS I registry: design, methodology, and early findings of a global disease registry for monitoring patients with Mucopolysaccharidosis Type I.* Mol Genet Metab, 2007. **91**(1): p. 37-47.
32. Scott, H.S., et al., *Identification of mutations in the alpha-L-iduronidase gene (IDUA) that cause Hurler and Scheie syndromes.* Am J Hum Genet, 1993. **53**(5): p. 973-86.
33. G, H., *Uber Einen Typ multiper Abartungen, vorwiegend am Skelettsystem.* Z Kinderheilk, 1919. **24**(220).
34. Ellis, R.W., *Gargoylism (Chondro-osteo-dystrophy, Corneal Opacities, Hepatosplenomegaly, and Mental Deficiency).* Proc R Soc Med, 1936. **30**(2): p. 158-60.
35. SCHEIE, H.G., G.W. HAMBRICK, and L.A. BARNESS, *A newly recognized forme fruste of Hurler's disease (gargoylism).* Am J Ophthalmol, 1962. **53**: p. 753-69.
36. MCKUSICK, V.A., *THE GENETIC MUCOPOLYSACCHARIDOSES.* Circulation, 1965. **31**: p. 1-4.
37. Wiesmann, U. and E.F. Neufeld, *Scheie and Hurler syndromes: apparent identity of the biochemical defect.* Science, 1970. **169**(3940): p. 72-4.
38. Bach, G., et al., *The defect in the Hurler and Scheie syndromes: deficiency of -L-iduronidase.* Proc Natl Acad Sci U S A, 1972. **69**(8): p. 2048-51.
39. Muenzer, J., et al., *Mucopolysaccharidosis I: management and treatment guidelines.* Pediatrics, 2009. **123**(1): p. 19-29.
40. Moore, D., et al., *The prevalence of and survival in Mucopolysaccharidosis I: Hurler, Hurler-Scheie and Scheie syndromes in the UK.* Orphanet J Rare Dis, 2008. **3**: p. 24.
41. Scott, H.S., et al., *Chromosomal localization of the human alpha-L-iduronidase gene (IDUA) to 4p16.3.* Am J Hum Genet, 1990. **47**(5): p. 802-7.
42. Scott, H.S., et al., *Structure and sequence of the human alpha-L-iduronidase gene.* Genomics, 1992. **13**(4): p. 1311-3.

43. Scott, H.S., et al., *A common mutation for mucopolysaccharidosis type I associated with a severe Hurler syndrome phenotype.* Hum Mutat, 1992. **1**(2): p. 103-8.
44. Scott, H.S., et al., *alpha-L-iduronidase mutations (Q70X and P533R) associate with a severe Hurler phenotype.* Hum Mutat, 1992. **1**(4): p. 333-9.
45. Terlato, N.J. and G.F. Cox, *Can mucopolysaccharidosis type I disease severity be predicted based on a patient's genotype? A comprehensive review of the literature.* Genet Med, 2003. **5**(4): p. 286-94.
46. Vijay, S. and J.E. Wraith, *Clinical presentation and follow-up of patients with the attenuated phenotype of mucopolysaccharidosis type I.* Acta Paediatr, 2005. **94**(7): p. 872-7.
47. Venturi, N., et al., *Molecular analysis of 30 mucopolysaccharidosis type I patients: evaluation of the mutational spectrum in Italian population and identification of 13 novel mutations.* Hum Mutat, 2002. **20**(3): p. 231.
48. Yogalingam, G., et al., *Identification and molecular characterization of alpha-L-iduronidase mutations present in mucopolysaccharidosis type I patients undergoing enzyme replacement therapy.* Hum Mutat, 2004. **24**(3): p. 199-207.
49. Wang, R.Y., et al., *Lysosomal storage diseases: diagnostic confirmation and management of presymptomatic individuals.* Genet Med, 2011. **13**(5): p. 457-84.
50. Rasalkar, D.D., et al., *Pictorial review of mucopolysaccharidosis with emphasis on MRI features of brain and spine.* Br J Radiol, 2011. **84**(1001): p. 469-77.
51. Wilson, S., et al., *Glycosaminoglycan-mediated loss of cathepsin K collagenolytic activity in MPS I contributes to osteoclast and growth plate abnormalities.* Am J Pathol, 2009. **175**(5): p. 2053-62.
52. Simonaro, C.M., et al., *Mechanism of glycosaminoglycan-mediated bone and joint disease: implications for the mucopolysaccharidoses and other connective tissue diseases.* Am J Pathol, 2008. **172**(1): p. 112-22.
53. Simonaro, C.M., et al., *Involvement of the Toll-like receptor 4 pathway and use of TNF-alpha antagonists for treatment of the mucopolysaccharidoses.* Proc Natl Acad Sci U S A, 2010. **107**(1): p. 222-7.

54. Novack, D.V. and S.L. Teitelbaum, *The osteoclast: friend or foe?* Annu Rev Pathol, 2008. **3**: p. 457-84.
55. Rodan, G.A., *Bone homeostasis.* Proc Natl Acad Sci U S A, 1998. **95**(23): p. 13361-2.
56. Kollet, O., A. Dar, and T. Lapidot, *The multiple roles of osteoclasts in host defense: bone remodeling and hematopoietic stem cell mobilization.* Annu Rev Immunol, 2007. **25**: p. 51-69.
57. Udagawa, N., et al., *Origin of osteoclasts: mature monocytes and macrophages are capable of differentiating into osteoclasts under a suitable microenvironment prepared by bone marrow-derived stromal cells.* Proc Natl Acad Sci U S A, 1990. **87**(18): p. 7260-4.
58. Boyle, W.J., W.S. Simonet, and D.L. Lacey, *Osteoclast differentiation and activation.* Nature, 2003. **423**(6937): p. 337-42.
59. Li, J., et al., *RANK is the intrinsic hematopoietic cell surface receptor that controls osteoclastogenesis and regulation of bone mass and calcium metabolism.* Proc Natl Acad Sci U S A, 2000. **97**(4): p. 1566-71.
60. Yasuda, H., et al., *Osteoclast differentiation factor is a ligand for osteoprotegerin/osteoclastogenesis-inhibitory factor and is identical to TRANCE/RANKL.* Proc Natl Acad Sci U S A, 1998. **95**(7): p. 3597-602.
61. Karsenty, G., H.M. Kronenberg, and C. Settembre, *Genetic control of bone formation.* Annu Rev Cell Dev Biol, 2009. **25**: p. 629-48.
62. Xiong, J. and C.A. O'Brien, *Osteocyte RANKL: new insights into the control of bone remodeling.* J Bone Miner Res, 2012. **27**(3): p. 499-505.
63. Feng, X. and J.M. McDonald, *Disorders of bone remodeling.* Annu Rev Pathol, 2011. **6**: p. 121-45.
64. Simonet, W.S., et al., *Osteoprotegerin: a novel secreted protein involved in the regulation of bone density.* Cell, 1997. **89**(2): p. 309-19.
65. Yasuda, H., et al., *Identity of osteoclastogenesis inhibitory factor (OCIF) and osteoprotegerin (OPG): a mechanism by which OPG/OCIF inhibits osteoclastogenesis in vitro.* Endocrinology, 1998. **139**(3): p. 1329-37.
66. Hofbauer, L.C. and M. Schoppet, *Clinical implications of the osteoprotegerin/RANKL/RANK system for bone and vascular diseases.* JAMA, 2004. **292**(4): p. 490-5.

67. Kwan Tat, S., et al., *The differential expression of osteoprotegerin (OPG) and receptor activator of nuclear factor kappaB ligand (RANKL) in human osteoarthritic subchondral bone osteoblasts is an indicator of the metabolic state of these disease cells.* Clin Exp Rheumatol, 2008. **26**(2): p. 295-304.
68. Nakashima, T. and H. Takayanagi, *Osteoimmunology: crosstalk between the immune and bone systems.* J Clin Immunol, 2009. **29**(5): p. 555-67.
69. Takayanagi, H., *Osteoimmunology: shared mechanisms and crosstalk between the immune and bone systems.* Nat Rev Immunol, 2007. **7**(4): p. 292-304.
70. Chen, G., et al., *Expression of RANKL/RANK/OPG in primary and metastatic human prostate cancer as markers of disease stage and functional regulation.* Cancer, 2006. **107**(2): p. 289-98.
71. Tat, S.K., et al., *OPG/membranous--RANKL complex is internalized via the clathrin pathway before a lysosomal and a proteasomal degradation.* Bone, 2006. **39**(4): p. 706-15.
72. Gatto, F., et al., *Hurler disease bone marrow stromal cells exhibit altered ability to support osteoclast formation.* Stem Cells Dev, 2012. **21**(9): p. 1466-77.
73. Khosla, S., *Minireview: the OPG/RANKL/RANK system.* Endocrinology, 2001. **142**(12): p. 5050-5.
74. Hikita, A., et al., *Negative regulation of osteoclastogenesis by ectodomain shedding of receptor activator of NF-kappaB ligand.* J Biol Chem, 2006. **281**(48): p. 36846-55.
75. Miyamoto, T., et al., *An adherent condition is required for formation of multinuclear osteoclasts in the presence of macrophage colony-stimulating factor and receptor activator of nuclear factor kappa B ligand.* Blood, 2000. **96**(13): p. 4335-43.
76. Nakashima, T., et al., *Protein expression and functional difference of membrane-bound and soluble receptor activator of NF-kappaB ligand: modulation of the expression by osteotropic factors and cytokines.* Biochem Biophys Res Commun, 2000. **275**(3): p. 768-75.
77. Suda, T., et al., *Modulation of osteoclast differentiation and function by the new members of the tumor necrosis factor receptor and ligand families.* Endocr Rev, 1999. **20**(3): p. 345-57.

78. Kobayashi, N., et al., *Segregation of TRAF6-mediated signaling pathways clarifies its role in osteoclastogenesis.* EMBO J, 2001. **20**(6): p. 1271-80.
79. D'Aco, K., et al., *Diagnosis and treatment trends in mucopolysaccharidosis I: findings from the MPS I Registry.* Eur J Pediatr, 2012. **171**(6): p. 911-9.
80. Muenzer, J., *Overview of the mucopolysaccharidoses.* Rheumatology (Oxford), 2011. **50 Suppl 5**: p. v4-12.
81. Muenzer, J., et al., *Mucopolysaccharidosis I: management and treatment guidelines.* Pediatrics, 2009. **123**(1): p. 19-29.
82. Volpi, N., et al., *Plasmatic dermatan sulfate and chondroitin sulfate determination in mucopolysaccharidoses.* J Pharm Biomed Anal, 2013. **85**: p. 40-5.
83. Campos, D., et al., *Identification of mucopolysaccharidosis I heterozygotes based on biochemical characteristics of L-iduronidase from dried blood spots.* Clin Chim Acta, 2014. **430**: p. 24-7.
84. Nakamura, K., K. Hattori, and F. Endo, *Newborn screening for lysosomal storage disorders.* Am J Med Genet C Semin Med Genet, 2011. **157C**(1): p. 63-71.
85. Kleijer, W.J., E.J. Thompson, and M.F. Niermeijer, *Prenatal diagnosis of the Hurler syndrome: report on 40 pregnancies at risk.* Prenat Diagn, 1983. **3**(3): p. 179-86.
86. Young, E.P., *Prenatal diagnosis of Hurler disease by analysis of alpha-iduronidase in chorionic villi.* J Inherit Metab Dis, 1992. **15**(2): p. 224-30.
87. Valayannopoulos, V. and F.A. Wijburg, *Therapy for the mucopolysaccharidoses.* Rheumatology (Oxford), 2011. **50 Suppl 5**: p. v49-59.
88. Fratantoni, J.C., C.W. Hall, and E.F. Neufeld, *Hurler and Hunter syndromes: mutual correction of the defect in cultured fibroblasts.* Science, 1968. **162**(3853): p. 570-2.
89. Prasad, V.K. and J. Kurtzberg, *Cord blood and bone marrow transplantation in inherited metabolic diseases: scientific basis, current status and future directions.* Br J Haematol, 2010. **148**(3): p. 356-72.
90. De Duve, C. and R. Wattiaux, *Functions of lysosomes.* Annu Rev Physiol, 1966. **28**: p. 435-92.
91. Phenix, C.P., et al., *Imaging of enzyme replacement therapy using PET.* Proc Natl Acad Sci U S A, 2010. **107**(24): p. 10842-7.

92. Barton, R.W. and E.F. Neufeld, *The Hurler corrective factor. Purification and some properties.* J Biol Chem, 1971. **246**(24): p. 7773-9.
93. Kakkis, E.D., et al., *Overexpression of the human lysosomal enzyme alpha-L-iduronidase in Chinese hamster ovary cells.* Protein Expr Purif, 1994. **5**(3): p. 225-32.
94. Shull, R.M., et al., *Enzyme replacement in a canine model of Hurler syndrome.* Proc Natl Acad Sci U S A, 1994. **91**(26): p. 12937-41.
95. Kakkis, E.D., et al., *Long-term and high-dose trials of enzyme replacement therapy in the canine model of mucopolysaccharidosis I.* Biochem Mol Med, 1996. **58**(2): p. 156-67.
96. Sifuentes, M., et al., *A follow-up study of MPS I patients treated with laronidase enzyme replacement therapy for 6 years.* Mol Genet Metab, 2007. **90**(2): p. 171-80.
97. Clarke, L.A., et al., *Long-term efficacy and safety of laronidase in the treatment of mucopolysaccharidosis I.* Pediatrics, 2009. **123**(1): p. 229-40.
98. Wraith, J.E., et al., *Enzyme replacement therapy for mucopolysaccharidosis I: a randomized, double-blinded, placebo-controlled, multinational study of recombinant human alpha-L-iduronidase (laronidase).* J Pediatr, 2004. **144**(5): p. 581-8.
99. Wraith, J.E., et al., *Enzyme replacement therapy in patients who have mucopolysaccharidosis I and are younger than 5 years: results of a multinational study of recombinant human alpha-L-iduronidase (laronidase).* Pediatrics, 2007. **120**(1): p. e37-46.
100. Giugliani, R., et al., *A dose-optimization trial of laronidase (Aldurazyme) in patients with mucopolysaccharidosis I.* Mol Genet Metab, 2009. **96**(1): p. 13-9.
101. Kakkis, E.D., et al., *Enzyme-replacement therapy in mucopolysaccharidosis I.* N Engl J Med, 2001. **344**(3): p. 182-8.
102. Arora, R.S., et al., *Enzyme replacement therapy in 12 patients with MPS I-H/S with homozygous p.Leu490Pro mutation.* J Inherit Metab Dis, 2007. **30**(5): p. 821.
103. Pitz, S., et al., *Ocular changes in patients with mucopolysaccharidosis I receiving enzyme replacement therapy: a 4-year experience.* Arch Ophthalmol, 2007. **125**(10): p. 1353-6.

104. Braunlin, E.A., J.M. Berry, and C.B. Whitley, *Cardiac findings after enzyme replacement therapy for mucopolysaccharidosis type I.* Am J Cardiol, 2006. **98**(3): p. 416-8.
105. Muenzer, J. and A. Fisher, *Advances in the treatment of mucopolysaccharidosis type I.* N Engl J Med, 2004. **350**(19): p. 1932-4.
106. Kakkis, E., et al., *Intrathecal enzyme replacement therapy reduces lysosomal storage in the brain and meninges of the canine model of MPS I.* Mol Genet Metab, 2004. **83**(1-2): p. 163-74.
107. Chen, A., et al., *Glycosaminoglycan storage in neuroanatomical regions of mucopolysaccharidosis I dogs following intrathecal recombinant human iduronidase.* APMIS, 2011. **119**(8): p. 513-21.
108. Boado, R.J., et al., *Reversal of lysosomal storage in brain of adult MPS-I mice with intravenous Trojan horse-iduronidase fusion protein.* Mol Pharm, 2011. **8**(4): p. 1342-50.
109. Wang, D., et al., *Engineering a lysosomal enzyme with a derivative of receptor-binding domain of apoE enables delivery across the blood-brain barrier.* Proc Natl Acad Sci U S A, 2013. **110**(8): p. 2999-3004.
110. Connock, M., et al., *A systematic review of the clinical effectiveness and cost-effectiveness of enzyme replacement therapies for Fabry's disease and mucopolysaccharidosis type 1.* Health Technol Assess, 2006. **10**(20): p. iii-iv, ix-113.
111. Wraith, J.E., *Enzyme replacement therapy in mucopolysaccharidosis type I: progress and emerging difficulties.* J Inherit Metab Dis, 2001. **24**(2): p. 245-50.
112. Baron, F., R. Storb, and M.T. Little, *Hematopoietic cell transplantation: five decades of progress.* Arch Med Res, 2003. **34**(6): p. 528-44.
113. Lutzko, C., et al., *Genetically corrected autologous stem cells engraft, but host immune responses limit their utility in canine alpha-L-iduronidase deficiency.* Blood, 1999. **93**(6): p. 1895-905.
114. Zheng, Y., et al., *Treatment of the mouse model of mucopolysaccharidosis I with retrovirally transduced bone marrow.* Mol Genet Metab, 2003. **79**(4): p. 233-44.
115. Slavin, S., et al., *Nonmyeloablative stem cell transplantation and cell therapy as an alternative to conventional bone marrow transplantation with lethal cytoreduction for the treatment of*

malignant and nonmalignant hematologic diseases. Blood, 1998. **91**(3): p. 756-63.
116. Peters, C., *Effective treatment of the central nervous system in lysosomal storage diseases: save that brain!* J Lab Clin Med, 2003. **142**(6): p. 361-3.
117. Knudson, A.G., N. Di Ferrante, and J.E. Curtis, *Effect of leukocyte transfusion in a child with type II mucopolysaccharidosis.* Proc Natl Acad Sci U S A, 1971. **68**(8): p. 1738-41.
118. Aldenhoven, M., J.J. Boelens, and T.J. de Koning, *The clinical outcome of Hurler syndrome after stem cell transplantation.* Biol Blood Marrow Transplant, 2008. **14**(5): p. 485-98.
119. Teo, A.K. and L. Vallier, *Emerging use of stem cells in regenerative medicine.* Biochem J, 2010. **428**(1): p. 11-23.
120. Watt, F.M. and B.L. Hogan, *Out of Eden: stem cells and their niches.* Science, 2000. **287**(5457): p. 1427-30.
121. Gluckman, E., et al., *Outcome of cord-blood transplantation from related and unrelated donors. Eurocord Transplant Group and the European Blood and Marrow Transplantation Group.* N Engl J Med, 1997. **337**(6): p. 373-81.
122. Tse, W. and M.J. Laughlin, *Umbilical cord blood transplantation: a new alternative option.* Hematology Am Soc Hematol Educ Program, 2005: p. 377-83.
123. Becker, A.J., C.E. Mc, and J.E. Till, *Cytological demonstration of the clonal nature of spleen colonies derived from transplanted mouse marrow cells.* Nature, 1963. **197**: p. 452-4.
124. Till, J.E. and C.E. Mc, *A direct measurement of the radiation sensitivity of normal mouse bone marrow cells.* Radiat Res, 1961. **14**: p. 213-22.
125. Brazelton, T.R., et al., *From marrow to brain: expression of neuronal phenotypes in adult mice.* Science, 2000. **290**(5497): p. 1775-9.
126. Ferrari, G., et al., *Muscle regeneration by bone marrow-derived myogenic progenitors.* Science, 1998. **279**(5356): p. 1528-30.
127. Lagasse, E., et al., *Purified hematopoietic stem cells can differentiate into hepatocytes in vivo.* Nat Med, 2000. **6**(11): p. 1229-34.
128. Bjornson, C.R., et al., *Turning brain into blood: a hematopoietic fate adopted by adult neural stem cells in vivo.* Science, 1999. **283**(5401): p. 534-7.

129. Galli, D., et al., *Mesoangioblasts, vessel-associated multipotent stem cells, repair the infarcted heart by multiple cellular mechanisms: a comparison with bone marrow progenitors, fibroblasts, and endothelial cells.* Arterioscler Thromb Vasc Biol, 2005. **25**(4): p. 692-7.
130. Beltrami, A.P., et al., *Adult cardiac stem cells are multipotent and support myocardial regeneration.* Cell, 2003. **114**(6): p. 763-76.
131. McKay, R., *Stem cells in the central nervous system.* Science, 1997. **276**(5309): p. 66-71.
132. Takahashi, K., et al., *Induction of pluripotent stem cells from adult human fibroblasts by defined factors.* Cell, 2007. **131**(5): p. 861-72.
133. Yamashita, A., S. Nishikawa, and D.E. Rancourt, *Identification of five developmental processes during chondrogenic differentiation of embryonic stem cells.* PLoS One, 2010. **5**(6): p. e10998.
134. Yamanaka, S. and H.M. Blau, *Nuclear reprogramming to a pluripotent state by three approaches.* Nature, 2010. **465**(7299): p. 704-12.
135. Briggs, R. and T.J. King, *Transplantation of Living Nuclei From Blastula Cells into Enucleated Frogs' Eggs.* Proc Natl Acad Sci U S A, 1952. **38**(5): p. 455-63.
136. Gurdon, J.B., *The developmental capacity of nuclei taken from intestinal epithelium cells of feeding tadpoles.* J Embryol Exp Morphol, 1962. **10**: p. 622-40.
137. Gurdon, J.B., *Adult frogs derived from the nuclei of single somatic cells.* Dev Biol, 1962. **4**: p. 256-73.
138. Wilmut, I., et al., *Viable offspring derived from fetal and adult mammalian cells.* Nature, 1997. **385**(6619): p. 810-3.
139. Yang, X., et al., *Nuclear reprogramming of cloned embryos and its implications for therapeutic cloning.* Nat Genet, 2007. **39**(3): p. 295-302.
140. Blau, H.M., C.P. Chiu, and C. Webster, *Cytoplasmic activation of human nuclear genes in stable heterocaryons.* Cell, 1983. **32**(4): p. 1171-80.
141. Blau, H.M., et al., *Plasticity of the differentiated state.* Science, 1985. **230**(4727): p. 758-66.
142. Pavlath, G.K. and H.M. Blau, *Expression of muscle genes in heterokaryons depends on gene dosage.* J Cell Biol, 1986. **102**(1): p. 124-30.

143. Tada, M., et al., *Nuclear reprogramming of somatic cells by in vitro hybridization with ES cells.* Curr Biol, 2001. **11**(19): p. 1553-8.
144. Tada, M., et al., *Embryonic germ cells induce epigenetic reprogramming of somatic nucleus in hybrid cells.* EMBO J, 1997. **16**(21): p. 6510-20.
145. Silva, J., et al., *Nanog promotes transfer of pluripotency after cell fusion.* Nature, 2006. **441**(7096): p. 997-1001.
146. Bhutani, N., et al., *Reprogramming towards pluripotency requires AID-dependent DNA demethylation.* Nature, 2010. **463**(7284): p. 1042-7.
147. Pereira, C.F., et al., *Heterokaryon-based reprogramming of human B lymphocytes for pluripotency requires Oct4 but not Sox2.* PLoS Genet, 2008. **4**(9): p. e1000170.
148. Schneuwly, S., R. Klemenz, and W.J. Gehring, *Redesigning the body plan of Drosophila by ectopic expression of the homoeotic gene Antennapedia.* Nature, 1987. **325**(6107): p. 816-8.
149. Gehring, W.J., *The master control gene for morphogenesis and evolution of the eye.* Genes Cells, 1996. **1**(1): p. 11-5.
150. Davis, R.L., H. Weintraub, and A.B. Lassar, *Expression of a single transfected cDNA converts fibroblasts to myoblasts.* Cell, 1987. **51**(6): p. 987-1000.
151. Yamanaka, S., *Strategies and new developments in the generation of patient-specific pluripotent stem cells.* Cell Stem Cell, 2007. **1**(1): p. 39-49.
152. Lengerke, C., et al., *Hematopoietic development from human induced pluripotent stem cells.* Ann N Y Acad Sci, 2009. **1176**: p. 219-27.
153. Raya, A., et al., *Disease-corrected haematopoietic progenitors from Fanconi anaemia induced pluripotent stem cells.* Nature, 2009. **460**(7251): p. 53-9.
154. Karumbayaram, S., et al., *Directed differentiation of human-induced pluripotent stem cells generates active motor neurons.* Stem Cells, 2009. **27**(4): p. 806-11.
155. Gai, H., et al., *Generation and characterization of functional cardiomyocytes using induced pluripotent stem cells derived from human fibroblasts.* Cell Biol Int, 2009. **33**(11): p. 1184-93.
156. Taura, D., et al., *Adipogenic differentiation of human induced pluripotent stem cells: comparison with that of human embryonic stem cells.* FEBS Lett, 2009. **583**(6): p. 1029-33.

157. Chin, M.H., et al., *Induced pluripotent stem cells and embryonic stem cells are distinguished by gene expression signatures.* Cell Stem Cell, 2009. **5**(1): p. 111-23.
158. Ghosh, Z., et al., *Persistent donor cell gene expression among human induced pluripotent stem cells contributes to differences with human embryonic stem cells.* PLoS One, 2010. **5**(2): p. e8975.
159. Kim, K., et al., *Donor cell type can influence the epigenome and differentiation potential of human induced pluripotent stem cells.* Nat Biotechnol, 2011. **29**(12): p. 1117-9.
160. Bock, C., et al., *Reference Maps of human ES and iPS cell variation enable high-throughput characterization of pluripotent cell lines.* Cell, 2011. **144**(3): p. 439-52.
161. Rouhani, F., et al., *Genetic background drives transcriptional variation in human induced pluripotent stem cells.* PLoS Genet, 2014. **10**(6): p. e1004432.
162. Polo, J.M., et al., *Cell type of origin influences the molecular and functional properties of mouse induced pluripotent stem cells.* Nat Biotechnol, 2010. **28**(8): p. 848-55.
163. Takahashi, K. and S. Yamanaka, *A developmental framework for induced pluripotency.* Development, 2015. **142**(19): p. 3274-85.
164. Stadtfeld, M., et al., *Induced pluripotent stem cells generated without viral integration.* Science, 2008. **322**(5903): p. 945-9.
165. Jia, F., et al., *A nonviral minicircle vector for deriving human iPS cells.* Nat Methods, 2010. **7**(3): p. 197-9.
166. Yu, J., et al., *Human induced pluripotent stem cells free of vector and transgene sequences.* Science, 2009. **324**(5928): p. 797-801.
167. Kaji, K., et al., *Virus-free induction of pluripotency and subsequent excision of reprogramming factors.* Nature, 2009. **458**(7239): p. 771-5.
168. Yusa, K., et al., *Generation of transgene-free induced pluripotent mouse stem cells by the piggyBac transposon.* Nat Methods, 2009. **6**(5): p. 363-9.
169. Fusaki, N., et al., *Efficient induction of transgene-free human pluripotent stem cells using a vector based on Sendai virus, an RNA virus that does not integrate into the host genome.* Proc Jpn Acad Ser B Phys Biol Sci, 2009. **85**(8): p. 348-62.
170. Nishimura, K., et al., *Development of defective and persistent Sendai virus vector: a unique gene delivery/expression system*

ideal for cell reprogramming. J Biol Chem, 2011. **286**(6): p. 4760-71.
171. Warren, L., et al., *Highly efficient reprogramming to pluripotency and directed differentiation of human cells with synthetic modified mRNA.* Cell Stem Cell, 2010. **7**(5): p. 618-30.
172. Kim, D., et al., *Generation of human induced pluripotent stem cells by direct delivery of reprogramming proteins.* Cell Stem Cell, 2009. **4**(6): p. 472-6.
173. Hou, P., et al., *Pluripotent stem cells induced from mouse somatic cells by small-molecule compounds.* Science, 2013. **341**(6146): p. 651-4.
174. Hanna, J., et al., *Treatment of sickle cell anemia mouse model with iPS cells generated from autologous skin.* Science, 2007. **318**(5858): p. 1920-3.
175. Tsuji, O., et al., *Therapeutic potential of appropriately evaluated safe-induced pluripotent stem cells for spinal cord injury.* Proc Natl Acad Sci U S A, 2010. **107**(28): p. 12704-9.
176. Wernig, M., et al., *Neurons derived from reprogrammed fibroblasts functionally integrate into the fetal brain and improve symptoms of rats with Parkinson's disease.* Proc Natl Acad Sci U S A, 2008. **105**(15): p. 5856-61.
177. Bellin, M., et al., *Induced pluripotent stem cells: the new patient?* Nat Rev Mol Cell Biol, 2012. **13**(11): p. 713-26.
178. Deans, R.J. and A.B. Moseley, *Mesenchymal stem cells: biology and potential clinical uses.* Exp Hematol, 2000. **28**(8): p. 875-84.
179. Dominici, M., et al., *Minimal criteria for defining multipotent mesenchymal stromal cells. The International Society for Cellular Therapy position statement.* Cytotherapy, 2006. **8**(4): p. 315-7.
180. Ko, J.Y., S. Park, and G.I. Im, *Osteogenesis from human induced pluripotent stem cells: an in vitro and in vivo comparison with mesenchymal stem cells.* Stem Cells Dev, 2014. **23**(15): p. 1788-97.
181. Xie, J., et al., *Osteogenic differentiation and bone regeneration of iPSC-MSCs supported by a biomimetic nanofibrous scaffold.* Acta Biomater, 2016. **29**: p. 365-79.
182. Nasu, A., et al., *Genetically matched human iPS cells reveal that propensity for cartilage and bone differentiation differs with clones, not cell type of origin.* PLoS One, 2013. **8**(1): p. e53771.

183. Kim, D., et al., *Impaired osteogenesis in Menkes disease-derived induced pluripotent stem cells.* Stem Cell Res Ther, 2015. **6**: p. 160.
184. Guzzo, R.M., et al., *Efficient differentiation of human iPSC-derived mesenchymal stem cells to chondroprogenitor cells.* J Cell Biochem, 2013. **114**(2): p. 480-90.
185. Koyama, N., et al., *Human induced pluripotent stem cells differentiated into chondrogenic lineage via generation of mesenchymal progenitor cells.* Stem Cells Dev, 2013. **22**(1): p. 102-13.
186. zur Nieden, N.I., G. Kempka, and H.J. Ahr, *In vitro differentiation of embryonic stem cells into mineralized osteoblasts.* Differentiation, 2003. **71**(1): p. 18-27.
187. Jukes, J.M., et al., *Endochondral bone tissue engineering using embryonic stem cells.* Proc Natl Acad Sci U S A, 2008. **105**(19): p. 6840-5.
188. Villa-Diaz, L.G., et al., *Derivation of mesenchymal stem cells from human induced pluripotent stem cells cultured on synthetic substrates.* Stem Cells, 2012. **30**(6): p. 1174-81.
189. Lou, X., *Induced Pluripotent Stem Cells as a new Strategy for Osteogenesis and Bone Regeneration.* Stem Cell Rev, 2015. **11**(4): p. 645-51.
190. Hwang, N.S., et al., *In vivo commitment and functional tissue regeneration using human embryonic stem cell-derived mesenchymal cells.* Proc Natl Acad Sci U S A, 2008. **105**(52): p. 20641-6.
191. Yamashita, A., et al., *Cartilage tissue engineering identifies abnormal human induced pluripotent stem cells.* Sci Rep, 2013. **3**: p. 1978.
192. Kino-Oka, M., et al., *Subculture of chondrocytes on a collagen type I-coated substrate with suppressed cellular dedifferentiation.* Tissue Eng, 2005. **11**(3-4): p. 597-608.
193. Farrell, E., et al., *In-vivo generation of bone via endochondral ossification by in-vitro chondrogenic priming of adult human and rat mesenchymal stem cells.* BMC Musculoskelet Disord, 2011. **12**: p. 31.
194. Saitta, B., et al., *Patient-derived skeletal dysplasia induced pluripotent stem cells display abnormal chondrogenic marker expression and regulation by BMP2 and TGFbeta1.* Stem Cells Dev, 2014. **23**(13): p. 1464-78.

CHAPTER 2

Osteogenic differentiation capability of induced pluripotent stem cells isolated from mucopolysaccharidosis type I patients (Hurler syndrome) through the generation of mesenchymal stromal cells

Anna Montagna[1], Ludovica Santi[1], Francesca Gatto[1], Lucia Cardinale[1], Pietro G. Mazzara[2], Cinzia Cancellieri[2], Catherine M. Verfaillie[3], Vania Broccoli[2], Andrea Biondi[4], Marta Serafini[1]

[1]Dulbecco Telethon Institute at Centro Ricerca M. Tettamanti, Department of Paediatrics, University of Milano-Bicocca, San Gerardo Hospital, via Pergolesi, 33, 20900, Monza, MB, Italy.

[2]Stem Cells and Neurogenesis Unit, Division of Neuroscience, DIBIT H San Raffaele, 20132 Milan, Italy.

[3]Department of Development and Regeneration, Stem Cell Biology and Embryology, KU Leuven, Leuven, Belgium.

[4]Centro Ricerca M. Tettamanti, Department of Paediatrics, University of Milano-Bicocca, Via Pergolesi, 33, Monza, 20900, Italy.

*Please address correspondence to: anna.montagna87@gmail.com

Manuscript in preparation

Abstract

Bone abnormalities, known as *dysostosis multiplex*, are one of the major manifestation of mucopolysaccharidosis type I Hurler syndrome (MPS IH) and represent a real, clinical burden for these patients. Complex cellular and molecular mechanisms underlie the patient clinical symptoms but they are still poorly understood. Induced pluripotent stem cells (iPSCs) represent a useful tool to elucidate these mechanisms, due to their high proliferation capability in culture, the possibility to generate patient- specific cell types and, mostly, to their ability to mimic development. We thus proposed a standardized osteogenic differentiation protocol for healthy donor (HD)-iPSCs, through the intermediate generation of *bona-fide* mesenchymal stem cells (hereafter named MSC-like cells). Consequently, we generated and characterized MPS MSC-like cells and MPS-derived osteoblasts (MPS-OBs) to elucidate their role in osteogenesis. Patient-derived stromal cells exhibited a similar expression of typical MSCs surface markers as HD MSC-like cells, whereas the kinetic of growth was significantly different between the two groups. Interestingly, MPS-OBs were obtained but the expression level of key osteogenic markers revealed an altered differentiation process. Additionally, we initially investigated the involvement of MPS MSCs-like cells and MPS-OBs in osteoclastogenesis. MPS MSCs-like cells displayed increased capacity to produce RANKL compared to HD.

Overall, we observed that a compromised phenotype was already evident at early pathological stage.

Introduction

Mucopolysaccharidosis type I (MPS I) is an autosomal recessive metabolic disorder caused by mutations in the IDUA gene, leading to inactivity of the lysosomal enzyme α-L-iduronidase (IDUA). This causes a progressive intracellular accumulation of non-metabolized glycosaminoglycans (GAGs), in particular dermatan and heparan-sulfate [1, 2]. This accumulation disrupts cell functions and gives rise to multiorgan dysfunction. Moreover, MPS I is a highly heterogeneous disorder with a wide spectrum of clinical manifestations. MPS I Hurler syndrome (MPS IH) is the most severe form of the pathology, affecting approximately 50% of all patients with MPS. The condition is marked by hepatosplenomegaly, obstructive airway disease complicated by respiratory infections, cardiac failure, and progressive mental retardation. The array of musculoskeletal abnormalities observed in Hurler syndrome is known as *dysostosis multiplex*, which is distinctive of these patients. These abnormalities arise from a disarray of skeletal remodelling, disordered endochondral and intramembranous ossification, and infiltration of GAGs into ligaments, tendons, joint capsules, and other soft tissue structures. This leads most often to gibbus deformity, prominent sternum, bulging forehead, slowing of physical growth, joint contractures, kyphoscoliosis and subluxation of the hip joints, and underlies the typical dwarfism and gargoyle-like features [3]. Enzyme replace therapy (ERT), hematopoietic stem cell transplantation (HSCT), gene therapy and anti-inflammatory drug administration for intervene in bone disease progression are not perfect and palliative means. In order to address these unmet medical needs a

clearer understanding of skeletal and connective tissue disease pathogenesis is required. Historically, the pathogenesis of the mucopolysaccharidoses has been assumed to directly relate to progressive storage of GAGs. It is now clear that more complex pathogenic mechanisms underlie patients' clinical symptoms [4].

Compare to other cells sources, including mesenchymal stem cells (MSCs), induced pluripotent stem cells (iPSCs) represent a useful tool to achieve this purpose, due to their high proliferation capability in culture and, mostly, to their ability to mimic development. Moreover, patient-specific iPSCs allows us to reproduce the pathological phenotype *in vitro*, creating a perfect disease model. Thus, they demonstrate great potential for investigating the osteogenic differentiation process at early stages. This is a key point because it has been demonstrated that disruption of extra-cellular matrix components, that lead to biomechanically compromised chondro-osseous tissue, already occurred in MPS I embryos and postnatal mice [4]. This alteration could be the onset of the musculoskeletal disorders that appear during the life of the patient. Moreover, prenatal lysosomal GAGs storage in chondrocytes has been demonstrated in MPS patients and animal models [5, 6]. The importance in the understanding of the early events that occur during osteogenesis is highlight by our recent study demonstrated superior long-term clinical outcome in bone structure for MPS I mice when neonatal HSCT was performed [7]. Other works support this observations[8, 9]. The more we are able to understand early events that occur during the pathology, the sooner we can intervene and ameliorate the severe osteogenic phenotype.

Bone remodelling also plays a major role in the maintenance of the skeleton's mechanical integrity and a well-coordinated balance between bone formation (by osteoblast, OBs) and bone resorption (by osteoclasts) is required. Receptor activator of nuclear factor-κB (RANK), osteoprotegerin (OPG) and the RANK ligand (RANKL) have been identified as key partners of a system that directly regulates osteoclast differentiation and they are mainly produced by MSCs and OBs [10]. In particular, RANKL binds to RANK present on osteoclast precursors, inducing their differentiation into osteoclasts. OPG is a decoy receptor, which acts by neutralizing and preventing RANKL from binding to RANK, resulting in decreased osteoclast recruitment. Alterations in the balance of the OPG/RANK/RANKL molecular triad have been associated with numerous bone diseases [11]. In the present study, healthy donor (HD)-iPSCs were adopted to design a standardized osteogenic differentiation protocol *via* generation of *bona fide* MSC-like cells. MPS MSC-like cells and OBs were then investigated for their role in osteogenesis and bone remodeling.

Materials and Methods

Fibroblasts isolation from MPS IH patients

This study had ethical approval and patient consent. 3mm skin biopsies were collected from 3 MPS IH pediatric patients. Fibroblasts were isolated as follow: briefly, the biopsy was washed in PBS (Invitrogen, San Giuliano Milanese, IT), cut in thin fragments with surgical scissors and transferred in a T25 cm^2 flask (Nunc, Rochester, NY) with standard fibroblast culture (SFC) medium. SFC medium contains RPMI (Gibco, Grand Island, NY), 15% of FBS (Biosera, East Sussex, UK), 1% L-glutamine (Gibco) and 1% Penicillin/Streptomycin (Gibco). After 5 days of culture, the medium was replaced and the remaining floating fragments were removed from the culture. The fibroblasts attached to the flask were expanded in SFC medium until they reached 90% confluence. Cultures were maintained at 37°C in a humidified atmosphere of 5% CO_2.

Generation and culture of human iPSCs from MPS IH fibroblasts

Moloney murine leukemia virus–derived vectors, each containing the coding sequences of 1 of the 4 human genes OCT4, SOX2, c-Myc, and KLF4, and the corresponding viral particles were generated by Vectalys (Toulouse, France) and used to infect the fibroblasts as previously described [12]. On day 1, 10^5 fibroblasts were plated in each well of 6-well plates in SFC medium. The following day the cells were transduced with the four viruses at a multiplicity of infection of 10 for each virus, for 24 hours. On day 3, the cells were washed 3 times in PBS (Gibco) and then grown in medium containing FBS for 3

additional days. On day 7, the cells were mechanically transferred onto mitomycin-treated mouse embryonic fibroblasts (iMEF, GlobalStem, Rockville, MD) and then grown for 2 additional days in medium containing FBS. After day 9, the cells were grown in standard human embryonic stem cell (hESC) culture medium consisted of 20% Knockout-SR (Gibco); DMEM/F12 (Gibco); 1 mM L-Glutamine (Euroclone); 10 U/mL penicillin-streptomycin (Euroclone), 1X nonessential amino acids (Gibco); 0,1 mM β-mercaptoethanol (Gibco) and + 4 ng/ml of basic fibroblast growth factor (bFGF) (Gibco). The first iPS colonies appeared 15-18 days after plaiting and they could be picked 5-8 days later. Individual colonies were picked and transferred into a single well of 12-well plates containing iMEF feeders in hES medium. The resulting colonies were then expanded using enzymatic dissociation: cells were harvested using a solution of 1 mg/ml of dispase II and collagenase type IV (ratio 1:1) (Gibco).

3 different iPSCs lines were obtained from the 3 MPS IH patients (MPS IH-iPSCs) and we isolated approximately 10 different cell lines from each clone.

Immunofluorescence

MPS-iPSCs were fixed for 20 minutes at 4°C in 4% paraformaldehyde and then washed three times in PBS. Cells were incubated 15 minutes at RT with PBS/Tryton 0.1%. Cells were incubated for 30 minutes at room temperature in PBS containing 5% donkey serum (Jackson ImmunoResearch) and subsequently incubated overnight at 4°C with primary antibody diluted in Dako Antibody Diluent. For the dilutions of primary antibodies see Table S1. Cells were then washed three times

in PBS and incubated with Hoechst 33342 and secondary antibody anti-mouse IgG or anti-rabbit IgG (Invitrogen), for 30 minutes at RT, in Dako Antibody Diluent. Unbound secondary antibody was removed by three washes in PBS. Slides were mounted with ProLong Gold (Lifetechnologies). For HD-iPSCs immunofluorescence refer to Dr. Broccoli's Laboratory.

Teratoma formation

Human iPSCs were harvested with the enzymatic treatment immediately prior to implantation, and approximately $2x10^6$ cells were resuspended in mixture of PBS and Matrigel (BD Biosciences, Buccinasco, IT) (ratio 1:1) in a final volume of 400 µL. The cell suspensions were inoculated subcutaneously into the dorsal flank of 8 week-old Balb/c-Rag2 $^{-/-}\gamma C^{-/-}$ male mice. Within eight weeks after the injection, tumors were surgically dissected from the mice. Samples were fixed in PBS containing 4% formaldehyde and embedded in paraffin. Serially sections of 4 µm were stained with hematoxylineosin and characterized.

***In vitro* differentiation of human iPSCs into three germ layers**

iPSCs were then collected were harvested using a solution of 1 mg/ml of dispase II and collagenase type IV (ratio 1:1) (Gibco) and suspended as clumps in EB medium (20% Knockout-SR (Gibco); DMEM/F12 (Gibco); 1 mM L-Glutamine (Euroclone); 10 U/mL penicillin-streptomycin (Euroclone), 1X nonessential amino acids (Gibco); 0,1 mM β-mercaptoethanol (Gibco)). EBs were cultured for 7 days on Ultra low adherent dish (CC3262 Corning). The medium was changed every

day. Next, EBs were seeded onto gelatin-coated dishes in EB medium for 9 days. On days 0 and 9, transcript levels for the following genes were analysed by means of q-RTPCR: paired box 6 (PAX6), alpha fetoprotein (AFP), smooth muscle (SM22), fetal liver kinase (FLK), POU class 5 homeobox 1 (OCT4), SRY-box 2 (SOX2) and Nanog homeobox (NANOG).

Mutation analysis of the IDUA gene

Genomic DNA was extracted from human iPSCs using the Wizard Genomic DNA Purification kit (Promega, Madison, WI). Mutation analysis of the IDUA gene was limited to confirm the presence of mutations identified at diagnosis: p.P496R for patient 1(exon 10); p.Q70X (exon 2) and p.P496R for patient 2; p.W402X (exon 9) for patient 3. The exons 2, 9 and 10 were amplified and sequenced using intronic primers designed for both amplification and sequencing. Exons 2 was amplified in 25µl containing 100 ng of genomic DNA, Buffer 1X with MgCl2 1.5mM, dNTP mix 200mM, 15pmol of each primer, GCRICH solution 1X and 0.5U of the proofreading PWO SuperYeld DNA Polymerase (ROCHE, Monza, Italy). Exons 9-10 coamplification was carried out in 25µl volume containing 100 ng of genomic DNA, Buffer 1X with MgCl2 1.5mM, dNTP mix 200mM, 15pmol of each primer and 0.5U of the GoTaq DNA Polymerase (Promega). Cycling conditions were: initial denaturation at 96°C for 5 min, 30 cycles at the following conditions: denaturation at 96°C for 1 min, annealing at 67°C for exon 2, 65°C for exon 4 and 63°C for exons 9-10 for 1 min, extension at 72°C for 1 min, followed by final extension at 72°C for 7 min. PCR products were purified using an enzymatic reaction

containing 5U of Exonuclease I (Celbio, Pero, Italy) and 1U of Alkaline Phosphatase (Promega) using the following conditions: 15 min at 37°C followed by 15 min at 80°C. Purified fragments were sequenced in both forward and reverse directions using BigDye v3.1 terminator technology and then purified with the BigDye XTerminator Purification Kit. Sequence reactions were carried out and purified according to the manufacturer's instructions and were analyzed on an ABI Prism 3130 Avant Automatic Sequencer (Applied Biosystems, Foster City, CA).

α-L-iduronidase enzyme assay

Cells were resuspended in 150 mM NaCl and freeze-thawed 6 times. Protein extracts were assayed for total protein content using the Lowry assay. 5 µg of protein was added, in triplicate, to a solution containing 8 mM D-Saccharic acid 1,4-lactone and 2 mM 4-methylumbelliferyl-a-L-iduronide in 0.1 M sodium formate buffer, pH 3.2. Samples were incubated for 1 hr at 37°C before stopping the reaction by adding 1 ml of 0.5 M carbonate buffer, pH 10.7. The cleaved substrate was quantified on a Perkin Elmer fluorimeter. The enzyme activity was calculated from a reference curve obtained by using 4-methylumbelliferone and was expressed as nmoles/hr/mg.

Quantification of GAGs

Human iPSCs were digested with proteinase K (0.5 mg/ml in 100 mM K2HPO4 pH 8.0; 1 ml/tube) at 56º C overnight. After digestion, proteinase K was inactivated at 90º C for 10 min. Debris was removed by centrifugation (5000g, 10 min, 4º C) and 100 ul cleared lysate used for sulfated GAGs quantification in the Blyscan Assay (Biocolor Ltd.,

UK). GAGs levels were normalized by the DNA content of each sample, and expressed as GAGs (ug)/ DNA (ug).

Proliferation kinetics of MSC-like cells

The cumulative population doubling (PD) levels at each sub-cultivation were calculated from the cell count by use of the equation: $PD_n = PD_{n\,1} + [\log (C_1/C_0)] \log 2$, wherein C_0= cells number initially seeded and C_1= cells number harvested. Ten PDs were count for each MSC line. Each PD was done in triplicate. The living cell count was performed in a hemocytometer by means of trypan blue dye exclusion (Sigma-Aldrich)

Induction of iPSCs to MSC-like cells

For EB formation, iPSC colonies were harvested by treating with 1 mg/ml of dispase II and collagenase type IV (ratio 1:1) (Gibco) and suspended as clumps in EB medium. EBs were cultured for 7 days on Ultra low adherent dish (CC3262 Corning). The medium was changed every day. After 7 days as a suspension culture, EBs were transferred to gelatin-coated dishes and cultivated until they reached confluency (10 days) in mesenchymal induction medium consisting of MEM α, GlutaMAX (Lifetechnologies), 10% FBS (Biosera), 100 µM L-Ascorbic acid 2-phosphate (Sigma-Aldrich), 1 mM Sodium Pyruvate (Gibco), 50 U/mL penicillin, 50 µ/mL streptomycin (Euroclone), 1X non-essential amino and 10 mM of HEPES solution (Sigma). EBs and cells sprouted from EBs were harvested and dissociated with 0.25% trypsin/EDTA (Euroclone). Dissociated cells were passed through a 70-µm cell strainer to remove cell aggregates and cultivated in monolayers

at $7x10^3$ cells/cm^2 in mesenchymal induction medium, onto gelatin-coated dishes. When cells reached confluency, serial passaging were performed to obtain MSC-like cells. On days 0 transcript levels for the following genes were analysed by means of quantitative real-time polymerase chain reaction (q-RT-PCR): receptor activator for nuclear factor-κB ligand (RANKL) and osteoprotegerin (OPG).

Adipogenic differentiation

For adipogenic differentiation, MSC-like cells were seeded at a density of $2x10^4$ cells/cm^2 in mesenchymal induction medium. After 24 h, medium was switched to adipogenic induction medium consisting of DMEM high glucose (Invitrogen) supplemented with 10% FBS (Biosera), 1 µmol/L DEX (Sigma-Aldrich), 1 µmol/L indomethacin (Invitrogen), 500 µmol/L 3-isobutyl-1-methylxantine (Sigma-Aldrich) and 10 µg/mL human recombinant insulin (Sigma-Aldrich). For the detection of adipogenic differentiation, intracellular lipid droplets were stained with the use of Oil Red O solution (Sigma-Aldrich) on day 21 of differentiation.

Chondrogenic differentiation

MSC-like cells were seeded in a 15-mL conical tube at different cell density: $3x10^5$, $6x10^5$, $1x10^6$,$3x10^6$ and re-suspended in chondrogenic differentiation medium. CM1 consisting of DMEM high glucose (Invitrogen) supplemented with 100 ug/mL ITS (Collaborative Biomedical Products, Bedford, MA, USA), 1 mM/L sodium pyruvate (Lifetech), 50 µg/mL ascorbic acid 2-phosphate (Sigma-Aldrich), 100 µMl/L DEX (Sigma-Aldrich) and 10 ng/mL transforming growth

factor (TGF)-β1 (R and D). CM2 consisting of DMEM high glucose (Invitrogen) supplemented with 1X ITS+ Premix (Corning), 100 µM/L ascorbic acid 2-phosphate (Sigma-Aldrich), 50 U/mL penicillin, 50 µ/mL streptomycin (Euroclone), 2mM L-glutamine, 0,125% BSA (Sigma-Aldrich) and 10 ng/mL transforming growth factor (TGF)-β1 (R and D). Cells were grown as pellets for 3,4,5 or 6 weeks at 37°C, 5% CO_2. For immunostaining experiments, cartilage pellets were fixed in 4% formaldehyde in phosphate buffer, processed for paraffin embedding and sectioned serially. Five-micron-thick sections were stained with hematoxylin and eosin (Sigma-Aldrich).

Osteogenic differentiation

MSC-like cells were seeded at a density of $4x10^3$ cells/cm^2 in mesenchymal induction medium. After 24 h, medium was switched to osteogenic induction medium consisting of GlutaMAX (Lifetechnologies), 5% FBS (Biosera), 100 µM L-Ascorbic acid 2-phosphate (Sigma-Aldrich), 1 mM Sodium Pyruvate (Gibco), 50 U/mL penicillin, 50 µ/mL streptomycin (Euroclone), 2 mM L-Glutamine and 2mM inorganic phosphate (Sigma). The osteogenic differentiation was assessed through the use of Alizarin Red S (SigmaAldrich) staining on day 21 of differentiation. On days 0, 7, 14 and 21, transcript levels for the following genes were analyzed by means of q-RTPCR: alkaline phosphatase (ALPL), type I collagen (COL1A2), osteonectin (OTN), runt-related transcription factor 2 (RUNX2), osteopontin (OPN), osteocalcin (OTC), receptor activator for nuclear factor-κB ligand (RANKL) and osteoprotegerin (OPG).

Flow cytometric analysis

MSC-like cells were labelled with phycoerythrin-conjugated or fluorescein isothiocyanate-conjugated antibodies against CD90 (clone 5E10; eBioscience), CD73 (clone AD2; BD Biosciences), CD105 (clone SN6; eBioscience), CD146 (clone P1H12; BD Biosciences), TRA-1-60 (clone TRA-1-60; Millipore) Isotype antibodies were used as control. Flow cytometric analysis was performed on 20,000 events with the use of a FACS Canto II cytometer, and data were analysed with the use of Diva software (BD Biosciences) and FlowJo software (LLC).

RNA isolation and q-RT-PCR

Total RNA was extracted with the use of TRIZOL reagent (Invitrogen), following the manufacturer's protocol; 1 μg of RNA was then reverse-transcribed with the use of a SuperScript II Reverse Transcriptase kit (Invitrogen) in the presence of random hexamers. Quantitative real-time polymerase chain reaction assays were performed in triplicate on an ABI 7900 Real-Time PCR system thermal cycler with the qPCR Mastermix (Applied BiosystemsInvitrogen). All TaqMan gene expression assays were provided by Applied Biosystems (Table S2). For primers sequence of PAX6, AFP, SM22, FLK, OCT4, SOX2 and NANOG refer to Dr. C. Verfaillie.

After having verified the stable expression of GAPDH, this gene was included as endogenous control. The level of each target gene was normalized to GAPDH levels and expressed relative to the control culture levels or to a specific time point (DDCt method). Graphs represent the level of the interested gene normalized to GAPDH (relative expression to GAPDH).

Results

Generation and characterization of iPSC lines from HD and MPS IH fibroblasts

Three MPS-iPSC lines were previously generated in our laboratory from skin biopsies of three MPS IH pediatric patients, by overexpressing the four transcription factors c-Myc, Oct-4, Klf-4 and Sox2 (Gatto et al, manuscript in preparation).

For comparative studies, we adopted a healthy donor-derived iPSC line (HD-iPSCs), kindly provided by Dr. V. Broccoli (Stem Cells and Neurogenesis Unit, San Raffaele Scientific Institute, Milan, Italy).

The generated lines had the typical iPSCs morphology with round-colony shape, consisting of cells with scant cytoplasm and large nucleoli (Fig.1A). MPS- and HD-iPSCs were characterized for pluripotency: q-RT-PCR assay revealed that both lines expressed Oct4, Sox2 and Nanog even if at different level (Fig.1B). The expression of pluripotent genes was also confirmed by immunofluorescence at the protein level, by which we confirmed the presence of the pluripotency genes Oct4 and Nanog, as also as the presence of the cell surface markers TRA-1-60 and SSEA on both iPSC lines (Fig.1C). TRA-1-60 antigen was even quantified by flow cytometry analysis, showing high expression level in HD-iPSCs and MPS IH-iPSCs (Fig.1D). The number of transgene copies inserted in the genome of the isolated MPS-iPSCs and silencing of the exogenous transgenes were performed. (Fig.1S-A, B).

MPS-iPSCs generated teratomas after subcutaneous injection into immunodeficient mice and retained the capacity to differentiate into

cell types of the three germ layers (Fig. 2A). EBs formation method was used to assess iPSCs capacity to originate cells differently committed *in vitro* (Fig. 2B). Genes of the neuroectoderm (Pax6), of the primitive endoderm (AFP) and of the mesoderm (SM22, FLK) were upregulated at day 16 of EB culture, compared to day 0, with the exception of FLK. The gene expression trend was similar in MPS-iPSCs and HD-iPSCs. As expected, during the differentiation process, the pluripotency genes decreased their expression.

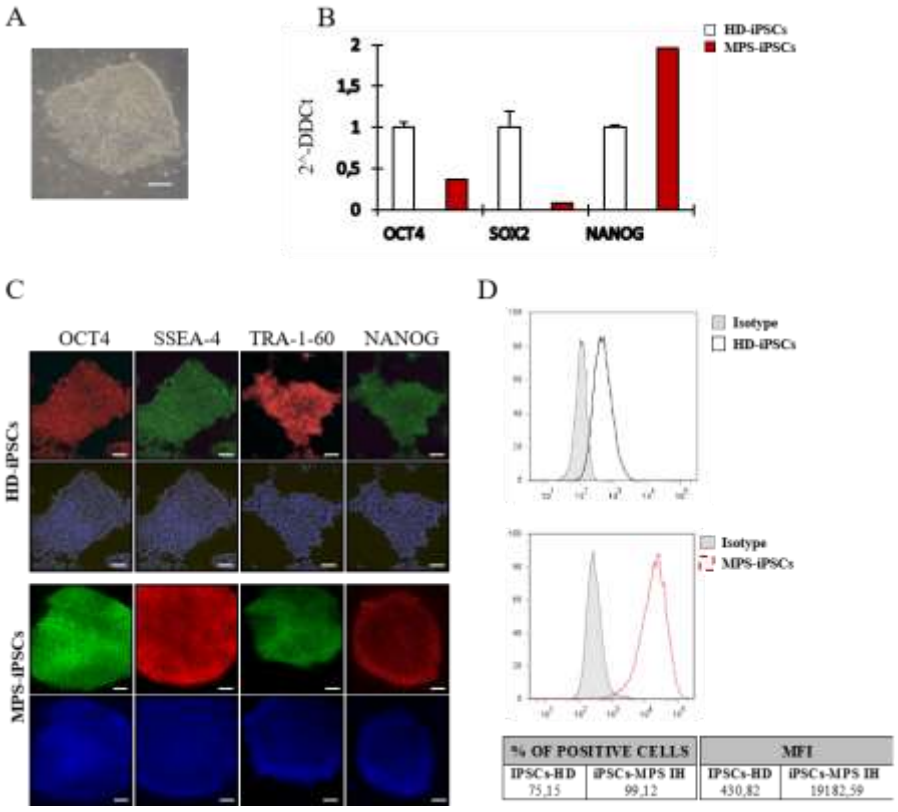

Fig. 1: Pluripotency of HD and MPS-iPSCs. (A) Morphology of iPSCs clone. **(B)** Gene expression of OCT4, SOX2, NANOG normalised to GAPDH and relative to HD-iPSCs. Data are presented as means ± SD. **(C)** Immunostaining of pluripotency markers OCT4, SSEA-4, TRA-1-60 and NANOG in HD-iPSCs and MPS-iPSCs.

DAPI stained nuclei blue fluorescence. **(D)** FACS staining for cell surface marker TRA-1-60 in HD-iPSCs and MPS-iPSCs. Filled histogram show isotype control and open histogram show tested sample. Percentage (%) of positive cells and mean fluorescence intensity (MFI) are shown. Data are representative of patient #2. Scale bar = 100 µm

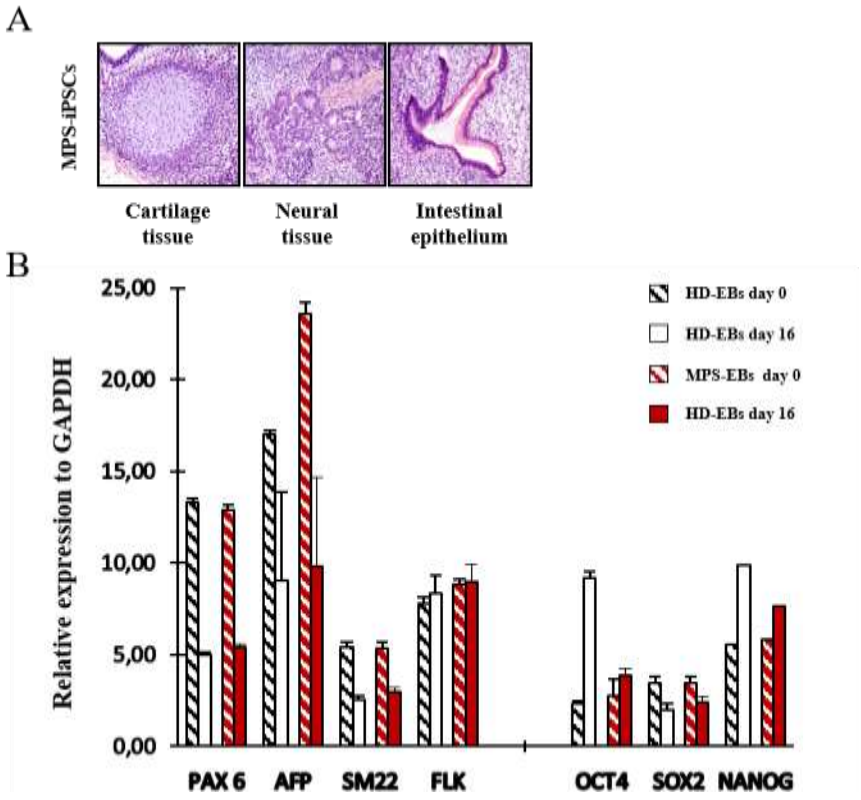

Fig. 2: Differentiation potential *in vivo* and *in vitro* of HD and MPS-iPSCs

(A) Teratoma formation of MPS-iPSCs in immunodeficient mice. This experiment was repeated two times. **(B)** Embryoid bodies formation. Gene expression normalised to GAPDH for HD-iPSCs and MPS-iPSCs, at day 0 and 16. Graph represent mean ± SD of three independent experiments. Data are representative of patient #2.

Genotypic and phenotypic characterization of MPS IH-iPSCs

We certified that MPS-iPSCs maintained the affected phenotype in terms of gene mutations, IDUA enzyme activity and GAGs accumulation within the cells.

Gene sequencing analysis revealed the same mutations that were detected in the skin biopsies of the MPS IH patients at the time of diagnosis (Fig 3A). Patient 1 (Pt1) was homozygote for the p.P496R, a missense mutation in exon 10 (c.1487C>G) resulted in a non-conserved aminoacid change (Proline > Arginine) at position 496 of protein chain. Patient 2 (Pt 2) revealed a compound heterozygosity for p.Q70X and p.P496R mutations. The p.Q70X mutation (c.208C>T) in exon 2 caused a premature STOP codon at position 70 of protein chain. Patient 3 (Pt 3) was homozygote for the p.W402X mutation in exon 9 (c.1205G>A), which introduced a premature STOP codon at position 402 of protein chain.

IDUA enzymatic activity was significantly lower in MPS-iPSC lines compared to HD-iPSCs (median HD-iPSCs 13,60 nmol/h/mg, range from 4,85 to 54,10 *vs.* median MPS-iPSCs 1,15 nmol/h/mg, range from 0 to 11,30, p = 0.0043) (Fig. 3B, left panel). As expected, GAGs cellular content was significantly higher in patients than in HD (median HD-iPSCs 0,076 µg/µg DNA, range from 0 to 0,189 *vs.* median MPS -iPSCs 0,332 µg/µg DNA, range from 0,265 to 0,49, p = 0,0011) (Fig. 3B, right panel).

A

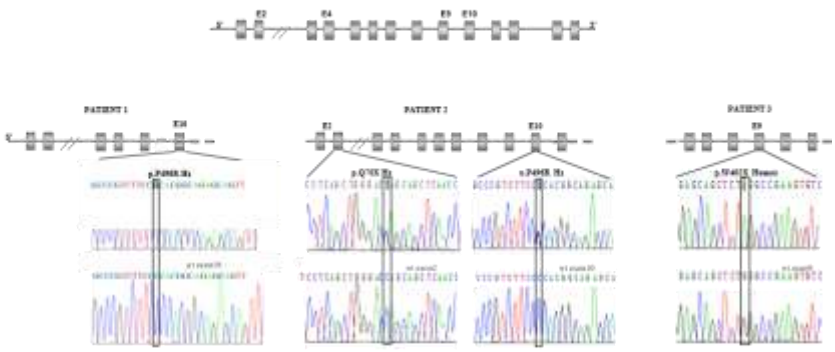

Patient	Genotype	Phenotype
1	p.P496R/p.P496R	Hurler
2	Q70X / P496R	Hurler
3	W402X / W402X	Hurler

B

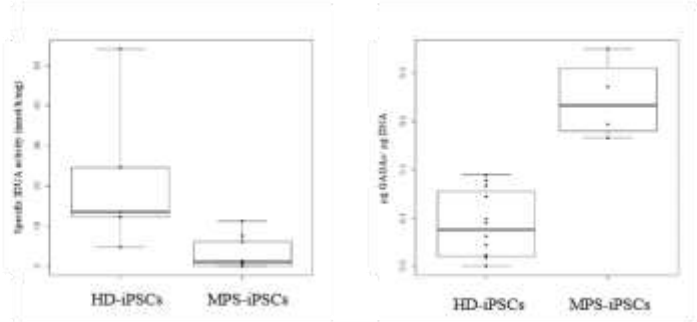

Fig. 3: Genotypic and phenotypic characterization of MPS IH-iPSCs. (A) Electroferograms show the position of the mutations in MPS-iPSCs (upper panel) compared with wild-type (lower panel). In the table are reported the genotypes of the three patients. **(B)** IDUA enzymatic activity (left panel) and GAGs accumulation level (right panel) of MPS-iPSCs compare to HD-iPSCs. Boxplot explanation: upper horizontal line of box represents the 75th percentile, the lower horizontal line of box represents the 25th percentile, the horizontal bar within the box represents the median, the dots within box represents the mean, and vertical lines outside the box represent the minimum and maximum. *P* value was calculated using Wilcoxon nonparametric

unpaired test, 1 side. For IDUA activity, the final values are the mean of 5 samples for HD and 10 samples for the three MPS-iPSC patient lines. For GAGs content, the final values are the mean of twelve samples for HD and four samples for the three MPS-iPSC patient lines.

Generation of mesenchymal stromal cells from HD-iPSCs

For this study, one HD-iPSCs and two MPS-iPSCs lines, derived from patient 1 and 2 (PT-1; PT-2), were used.

In order to recapitulate the osteogenic process, we designed a reliable, multi-step differentiation protocol, including a transition step through *bona fide* "MSC-like" cells, which are known to be osteoblast precursors. We first standardized the protocol on HD-iPSCs. Briefly, the process included: EBs formation, cell outgrowth from EBs, monolayer culture of sprouted cells from EBs, and a series of passages in culture until cells reach a fibroblast-like morphology (Fig.4 A).

HD-iPSCs were grown as a suspension culture for 1 week onto low-adherent plates to allow EBs formation (Fig.4 B-II). Then, they were transferred on gelatin-coated dishes for 10 days to permit EBs attachment. Starting from day 2 sprouted cells from EB were observed and they reached almost 100% confluency in 10 days, looking as a heterogeneous population of cells (Fig. 4B-III). Subsequently, cells were cultured in mesenchymal induction medium until the generation of MSC-like cells. We included monolayer culture steps (from P_0 to P_n) to deplete residual undifferentiated cells and to purify the MSCs-like population. Unlike undifferentiated cells, these cells are able to attach to regular culture dishes and to proliferate in the MSCs growth medium. The first passage (P_0) was extremely important for the outcome of the experiment. Indeed, for this step gelatin coated-dishes were used to

permit the adherence of cells presenting a transitional phenotype and not completely able to be attached to the dish. The initial density was also crucial. We tried a range of seeding density and define that a concentration of 7.000 cells/cm^2 was ideal for a 7 days culture as monolayer (data not shown). When cells were seeded at lower density, they tend to acquire a large, flattened and irregular morphology and to undergo mitotic arrest. On the contrary, higher cell concentration generated clusters (data not shown). Since the first step of monolayer culture, iPSCs undergo significant morphological changes: from round-shaped single cells organised in colonies to a monolayer culture of dermal/fibroblast-like morphology (Fig. 4B I and IV). At P_0, the cells still exhibited a heterogeneous morphology (Fig. 4B IV). In subsequent passages, there was an increase in the proportion of cells with a fibroblast-like morphology and by P_4 cells exhibited a more uniform morphology (Fig. 4 B-V, VI, VII) similar to BM-MSCs (Fig. 4B-VIII).

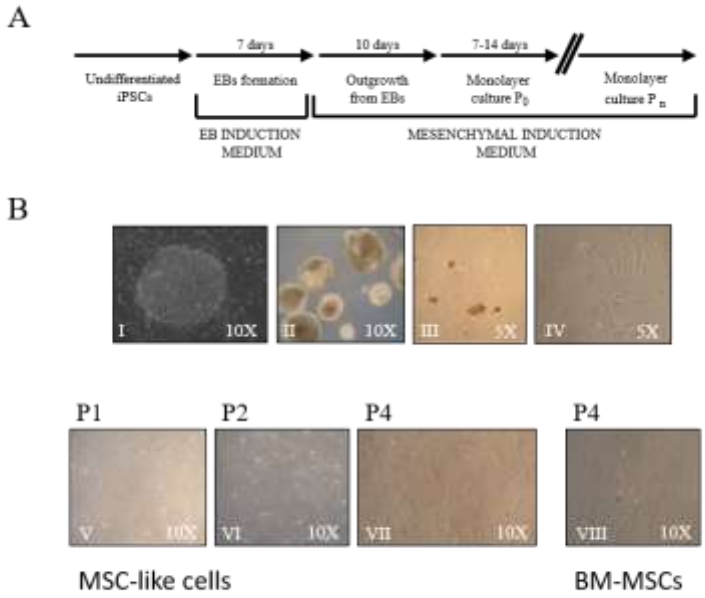

Fig. 4: (A) Schematic protocol for the differentiation of HD and MPS-iPSCs into MSC-like cells. **(B)** Representative images of the different steps of the differentiation protocol: EBs formation, cell outgrowth from EBs, monolayer culture steps from P_0-P_4.

Immunophenotype and proliferation capacity of MSC-like cells

To determine if the mesenchymal differentiation was accomplished, we first evaluated the expression of classical MSCs surface markers on HD-iPSCs, by flow cytometry. They resulted strongly positive for CD90 (99,9%), CD105 (99,9%), CD146 (95,7%), partially positive for MHC I (45,9%), and negative for MHC II. Of note, HD-iPSCs were slightly positive for a typical MSC marker CD73 (4,1%) (Fig. 5). Thus, we selected CD73 positivity as our marker for the appearance of MSC-like cells. The more the expression was increased, the more the cells were acquiring a mesenchymal-like phenotype. Due to the reduced initial number of differentiating cells, before performing the complete

phenotype panel already from P_0, we just looked at the expression of CD73, CD90 and TRA-1-60. CD90 was enrolled as positive control, while TRA-1-60 as negative one. An expression of $\geq$ 90% for CD73 was consider as our cut-off before proceeding with the complete phenotype characterization (Fig. 6A). At P_0 MSC-like cells did not express CD73, whereas CD90 was already 99,47%. By P_2, more than 99,3% of MSCs-like cells expressed CD73 marker and it remained until P_4. CD 90 expression maintained a similar expression level for all steps. For the entire period of culture, MSC-like cells were negative for the pluripotent marker TRA-1-60. CD105, CD146, MHC I and MHC II markers were then evaluated. (Fig. 6B). At P_3 MSC-like cells were highly positive for CD105, CD146, MHC I, while they were negative for MHC II. As the culture proceeded, the cell population increasingly expressed all the MSCs markers, reaching values comparable with BM-MSCs.

MSC-like cells were culture up to P16 without undergo senescence, as demonstrated by population doubling assay (Fig. 6C). They grew for an extensive period of time *in vitro* and presented strong resistance to freeze-thaw cycles (data not shown).

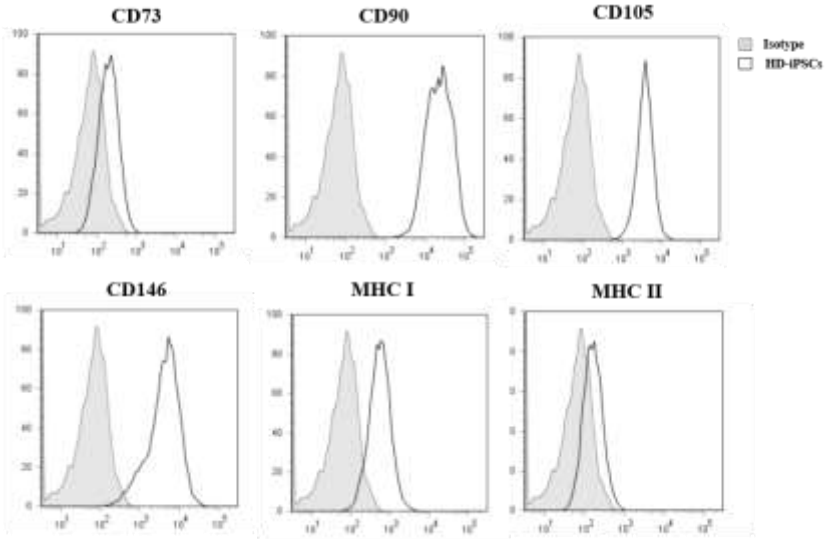

% OF POSITIVE CELLS					
CD 73	**CD90**	**CD105**	**CD146**	**MHC I**	**MHC II**
HD-iPSCs	HD-iPSCs	HD-iPSCs	HD-iPSCs	HD-iPSCs	HD-iPSCs
4,1	99,9	99,9	95,7	45,9	neg.

MFI					
CD 73	**CD90**	**CD105**	**CD146**	**MHC I**	**MHC II**
HD-iPSCs	HD-iPSCs	HD-iPSCs	HD-iPSCs	HD-iPSCs	HD-iPSCs
103	144662	2147	2512	303	78,8

Fig. 5: Immunophenotype of HD-iPSCs. FACS staining for MSCs cell surface markers in HD-iPSCs. Filled histogram show isotype control and open histogram show tested sample. Percentage (%) of positive cells and mean fluorescence intensity (MFI) are shown.

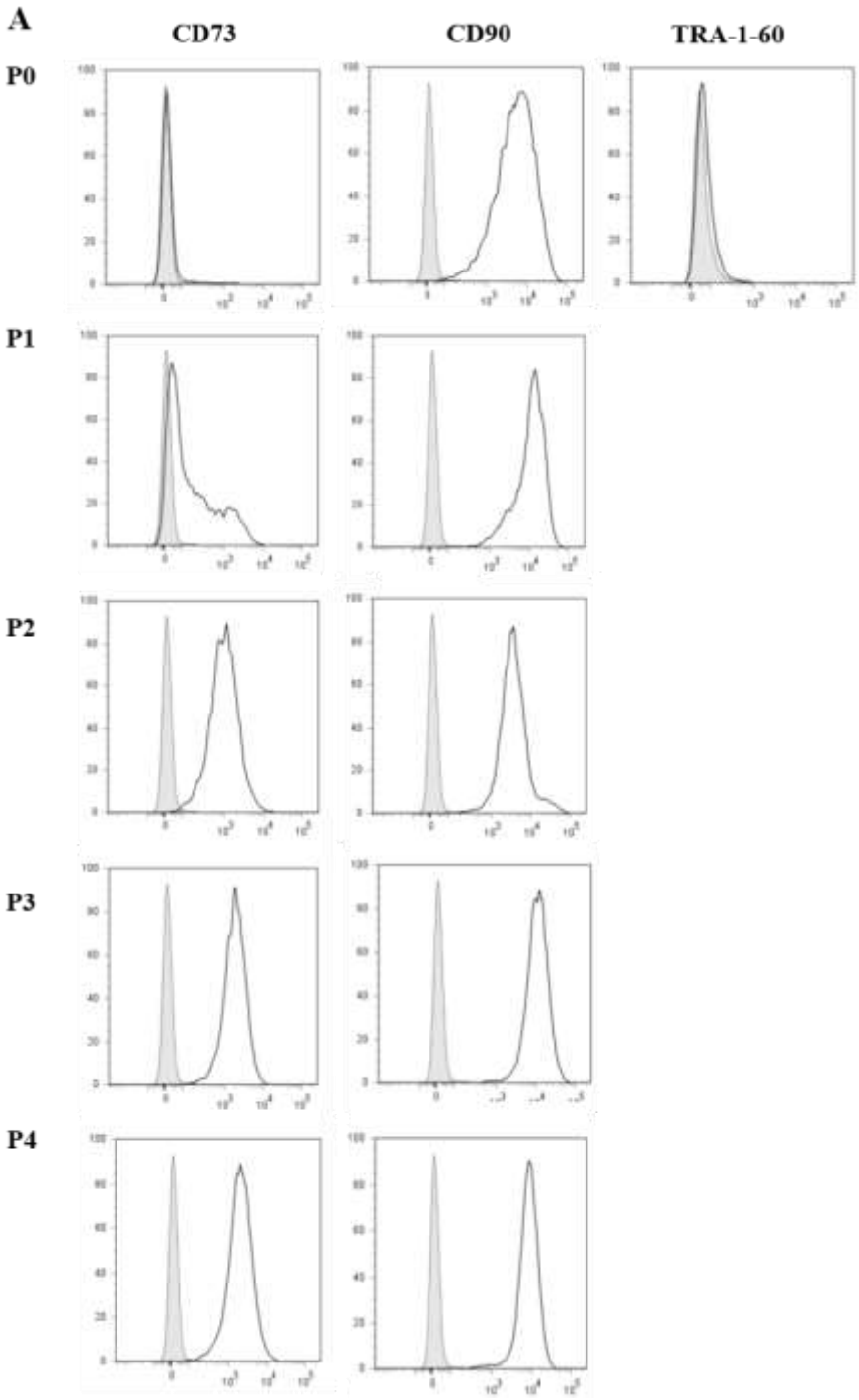
A
CD73
CD90
TRA-1-60
P0
P1
P2
P3
P4

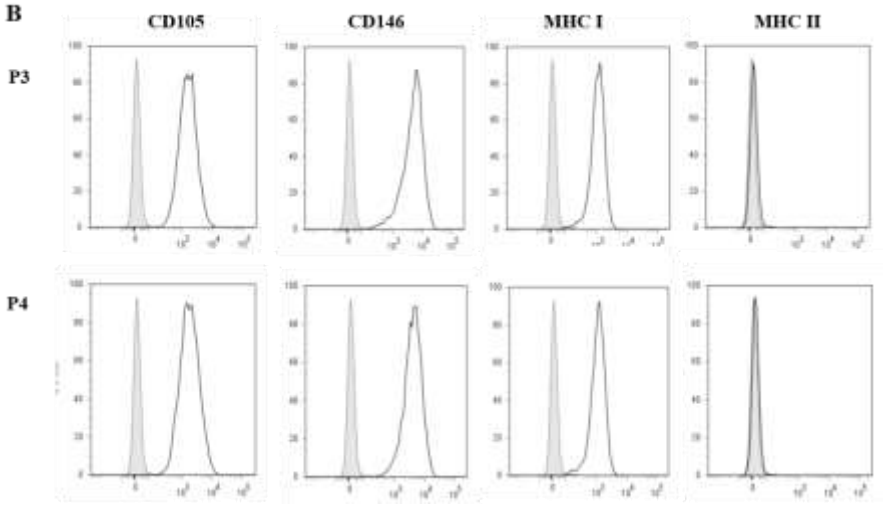

	% OF POSITIVE CELLS						
	CD 90	**CD 73**	**CD105**	**CD146**	**MHC I**	**MHC II**	**TRA-1-60**
	HD-iPSCs	HD-iPSCs	HD-iPSCs	HD-iPSCs	HD-iPSCs	HD-iPSCs	HD-iPSCs
P0	99,47	neg.					neg.
P1	99,96	51,27					neg.
P2	99,93	99,43					neg.
P3	99,85	99,67	99,99	99,72	99,21	neg.	neg.
P4	99,96	99,24	99,99	99,83	99,26	neg.	neg.

	MFI						
	CD 90	**CD 73**	**CD105**	**CD146**	**MHC I**	**MHC II**	**TRA-1-60**
	HD-iPSCs	HD-iPSCs	HD-iPSCs	HD-iPSCs	HD-iPSCs	HD-iPSCs	HD-iPSCs
P0	5089,11	neg.					neg.
P1	12031,86	99,46					neg.
P2	3467,33	964,76					neg.
P3	8475,05	1795,89	1480,01	4826,70	1049,52	neg.	neg.
P4	8142,94	1825,51	1709,29	3943,99	1085,65	neg.	neg.

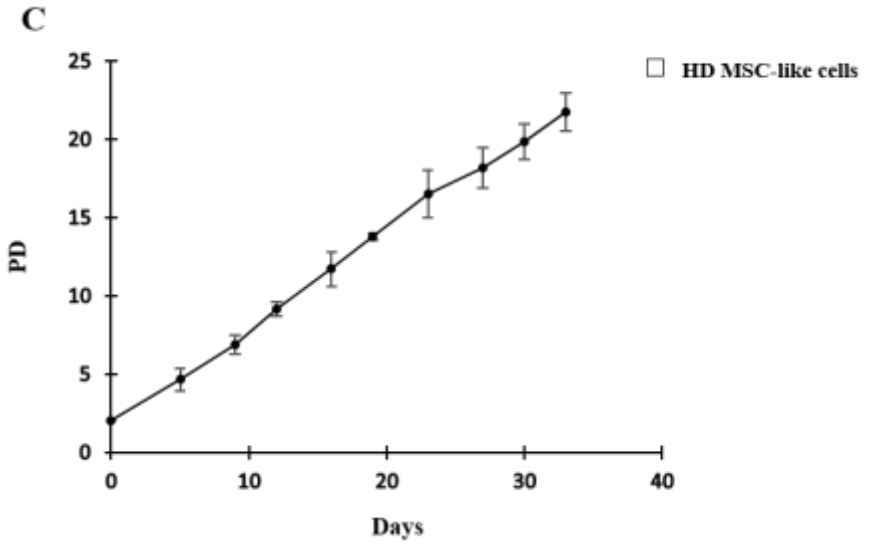

Fig. 6: Immunophenotype and proliferation capacity of HD MSC-like cells. (A) Immunostaining for CD73, CD90 and TRA-1-60 from P_0-P_4; and for CD105, CD146, MHC I, MHC II from P_3-P_4 **(B)**. Filled histogram show isotype control and open histogram show tested sample. Percentage (%) of positive cells and mean fluorescence intensity (MFI) are shown. **(C)** Expansion curve of HD MSC-like cells. Graph represent mean ± SD of three independent experiments.

Adipogenic and chondrogenic differentiation of MSC-like cells

Since one of the typical MSCs properties is their capacity to differentiate *in vitro* into cells of the mesoderm lineage, we assessed MSC-like cells for their ability to differentiate into adipocytes and chondroid pellets.

For adipogenic differentiation we tried different cell concentrations (data not shown) and defined a proper seeding density of $2x10^4$ cells/cm^2. The cells were induced to differentiate 24h after seeding by adipogenic induction medium and maintained in culture for 21 days. Intracytoplasmic lipid droplets were detected with oil red O staining.

After adipogenic induction, 71% of MSC-like cell lines (5 out of 7 samples analized) showed an adipogenic phenotype (Fig. 7A).

For chondrogenic differentiation we used a 3D pellet culture method standardised in our laboratory for BM-MSCs [13] and adapted for MSC-like cells. To determine the duration of the culture period, we incubated $3x10^5$ MSC-like cells in chondrogenic medium (CM1) enriched with TGF-β1, at different time points (21, 28, 34, or 42 days) (Fig. 7B). Histological section revealed that a prolonged culture in the induction medium caused enhanced necrosis within the pellets. A culture of either 21 and 28 days was optimal to preserve cell vitality and reduced necrosis. Moreover, the cell density used in this first set of experiments ($3x10^5$ cells), was too low because the pellets obtained were often excessively small to be analysed. Overall, we could detect only an initial chondrogenic differentiation. Thus, we designed a new set of experiments to determine the best cell density and to test if a CM optimized for iPSCs-derived MSCs (CM2) could be more suitable. MSC-like cells were cultured for 28 days, either with CM1 or CM2, at cell densities of $6x10^5$, $1x10^6$ and $3x10^6$ (Fig. 7C). The lowest density seemed to be ideal allowing to obtain the best cellularity and cell viability within the generated pellets. Although, in both culture conditions we were unable to observe a histologically-proven chondrogenic differentiation but an initial one.

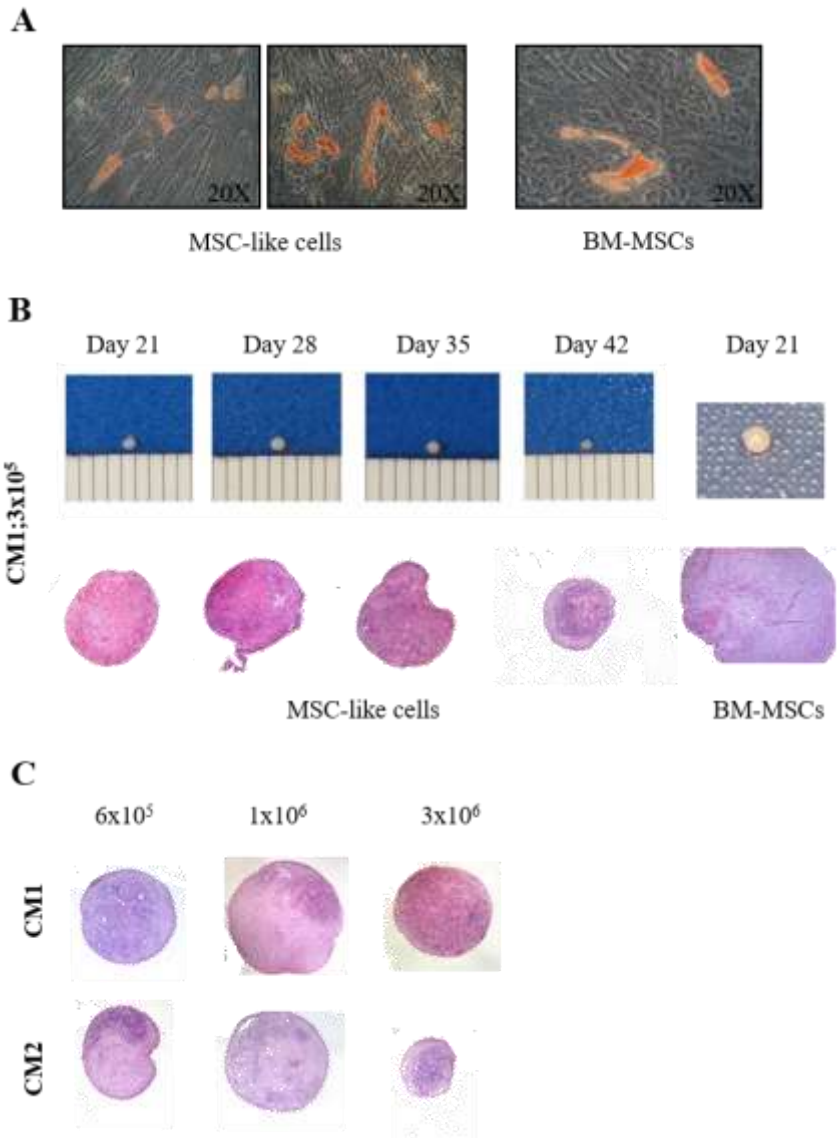

Fig. 7: Adipogenic and chondrogenic differentiation of HD MSC-like cells. (A) Adipogenic differentiation of HD MSC-like cells (left panles) and BM-MSCs (right panel) is demonstrated by the accumulation of lipid vacuoles stained by Oil Red O. n=5 out of 7. **(B)** Chondrogenic differentiation capability of HD MSC-like cells (left panels) in chondrogenic medium 1 (CM1), at cell density of $3x10^5$, at different time points. n=3 for each condition. **(C)** Chondrogenic differentiation capability of HD MSC-like cells in CM1 and CM2, at different cell density. N= 3 for each condition of

pellets at $6x10^5$ and $1x10^6$ cell density. n=2 for each condition of pellets at $3x10^6$. Pellets generated from BM-MSCs are used as a control (B, right panel). Hematoxylin and eosin staining of pellets are represented.

Osteogenic differentiation of HD MSC-like cells

To develop an osteogenic differentiation protocol, we had to set up the best conditions, focussing in particular on: 1- seeding cell density; 2- induction medium; 3- differentiation starting point; 4- differentiation endpoint.

At an initial cell density of $7x10^3$ cells/cm^2, the cells were already confluent at day 2 post-induction (Fig. 8A-I) and it was not possible to maintain the culture for more than 14 days, when the differentiation process was not yet completed (Fig. 8A-II) or not even started (Fig. 8A-III). We found that a cell density of $4x10^3$ cells/cm^2 was ideal for maintaining a subconfluent monolayer for a sufficient period (data not shown).

We tested two different osteogenic induction media (OM): one already used by our laboratory for osteogenic differentiation of MSCs (MSC-OM); and a second one optimised for iPSCs-based differentiation protocols (iPSC-OM). Only 14% of differentiation processes performed using MSC-OM turned positive after Alizarin Red staining (one out of seven), while 71% (fifteen out of twenty-one) positively stained when iPSC-OM was used (Fig 8B). We did not observe any difference due to the time of the induction after cell seeding (24h, 48h, 72h), because in all conditions osteogenic differentiation was equally achieved (data not shown).

As previously mentioned, we verified that a 21 days incubation period was sufficient to accomplish the differentiation process, as it is reported

in literature. In fact, at day 14 we could not -or partially- detect the Alizarin Red staining, whereas at day 21 the cells became strongly red. (Fig. 8C upper panel). Therefore, we concluded that an initial cell density of $4x10^3$ cells/cm^2 and an incubation period of 21 days in iPSC-OM were optimal conditions for osteoblasts derivation. The differentiation stage achieved by our protocol was similar, if not superior, to BM-MSC osteogenic differentiation, as visible by hydroxyapatite matrix staining (Fig. 8C, lower panel) and confirmed by Alizarin Red quantification (Fig. 8D).

To further analyse the accomplishment of the osteogenic differentiation process, we verified the expression of key osteogenic markers such as OPN, RUNX2, OTC, OTN, ALP and COL1A2 at day 0, 7, 14, 21 of differentiation (Fig. 8). The analysis revealed a nearly constant upregulation for all the genes, showing a similar expression profile between MSC-like cells (Fig. 8E) and BM-MSC-derived osteoblasts (Fig. 8F).

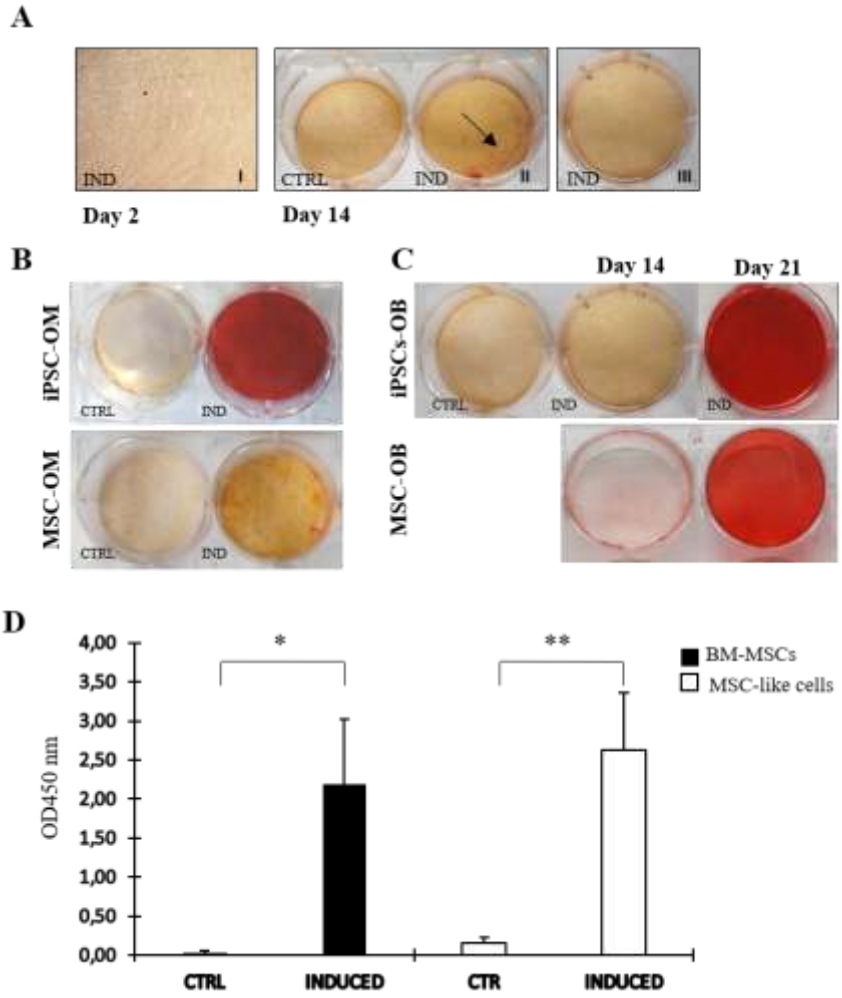
A
IND
I
CTRL
IND
II
IND
III
Day 2
Day 14
B
iPSC-OM
CTRL
IND
MSC-OM
CTRL
IND
C
Day 14
Day 21
iPSCs-OB
CTRL
IND
IND
MSC-OB
D
OD450 nm
4,00
3,50
3,00
2,50
2,00
1,50
1,00
0,50
0,00
*
**
BM-MSCs
MSC-like cells
CTRL
INDUCED
CTR
INDUCED

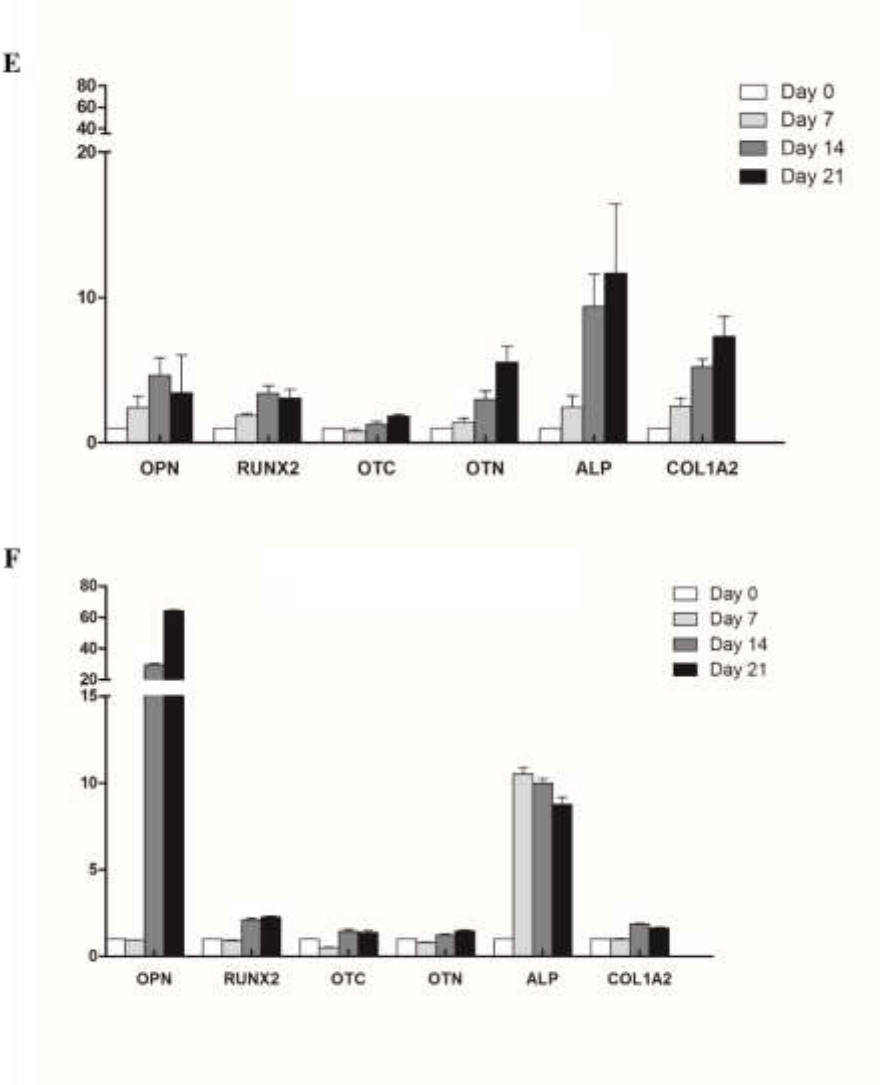

Fig. 8: Osteogenic differentiation of HD MSC-like cells. (A) Osteogenic differentiation of HD MSC-like cells at $7x10^3$ cells/cm^2, at day 2 and day 14 post-induction. **(B)** Osteogenic differentiation of HD MSC-like cells at $4x10^3$ cells/cm^2 in osteogenic differentiation medium optimised for MSCs (MSC-OM); and in osteogenic differentiation medium optimised for iPSCs (iPSC-OM). n= 1 out of 7 for MSC-OM; n= 15 out of 20 for iPSC-OM. **(C)** Comparison between iPSC-derived osteoblast (iPSC-OB) and BM-MSC-derived osteoblast (MSC-OB). Alizarin Red staining is performed at day 14 and 21 post induction. **(D)** Quantification of Alizarin Red staining 3 weeks after osteogenic induction. **(E-F)** Expression of osteogenesis-

related genes detected by RT-PCR after 7, 14 and 21 days of culture in MSC-OB **(E)** and iPSC-OB **(F).** Gene expression is normalised to GAPDH and relative to day 0 of the differentiation protocol. Graphs represent mean ± SD of three independent experiments. *p<0.05, **p<0.01. CTRL= control cells; IND= induced cells.

Generation and characterization of MPS MSC-like cells

We applied the mesenchymal differentiation protocol previously described to obtain MPS MSC-like cells. In the specific, four different strains were obtained.

MPS-iPSCs showed a lower expression for all of the MSC markers analysed compared to the HD population. (Fig. 10).

During the monolayer formation, CD90 was similarly expressed by MPS and HD MSC-like cells at P_0. Of note, MPS MSC-like cells presented a higher level of CD73 marker (92,58%) already at P_0. That was not the case of HD MSC-like cells that reached 99,4% of CD73 positivity only by P_2. Moreover, CD73 and CD90 expression was higher on MPS compared to HD MSC-like cells, at P_4. TRA-1-60 surface marker stained negatively for both populations (Fig. 11A). As previously mentioned, CD73 was consider as our marker of MSCs differentiation. Since MPS MSC-like cells have already reached an expression level of CD73 greater than 90% at P_0, we performed the complete phenotype characterization already at P_1. By the end of the characterization (P_4), the expression level of CD150, CD146 and MHC I in MPS and HD cells were the same. The hematopoietic marker MHC II was negative for both populations (Fig. 11B). Interestingly, cell proliferation of MPS MSC-like cells was significantly lower compared to HD MSC-like cells, already at half of the culture. (Fig. 11C). In

particular, for PT-2 EBs were hardly obtained and MSC-like cells stopped to proliferate after a few passages of culture.

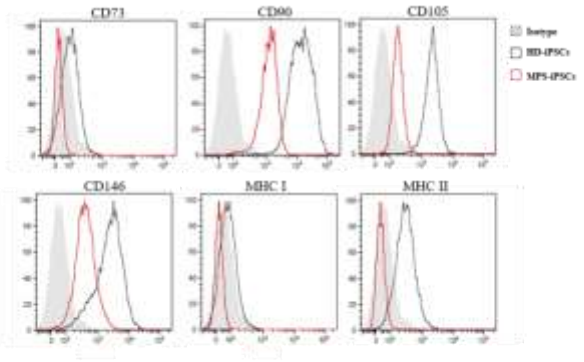

% OF POSITIVE CELLS																	
CD 73			CD90			CD105			CD146			MHC I			MHC II		
HD	PT-1	PT-2	HD	PT-1	PT-2	HD	PT-1	PT-2	HD	PT-1	PT-2	HD	PT-1	PT-2	HD	PT-1	PT-2
4,1	neg.	neg.	99,9	97,6	94	99,9	51,1	neg.	95,7	75,3	94,7	45,9	neg.	neg.	neg.	neg.	neg.

MFI																	
CD 73			CD90			CD105			CD146			MHC I			MHC II		
HD	PT-1	PT-2	HD	PT-1	PT-2	HD	PT-1	PT-2	HD	PT-1	PT-2	HD	PT-1	PT-2	HD	PT-1	PT-2
103	18,9	19	144662	1335	1327	2147	194	188	2512	420	416	303	29,9	30	78,8	17,4	17

Fig. 10: Immunophenotype of HD and MPS-iPSCs. FACS staining for MSCs cell surface markers in HD and MPS-iPSCs. Filled histograms show isotype control, open black histograms show HD sample and open red histograms show MPS sample. Patient-1 iPSCs (PT-1) is represented. Percentage (%) of positive cells and mean fluorescence intensity (MFI) are shown for HD-iPSCs and for both PT-1 and PT-2 iPSCs.

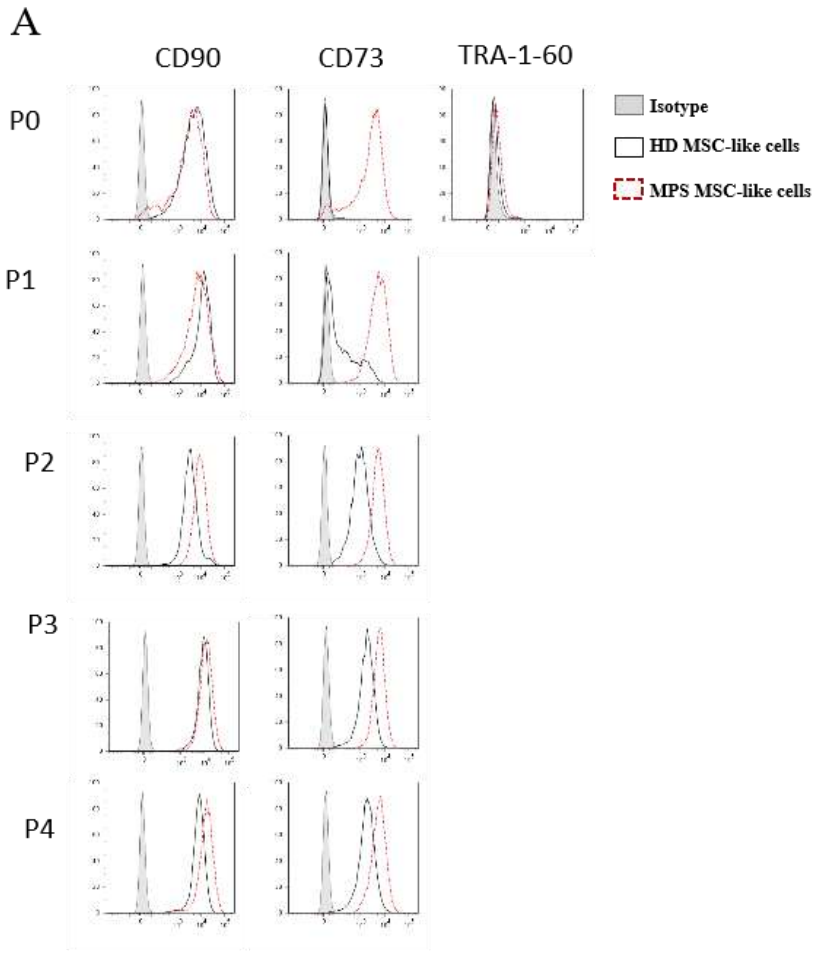
A
CD90
CD73
TRA-1-60
P0
P1
P2
P3
P4
Isotype
HD MSC-like cells
MPS MSC-like cells

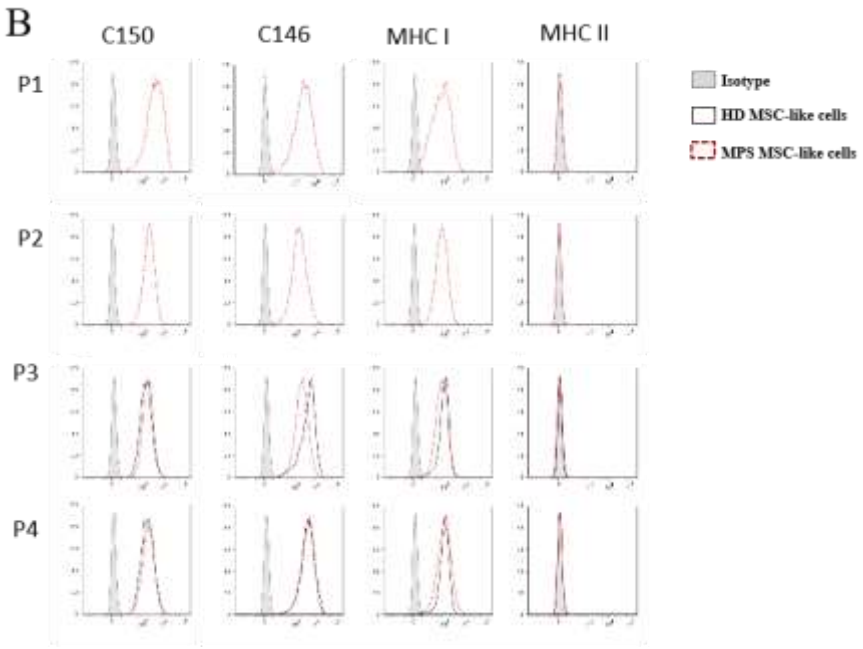

% OF POSITIVE CELLS																					
	CD90			CD 73			CD105			CD146			MHC I			MHC II			TRA-1-60		
	HD	PT-1	PT-2	HD	PT-1	PT-2	HD	PT-1	PT-2	HD	PT-1	PT-2	HD	PT-1	PT-2	HD	PT-1	PT-2	HD	PT-1	PT-2
P0	99,47	94,58	98,5	neg.	92,58	77,8													neg.	neg.	neg.
P1	99,96	99,57	100	51,27	99,88	99,3		99,95	100		99,24	96		96,74	96,4		neg.	neg.	neg.	neg.	neg.
P2	99,93	99,95	100	99,43	99,98	99		100	100		99,80	93		99,42	95,6		neg.	neg.	neg.	neg.	neg.
P3	99,85	100	100	99,67	99,99	100	99,99	100	100	99,72	99,94	98	99,21	99,07	94,4	neg.	neg.	neg.	neg.	neg.	neg.
P4	99,4	100	100	99,2	99,97	100	99,99	100	100	99,83	99,95	98	99,26	99,20	96	neg.	neg.	neg.	neg.	neg.	neg.

MFI																					
	CD90			CD 73			CD105			CD146			MHC I			MHC II			TRA-1-60		
	HD	PT-1	PT-2	HD	PT-1	PT-2	HD	PT-1	PT-2	HD	PT-1	PT-2	HD	PT-1	PT-2	HD	PT-1	PT-2	HD	PT-1	PT-2
P0	5089	3581	5340	neg.	2947	2305										<20	<50	<60	<100	<100	<100
P1	12031	7406	17917	99	5404	4197		4362	6959		2724	2981		768	2043	<20	<50	<60	<100	<100	<100
P2	3467	9044	21803	964	5247	4206		2097	3517		1592	3655		995	2480	<20	<50	<60	<100	<100	<100
P3	8475	11114	22316	1795	5900	5661	1480	1805	5241	4826	2136	4037	1049	778	1672	<20	<50	<60	<100	<100	<100
P4	8142	17109	50342	1825	5638	7529	1709	1956	6505	3943	4215	3825	1085	1045	2306	<20	<50	<60	<100	<100	<100

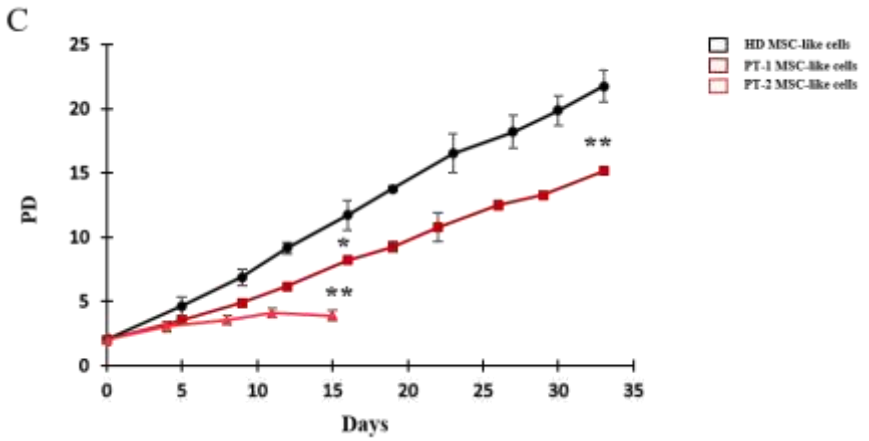

Fig. 11: Immunophenotype and proliferation capacity of HD and MPS MSC-like cells. (A) Immunostaining for CD73, CD90 and TRA-1-60 from P_0-P_4; and for CD105, CD146, MHC I, MHC II from P_3-P_4 **(B)**. Filled histograms show isotype control, open black histograms show HD sample and open red histograms show MPS sample. Patient-1 MSC-like cells (PT-1 MSC-like cells) is represented. Percentage (%) of positive cells and mean fluorescence intensity (MFI) are shown for HD MSC-like cells and both PT-1, PT-2 MSC-like cells **(C)** Expansion curve of HD MSC-like cells (black line), PT-1 MSC-like cells (red line) and PT-2 MSC-like cells (light red line). Graph represent mean ± SD. HD MSC-like n= 3 independent experiments; PT-1 MSC-like cells n= 2 independent experiments; PT-2 MSC-like cells n= 4 independent experiments. *p<0.05, **p<0.01. PD= population doubling

Osteogenic differentiation of MPS MSC-like cells

Since we were interested in the compromised bone phenotype of Hurler patients, we focused our attention in the differentiation of MPS MSC-like cells to osteoblasts, by adopting the previously described *in vitro* protocol. Alizarin Red quantification assay revealed that MPS-derived osteoblasts (MPS-OBs) produced less hydroxyapatite than their HD counterpart, although this difference was not statistically significant (Fig. 12A).

Interestingly, this different trend of expression was confirmed by the analysis of the osteogenic genes (Fig. 12B). Indeed, MPS-OBs displayed a lower expression level for the investigated genes, with the only exception for OTC gene. Of note, RUNX 2 and ALP, two of the main genes involved in osteogenesis, were markedly downregulated in patient- derived cells compared to HD cells.

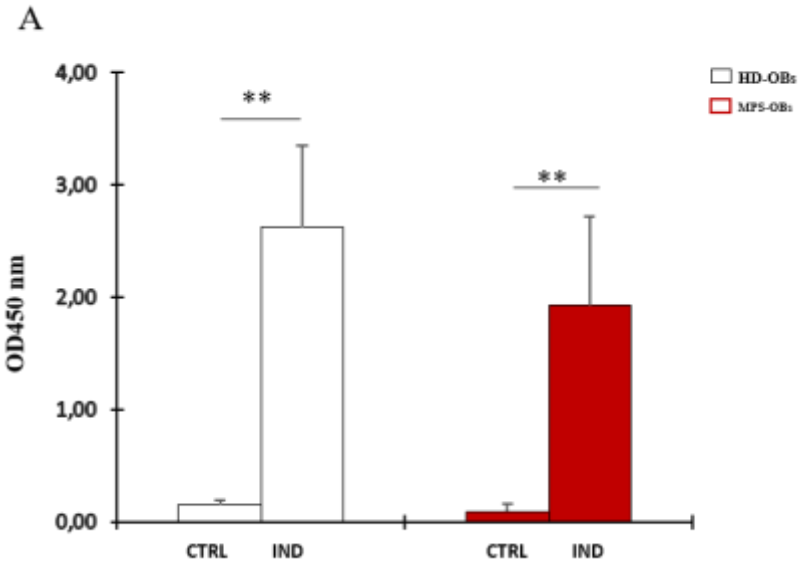

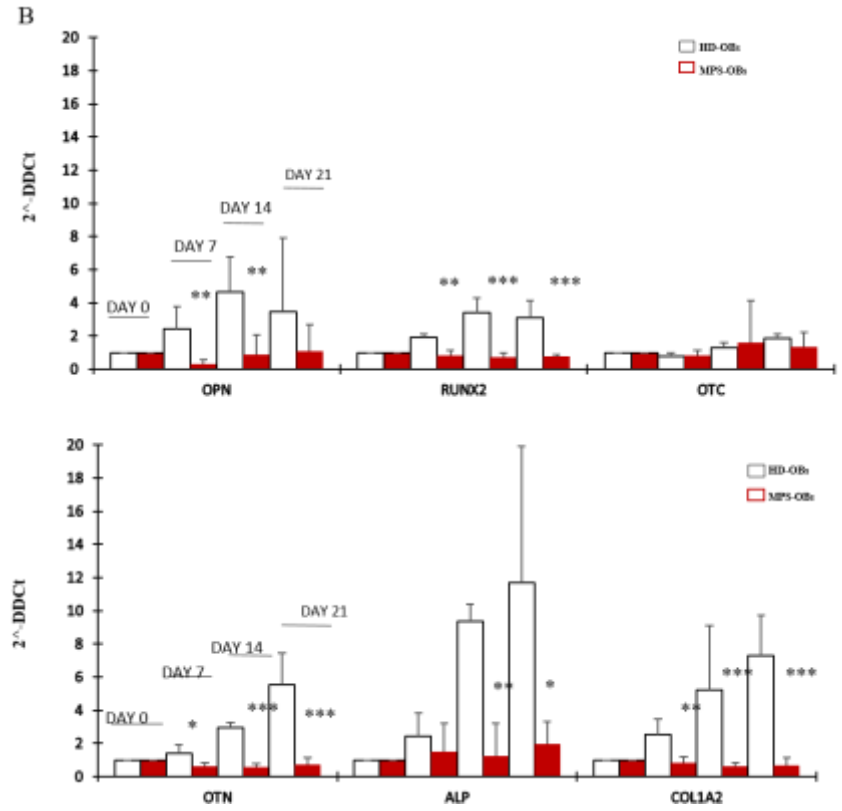

Fig. 12: Osteogenic differentiation of HD and MPS MSC-like cells. (A) Quantification of Alizarin Red staining 3 weeks after osteogenic induction. Graph represents mean ± SD. HD-OBs n= 3 independent experiments. MPS-OBs n=5 independent experiments. **(B)** Expression of osteogenesis-related genes detected by q-RT-PCR after 7, 14 and 21 days of culture in induction medium. Gene expression is normalised to GAPDH and relative to day 0 of the differentiation protocol for each group. Graph represent mean ± SD. HD-OBs n= 3 independent experiments. MPS-OBs n=7 independent experiments. *p<0.05, **p<0.01, ***p<0.001 CTRL= control cells;

RANKL and OPG expression level in MSC-like cells and derived OBs

RANKL and OPG are key regulators of osteoclastogenesis and bone resorption and are produced by different cell sources, including MSCs and OBs. Alteration in the balance of these molecules and, as a consequence, dysregulation of the osteoclasts differentiation, is the cause of different bone pathology. Thus, we measured the mRNA level of these genes in HD and MPS MSC-like cells and derived OBs. Interestingly, OPG expression level was not significantly different between the two MSC populations (Fig. 13A), while RANKL was only detectable in MPS MSC-like cells (Fig. 13B). This was not a problem of degraded mRNA for HD MSC-like cell samples because the expression of the housekeeping gene GAPDH was clearly detectable during q-RT-PCR assay. Moreover, the RANKL primers adopted were previously tested on BM-MSCs (Fig. 2S).

MPS-OBs showed a decrease expression of OPG compare to HD-OBs, which reached significance by day 14. HD-OBs had a nearly constant expression of this molecule (Fig. 14A). At the same time, RANKL expression was higher in HD-OBs compare with MPS-OBs, even though it was not significant (Fig. 14B). Moreover, the expression level of RANKL at the time point 21 of MP-OBs was clearly different within the two patients (Fig. 14C).

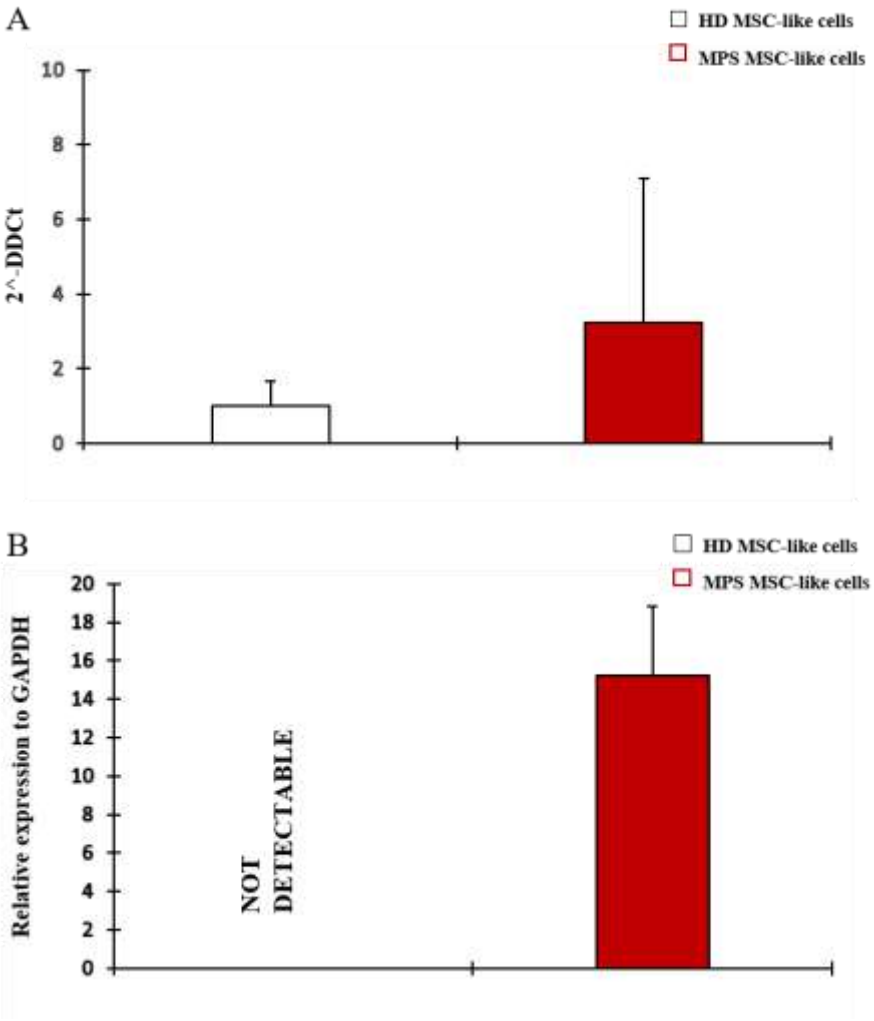

Fig. 13: RANKL and OPG expression level in HD and MPS MSC-like cells

Expression of OPG **(A)** and RANKL **(B)** was evaluated by q-RT-PCR in basal HD and MPS MSC-like cells. For graph (A), gene expression is normalised to GAPDH and relative to HD MSC-like cells. For graph (B), gene expression is relative to GAPDH. Bars represent mean ± SD. HD MSC-like cellss n= 3 independent experiments. MPS MSC-like cells n=7 independent experiments.

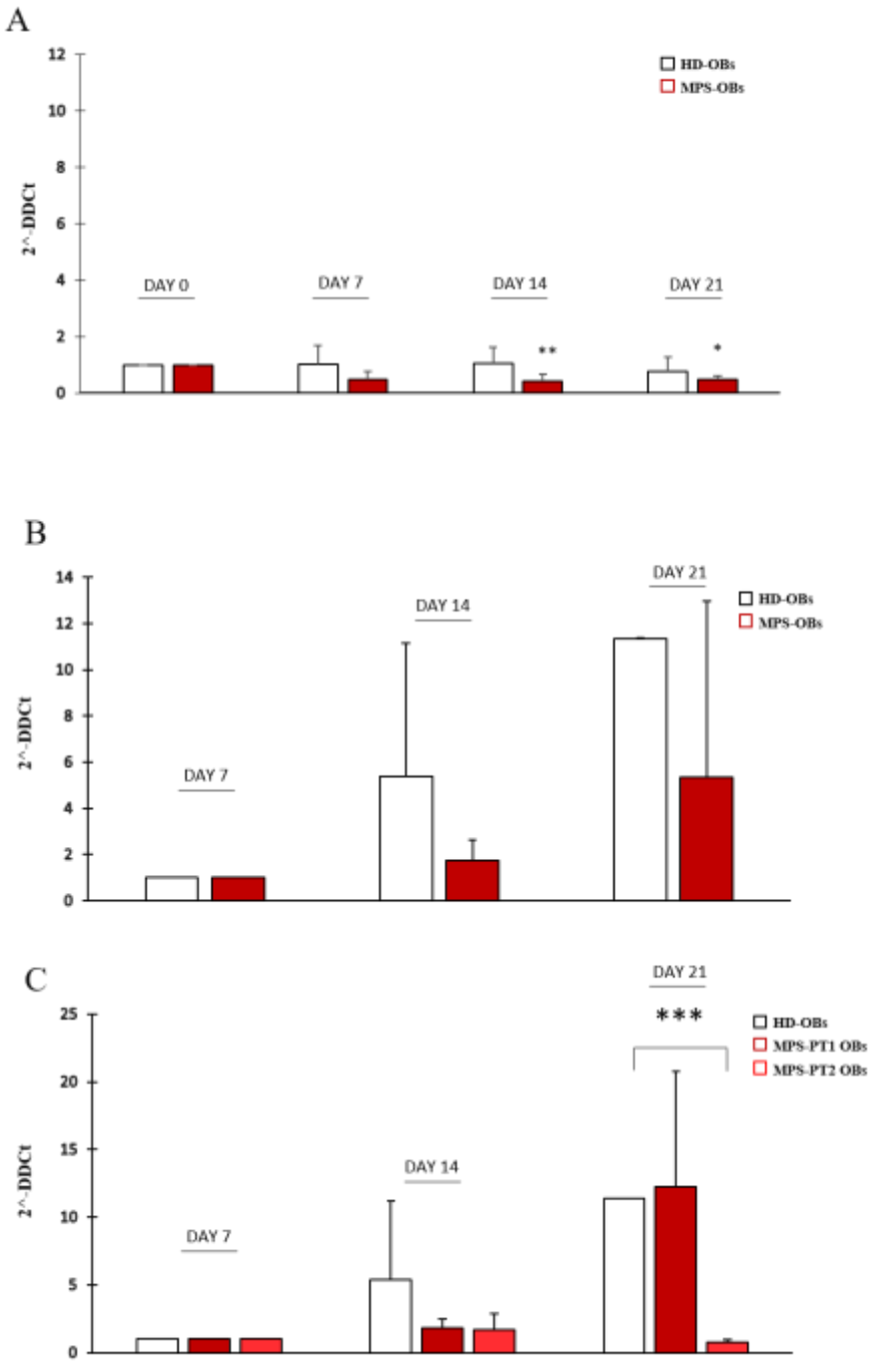
A
12
10
8
6
4
2
0
2^-DDCt
HD-OBs
MPS-OBs
DAY 0
DAY 7
DAY 14
DAY 21
**
*
B
14
12
10
8
6
4
2
0
2^-DDCt
DAY 7
DAY 14
DAY 21
HD-OBs
MPS-OBs
C
25
20
15
10
5
0
2^-DDCt
DAY 7
DAY 14
DAY 21
***
HD-OBs
MPS-PT1 OBs
MPS-PT2 OBs

Fig. 14: RANKL and OPG expression level in HD and MPS-OBs

Expression of OPG **(A)** and RANKL **(B-C)** was evaluated by q-RT-PCR in HD and MPS-OBs. At time point 7,14,21 of osteogenesis. For graph (A), gene expression is normalised to GAPDH and relative to day 0 of the differentiation protocol for each group. For graph (B-C), gene expression is normalised to GAPDH and relative to day 7 of the differentiation protocol for each group. Graph (B) represents RANKL gene expression as a mean of patient 1 (PT1) and patient 2 (PT2), while graph (C) represents the gene expression separately for PT1 and PT2.

Graph represent mean ± SD. HD-OBs n= 3 independent experiments. MPS-OBs n=7 independent experiments. *p<0.05, **p<0.01, ***p<0.001

Discussion

In the present study, we proposed an appropriate, humanized *in vitro* model to elucidate possible impaired mechanisms at the basis of the muscular-skeletal phenotype, affecting Hurler patients. In particular, we are interested in studying the early timeframe of bone formation because it has been poorly explored and initial insights suggest that skeletal alterations already occurred in MPS I embryos and postnatal mice [4-6]. iPSCs demonstrate great potential as a model for investigating the osteogenic differentiation process at early stages, due to their high proliferation capability in culture and, mostly, to their ability to mimic development. Our study is the first, within mucopolysaccaridoses, to propose an *in vitro* model to resemble osteogenesis development through the adoption of MPS-derived iPSCs. In our study, we have been able to generate MPS-iPSC from 3 different patients. Pluripotency of canonical ES genes and cell surface markers were evaluated by q-RT-PCR, immunofluorescence staining and FACS analysis. Both HD and MPS-iPSCs expressed these markers, with different grade of positivity. This is not surprising because it is well documented a range of variability in the expression profile among different lines of iPSCs and often within the same line. Notably is the high expression of Nanog, among the other genes, because it has been demonstrated that is a crucial gene for the maintenance of pluripotency [14, 15]. The hallmark of iPSCs of generating cells belonging to the three germ layers was confirmed by EBs *in vitro* formation and by *in vivo* teratoma generation.

The first aim of our work was to design an efficient and reproducible protocol for the isolation of osteoblasts. Unfortunately, there are only few protocols that attempt to differentiate human iPSCs to osteoblasts and each of them adopt different procedures. This process is still largely unknown and unexplored. Beside the lack of clear and univocal experimental procedures, there are also limited data from the literature. In this study, we proposed a multistep differentiation procedure through the generation of *bona fide* MSC-like cells, avoiding induced osteogenic genes expression and any genetic manipulation, or even the use of matrix scaffolds. In fact, we want to mimic as much as possible the physiological process that lead to osteoblasts formation, in order to make the protocol suitable for studying the mechanism of the genetic disease. At the same time, we want to study the contribution of precursors cells to bone formation, such as MSCs. For this reason, we adopted EBs culture method because it mimics early embryonic development, providing a spontaneous and gradually transition from pluripotent stem cells to more committed cells, in this case of the mesoderm lineage.

MSC-like cells generated with the proposed method, reflected the minimal criteria for MSCs, defined by the Mesenchymal and Tissue Stem Cell Committee [16]: plastic adhesion, expression of CD 73, CD90, CD 105, CD146 and absence of MHC II, and the ability to differentiate into adipocytes, osteoblast and chondrocytes. Actually, the percentage of positivity that we obtained for MSCs surface markers was higher than other published paper that adopted a transition step from iPSCs to MSCs [17, 18]. Anyhow, MSC-like cells seemed to retain an ”embryonic-like phenotype”, compare to adult MSC-lines. Indeed, they

expressed more intensely the cell surface markers MHC I, as perinatal tissue-derived MSCs [19], and demonstrated a more prolonged self-renewal capacity *in vitro* (over P20). Interestingly, MPS MSC-like cells showed a reduced growth kinetic, if compared to HD. Moreover, MSC-like cells derived from PT-2 were arrested in their proliferation after a few passages and EBs were hardly obtained. GAGs accumulation may be the causes of abnormal functionality of MSCs. The work of Meng 's group demonstrated a significantly decreased capability of EBs formation in mouse derived MPS VII-iPSCs [20]. Thus, additional investigation, such as cell-cycle analysis, apoptosis test and telomerase activity need to be done in MPS MSC-like cells.

The second point of interest of the study was the investigation of the features of *bona-fide* MPS MSCs-like cells and MPS-OBs in osteogenesis.

MPS-OBs isolated with our protocols revealed a significant downregulation of RUNX2 expression, compare to HD-OBs, already at day 7 of culture. This difference ulteriorly increased at later time points. RUNX2 is the most important factor involved in the osteogenic differentiation, Mice with its null mutation exhibit a complete lack of bone [21]. Its expression is up-regulated in proliferative chondrocytes for the initiation of differentiation of MSCs to osteoblast, and it reduces during the differentiation into mature osteoblasts; it is undetectable during the differentiation of osteoblasts into osteocytes [22]. This gene can be stimulated by multiple signal transduction pathways, and it can directly stimulate the transcription of osteoblast-related genes such as those encoding osteocalcin (OTC), type I collagen (COL1), osteopontin (OPN) and collagenase 3 [23, 24]. Taken together, these observations

could explain the markedly downregulation of OPN and COL1A2 genes observed in MPS-OBs, since they are directly regulated by RUNX2. Moreover, ALP is an important gene for calcium crystallization and mineralization during bone formation [25]. It has been reported that reduced ALP activity in osteoblasts derived-iPSCs, correlate with low expression of the matrix-related genes OPN and OTN [26], as we observed. Our data are also in accordance with the extracellular matrix disruption that has been seen during embryogenesis or in postnatal MPS I mice [4]. The essential role of RUNX2 during embryogenesis, is also emphasized by several works [27-29]. Thus, it could be reasonable to suppose that an early osteogenic disruption may occur in MPS I patients. Whether or not there is a correlation between altered MPS-MSCs and incomplete osteoblasts formation needs to be elucidated.

Bone remodelling also plays a major role in the maintenance of the skeleton's mechanical integrity and involves a well-coordinated balance between bone formation (by osteoblast) and bone resorption (by osteoclasts). While the role of increased activity of osteoclasts has been extensively studied, the involvement of MSCs and osteoblasts has been not well elucidated. Thus, we focused our attention on the contribution to osteoclastogenesis of MPS MSC-like cells and OBs by measuring mRNA level of RANKL and OPG. These molecules are two key regulators of osteoclastogenesis and their imbalanced production could cause alteration in bone remodelling.

Interestingly, our preliminary data showed that OPG expression level was similar in both HD and MPS MSCs-like cells, whereas RANKL was highly expressed in MPS MSC-like cells. HD-MSCs have an

undetectable expression of RANKL. These data are in accordance with our previously published work [30], where we demonstrated that RANKL expression was higher in MPS I BM-MSCs compared with HD BM-MSCs. Thus, it might be conceivable an enhanced osteoclastogenesis which could corroborate with bone alterations. Under question are the data of the expression level for OPG and RANKL of the osteoblasts population, which need to be confirmed with further experiments. This pathway needs to be further studied because it has been demonstrated that mutation in RANK, RANKL and OPG expression correlated with bone disorders, such as familial expansile osteolysis, autosomal recessive osteopetrosis and Juvenile Paget's disease [31]. Of particular interest are few works that correlate RUNX2 expression with RANKL gene transcription [32]. Thus, in addition to its essential role in osteoblast development and chondrocyte hypertrophy, RUNX2 may also regulate osteoclast function indirectly, through RANKL and OPG, which might correlate with what we have observed. Our model is appropriate for the investigation of the role of the triage in MPS-OBs because in normal condition, osteoblasts and chondrocytes are the major source of RANKL during skeletal development [33].

Here, we have developed a simplified and reproducible differentiation protocol for MPS-iPSCs, providing a useful technique for the study of different skeletal dysplasia. Moreover, we can conclude that bone abnormalities of Hurler patients might be due to an alteration in the osteoblast gene expression pathway with a concomitant increased osteoclastogenesis.

References

1. Clarke, L.A., *The mucopolysaccharidoses: a success of molecular medicine.* Expert Rev Mol Med, 2008. **10**: p. e1.
2. Neufeld, E.F.a.J.M., *The mucopolysaccharidoses, in The Metabolic and Molecular Bases of Inherited Disease.* 2001. **C.R. Scriver, et al., Editors**: p. p. 3427-3436.
3. Aldenhoven, M., et al., *Musculoskeletal manifestations of lysosomal storage disorders.* Ann Rheum Dis, 2009. **68**(11): p. 1659-65.
4. Heppner, J.M., F. Zaucke, and L.A. Clarke, *Extracellular matrix disruption is an early event in the pathogenesis of skeletal disease in mucopolysaccharidosis I.* Mol Genet Metab, 2015. **114**(2): p. 146-55.
5. Beck, M., et al., *Fetal presentation of Morquio disease type A.* Prenat Diagn, 1992. **12**(12): p. 1019-29.
6. Martin, J.J. and C. Ceuterick, *Prenatal pathology in mucopolysaccharidoses: a comparison with postnatal cases.* Clin Neuropathol, 1983. **2**(3): p. 122-7.
7. Pievani, A., et al., *Neonatal bone marrow transplantation prevents bone pathology in a mouse model of mucopolysaccharidosis type I.* Blood, 2015. **125**(10): p. 1662-71.
8. Sands, M.S., et al., *Treatment of murine mucopolysaccharidosis type VII by syngeneic bone marrow transplantation in neonates.* Lab Invest, 1993. **68**(6): p. 676-86.
9. Soper, B.W., et al., *Nonablative neonatal marrow transplantation attenuates functional and physical defects of beta-glucuronidase deficiency.* Blood, 2001. **97**(5): p. 1498-504.
10. Nakashima, T. and H. Takayanagi, *New regulation mechanisms of osteoclast differentiation.* Ann N Y Acad Sci, 2011. **1240**: p. E13-8.
11. Wada, T., et al., *RANKL-RANK signaling in osteoclastogenesis and bone disease.* Trends Mol Med, 2006. **12**(1): p. 17-25.
12. Takahashi, K. and S. Yamanaka, *Induction of pluripotent stem cells from mouse embryonic and adult fibroblast cultures by defined factors.* Cell, 2006. **126**(4): p. 663-76.

13. Serafini, M., et al., *Establishment of bone marrow and hematopoietic niches in vivo by reversion of chondrocyte differentiation of human bone marrow stromal cells.* Stem Cell Res, 2014. **12**(3): p. 659-72.
14. Chambers, I., et al., *Functional expression cloning of Nanog, a pluripotency sustaining factor in embryonic stem cells.* Cell, 2003. **113**(5): p. 643-55.
15. Mitsui, K., et al., *The homeoprotein Nanog is required for maintenance of pluripotency in mouse epiblast and ES cells.* Cell, 2003. **113**(5): p. 631-42.
16. Horwitz, E.M., et al., *Clarification of the nomenclature for MSC: The International Society for Cellular Therapy position statement.* Cytotherapy, 2005. **7**(5): p. 393-5.
17. Guzzo, R.M., et al., *Efficient differentiation of human iPSC-derived mesenchymal stem cells to chondroprogenitor cells.* J Cell Biochem, 2013. **114**(2): p. 480-90.
18. Koyama, N., et al., *Human induced pluripotent stem cells differentiated into chondrogenic lineage via generation of mesenchymal progenitor cells.* Stem Cells Dev, 2013. **22**(1): p. 102-13.
19. Pievani, A., et al., *Comparative analysis of multilineage properties of mesenchymal stromal cells derived from fetal sources shows an advantage of mesenchymal stromal cells isolated from cord blood in chondrogenic differentiation potential.* Cytotherapy, 2014. **16**(7): p. 893-905.
20. Meng, X.L., et al., *Induced pluripotent stem cells derived from mouse models of lysosomal storage disorders.* Proc Natl Acad Sci U S A, 2010. **107**(17): p. 7886-91.
21. Otto, F., et al., *Cbfa1, a candidate gene for cleidocranial dysplasia syndrome, is essential for osteoblast differentiation and bone development.* Cell, 1997. **89**(5): p. 765-71.
22. Lee, M.H., et al., *Transient upregulation of CBFA1 in response to bone morphogenetic protein-2 and transforming growth factor beta1 in C2C12 myogenic cells coincides with suppression of the myogenic phenotype but is not sufficient for osteoblast differentiation.* J Cell Biochem, 1999. **73**(1): p. 114-25.
23. Dalle Carbonare, L., et al., *Circulating mesenchymal stem cells with abnormal osteogenic differentiation in patients with osteoporosis.* Arthritis Rheum, 2009. **60**(11): p. 3356-65.

24. Kern, B., et al., *Cbfa1 contributes to the osteoblast-specific expression of type I collagen genes.* J Biol Chem, 2001. **276**(10): p. 7101-7.
25. Whyte, M.P., *Hypophosphatasia and the role of alkaline phosphatase in skeletal mineralization.* Endocr Rev, 1994. **15**(4): p. 439-61.
26. Kim, D., et al., *Impaired osteogenesis in Menkes disease-derived induced pluripotent stem cells.* Stem Cell Res Ther, 2015. **6**: p. 160.
27. Inada, M., et al., *Maturational disturbance of chondrocytes in Cbfa1-deficient mice.* Dev Dyn, 1999. **214**(4): p. 279-90.
28. Kim, I.S., et al., *Regulation of chondrocyte differentiation by Cbfa1.* Mech Dev, 1999. **80**(2): p. 159-70.
29. Otto, F., H. Kanegane, and S. Mundlos, *Mutations in the RUNX2 gene in patients with cleidocranial dysplasia.* Hum Mutat, 2002. **19**(3): p. 209-16.
30. Gatto, F., et al., *Hurler disease bone marrow stromal cells exhibit altered ability to support osteoclast formation.* Stem Cells Dev, 2012. **21**(9): p. 1466-77.
31. Nakashima, T. and H. Takayanagi, *Osteoimmunology: crosstalk between the immune and bone systems.* J Clin Immunol, 2009. **29**(5): p. 555-67.
32. Mori, K., et al., *Modulation of mouse RANKL gene expression by Runx2 and PKA pathway.* J Cell Biochem, 2006. **98**(6): p. 1629-44.
33. Xiong, J., et al., *Matrix-embedded cells control osteoclast formation.* Nat Med, 2011. **17**(10): p. 1235-41.

Supplementary materials

Table S1

Primary Antibody	**Supplier**	**Catalog Number**	**Dilution**
Oct-3/4	Santa Cruz Biotechnology	sc-9081	1:100
Sox2	Millipore	AB5603	1:500
Nanog	Invitrogen	PA1-097	1:500
TRA-1-60	Cell-Signaling	4746	1:200
Secondary Antibody	**Supplier**	**Catalog Number**	**Dilution**
Donkey anti-Mouse Alexa Fluor 555	Invitrogen	A-31570	1:500
Donkey anti-Rabbit Alexa Fluor 488	Invitrogen	A-21206	1:500

Table S2

GAPDH	4352934E
OPN	Hs00959010_m1
RUNX 2	Hs00231692_m1
OTC	Hs00609452_g1
OTN	Hs00234160_m1
ALP	Hs01029144_m1
COL 1A2	Hs01028970_m1
RANKL	Hs00243519_m1
OPG	Hs00171068_m1

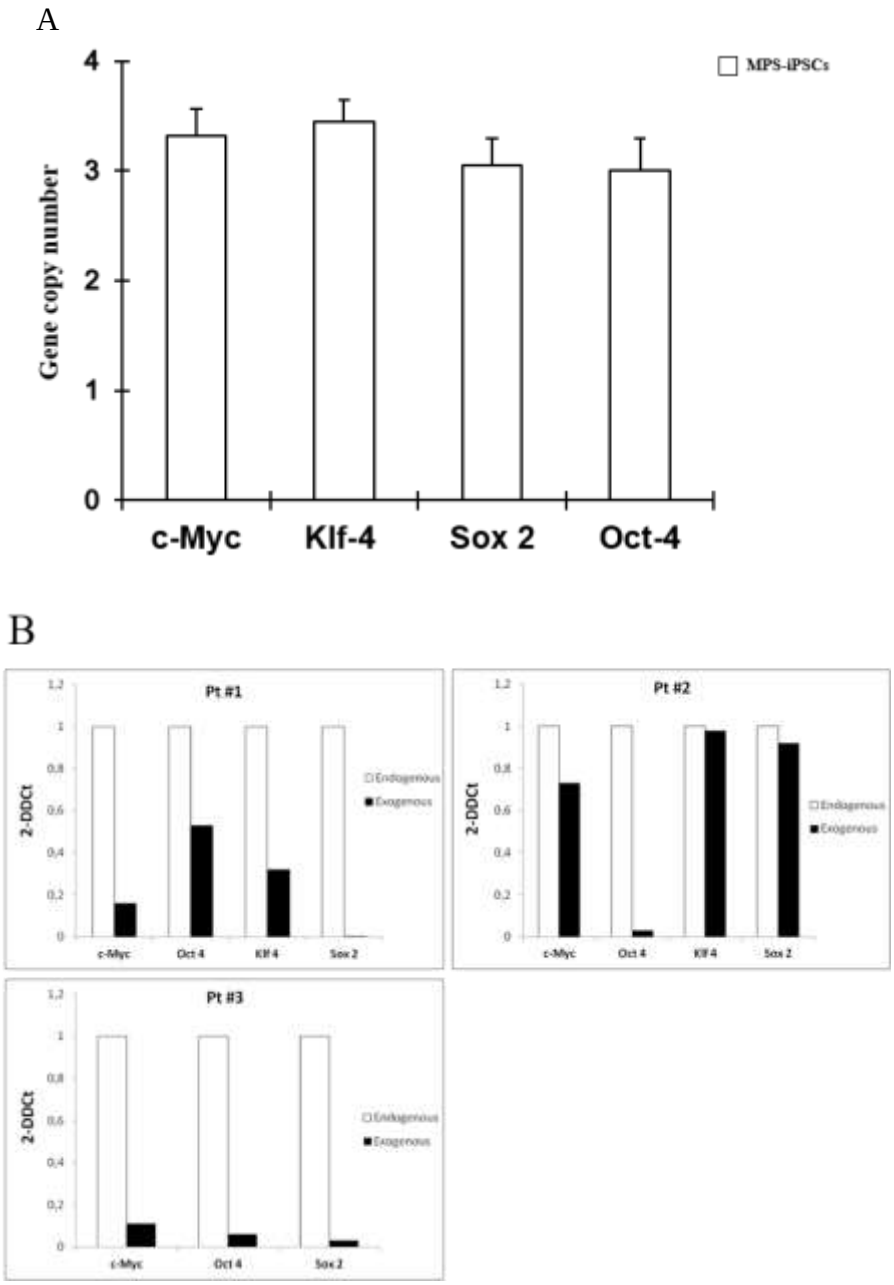

Fig. 1S: (A) Number of transgene copies in human iPSCs generated from MPS IH fibroblasts. Copy number for each gene used to reprogram MPS IH fibroblasts was determined using real-time PCR. The graph shows the mean of three different iPS cell lines derived from the same patient. Bars indicate ± SD. **(B)** Relative gene expression

of exogenous and endogenous c-Myc, Oct-4, Klf-4 and Sox2 in human iPSCs generated from fibroblasts of MPS IH patients, for the three patients. The graph shows the mean of three different iPS cell lines derived from the same patient. hESCs (H9 line) were used as reference control. Bars indicate ± SD.

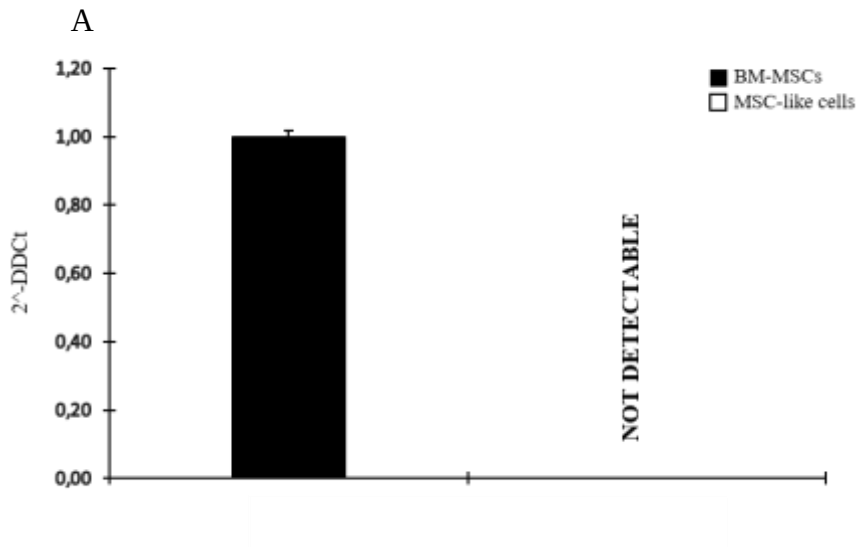

Fig. 2S: Fig. 13: RANKL expression level in BM-MSCs and HD MSC-like cells

CHAPTER 3:

Differentiation of MPS IH patient-derived human induced pluripotent stem cells into hepatocyte-like cells and neural cells suitable for disease modelling and drug screening.

F. Gatto[1,2,†], **A. Montagna**[1,2,†], L. Ordovas3, S. Raitano[3], J. Vanhove[3], I. Geti[4], R. Parini[5], A. Rovelli[5], S. Montefusco[6], I. Peluso[6], D.L. Medina[6], M. Riminucci[7], L. Vallier[4], A. Biondi[2,5], C.M. Verfaillie[3]§, M. Serafini1,[2]§*.

[1]Dulbecco Telethon Institute at Tettamanti Research Center, University of Milano-Bicocca, 20900 Monza, Italy

[2]Pediatric Department, Tettamanti Research Center, University of Milano-Bicocca, 20900 Monza, Italy.

[3]Stem Cell Institute, KU Leuven, 3000 Leuven, Belgium.

[4]The Anne McLaren Laboratory for Regenerative Medicine, Department of Surgery, University of Cambridge, Cambridge CB2 0SZ, United Kingdom

[5]Pediatric Department, University of Milano-Bicocca, 20900 Monza, Italy

[6]Telethon Institute of Genetics and Medicine (TIGEM), 80131 Naples, Italy

[7]Department of Molecular Medicine, La Sapienza University, 00161 Rome, Italy

§ These authors are equal last authors

†These authors equally contributed to this work

*Please address correspondence to: Marta Serafini, PhD; Dulbecco Telethon Institute at Tettamanti Research Center, University of Milano-Bicocca, via Pergolesi, 33 20900 Monza, Italy; email: serafinim72@gmail.com

Manuscript in preparation

Abstract

We have generated induced pluripotent stem cells (iPSCs) from patients affected by Mucopolysaccharidosis type IH (MPS IH; also termed Hurler syndrome), a lysosomal storage disorder in which mutations in the α-L-iduronidase (IDUA) gene results in the deficiency of IDUA enzyme activity and consequently, in intra-cellular accumulation of glycosaminoglycans (GAGs). Interestingly, differentiation towards hepatocyte-like cells and neural cells, two disease relevant cell types, was comparable for MPS-iPSCs and iPSCs from normal donors (ND). In particular, hepatocyte-like cells generated from MPS-iPSCs expressed markers of mature hepatocytes and exhibited normal hepatic functions *in vitro*, including albumin secretion and cytochrome activity. MPS-iPSCs were also able to differentiate into neural progenitors and cortical cells, as shown by a repertoire of molecular markers identifying neuronal populations. However, accumulation of GAGs occurred in MPS-iPSCs, as well as in teratomas. In conclusion, we demonstrate that the inherent ability of MPS IH iPSCs to hepatocytes and neural cells is unaffected by the accumulation of GAGs. Hepatocyte-like cells and cortical neurons were successfully produced from patient-derived iPSCs, thereby offering opportunities for further functional studies and drug screening of Hurler syndrome.

Introduction

Hurler syndrome (Mucopolysaccharidosis type IH; MPS IH) is a rare genetic, autosomal recessive disorder where the IDUA enzyme is missing, leading to accumulation of the glycosaminoglycans (GAGs) dermatan sulfate and heparan sulphate (Neufeld EF, Muenzer; Ballabio and Gieselmann 2009; Muenzer 2011). These GAGs build up in all tissues in the body causing progressive deterioration and abnormal function of multiple organs. In fact, patients affected by Hurler syndrome develop a cascade of multisystemic clinical manifestations in the first year of life, including the typical coarse facial features, hepatosplenomegaly, obstructive airway disease complicated by respiratory infections, cardiac failure, skeletal abnormalities and severe neurological deficits. Hematopoietic stem cell transplantation (HCT) is the recommended treatment for MPS IH patients (Peters 2004; Aldenhoven, Boelens et al. 2008). As IDUA is secreted by all cells and can be taken up by other cells, it is believed that IDUA secreted from donor monocytes becoming resident in all organs retards disease progression. However, the clinical success of HCT to treat MPS IH is compromised by the high frequency of graft rejection, leading to incomplete donor chimerism, which is insufficient to prevent deterioration of neurological and skeletal abnormalities associated with the disease (Aldenhoven, Boelens et al. 2008). For this reason, alternative stem cell sources and transplant procedures could offer important and innovative approaches.

The advent of induced pluripotent stem cell (iPSCs) technology, makes it now possible to generate autologous pluripotent stem cells from any

individual, suitable for the creation of *in vitro* disease models and potentially providing a source for cell replacement therapy (Takahashi, Tanabe et al. 2007). Different reports have demonstrated that iPSCs can recapitulate the disease-specific phenotype for numerous monogenic diseases (Park, Zhao et al. 2008), (Zhu, Lensch et al. 2011). iPSCs technology has been recently adopted for modelling of various lysosomal storage diseases, making it possible to obtain differentiated cell types relevant to the clinical disease manifestations (Meng, Shen et al. 2010) (Kawagoe, Higuchi et al. 2011) (Huang, Chen et al. 2011). Tolar et al. reported the generation and characterization of iPSCs from patients affected by MPS IH (Tolar, Park et al. 2011). Hurler iPSCs were genetically corrected by transduction with a lentiviral vector harbouring the human IDUA cDNA, and could be induced to differentiate into gene-corrected hematopoietic cells. The derivation of iPSCs from two Pompe disease patients was reported by Huang et al. (Huang, Chen et al. 2011). They demonstrated that as the typical low α-glucosidase activity and high glycogen content was also present in the iPSCs and their progeny, and could be reversed by exposure to recombinant human enzyme. Lemonnier et al. studied the neural differentiation capacity of human iPSCs generated from MPSIIIB fibroblasts (Lemonnier, Blanchard et al. 2011). They demonstrated that undifferentiated patient iPSCs and their neuronal progeny expressed cell disorders consisting of intracellular storage vesicles and severe disorganization of Golgi structure.

Here, we report the generation and characterization of iPSCs from MPS IH patient-derived mesenchymal stem cells (MSCs) and fibroblasts by introducing four reprogramming factors (Oct3/4, Sox2, Klf4 and c-

Myc), following the method described by Yamanaka's group (Takahashi and Yamanaka 2006). This allowed us to evaluate the ability of Hurler iPSC to differentiate to neural cells, which are particularly affected in Hurler syndrome and not optimally corrected by HSC transplantation (Aldenhoven, Boelens et al. 2008), as well as hepatocyte-like cells.

Materials and Methods

Human iPSCs isolation from MPS IH patients

After informed consent per institutionally approved protocols, fibroblasts and mesenchymal stem cells (MSCs) were collected from 4 MPS IH pediatric patients (aged 13 months, 20 months, 11 months and 11 months), as previously described (Takahashi and Yamanaka 2006) (Gatto, Redaelli et al. 2012).

Moloney murine leukemia virus–derived vectors, each containing the coding sequences of 1 of the 4 human genes OCT4, SOX2, c-Myc, and KLF4, and the corresponding viral particles were generated by Vectalys (Toulouse, France) and used to infect the fibroblasts as previously described (Takahashi and Yamanaka 2006) (Vallier, Touboul et al. 2009). On day 1, 10^5 fibroblasts were plated in each well of 6-well plates in SFC medium. The following day, the cells were transduced with the four viruses at a multiplicity of infection of 10 (for each virus) for 24 hours. On day 3, the cells were washed in PBS (Gibco, Grand Island, NY) and then grown in medium containing FBS for 3 additional days. On day 7, the cells were passaged on plastic plates containing irradiated mouse embryonic fibroblasts (iMEF, GlobalStem, Rockville, MD) and then grown for 2 additional days in medium with FBS. After day 9, the cells were grown in standard hESC culture conditions (knockout [KSR](Gibco) + FGF2 (4 ng/ml; R&D Systems Inc., Minneapolis, MN). The first iPSCs colonies appeared 15-18 days later and they could be picked after 5-8 additional days of culture. Individual colonies were picked and either transferred into a single well of 12-well plates containing iMEF feeders in KSR + FGF2. The resulting colonies

were then expanded using enzymatic dissociation, cells were harvested using a solution of 1 mg/ml dispase:collagenase IV (ratio 1:1) (Gibco). For comparative studies, normal donor-derived iPSCs (ND-iPSCs) were kindly provided by Professor C.M. Verfaillie (KU Leuven, Leuven, Belgium) and Professor E. Cattaneo (Università degli Studi di Milano, Milan, Italy).

In vitro differentiation of human iPSCs into three germ layers

For *in vitro* differentiation, human iPSCs were switched to a feeder-free condition of culture with Chemically Defined Medium (CDM or CDM-PVA) (Vallier, Touboul et al. 2009). Initially, iPSCs were grown for the first 2 days in CDM supplemented with recombinant Activin (10 ng/ml; R&D Systems Inc.) and FGF2 (12 ng/ml). To obtain extraembryonic tissue, iPSCs were grown for 7 days in CDM in the presence of bone morphogenic protein 4 (BMP4, 10 ng/ml, R&D Systems Inc.). To obtain neuroectoderm progenitors, iPSCs were grown in CDM-PVA in the presence of SB431542 (10 µM, Tocris Bioscience, Bristol, UK) and FGF2 (12 ng/ml) for 7 additional days. To obtain mesendoderm precursors, iPSCs were grown for the 3 following days in CDM-PVA in the presence of BMP4 (10 ng/ml), FGF2 (20 ng/ml), Activin (100 ng/ml) and LY294002 (10 µM, Promega, Madison, WI).

In vivo differentiation

Human iPSCs were harvested with enzymatic treatment immediately prior to implantation, and approximately $2x10^6$ cells were resuspended in mixture of PBS and Matrigel (BD Biosciences, Buccinasco, IT) (ratio 1:1) in a final volume of 400 µL. The cell suspensions were inoculated

subcutaneously into the dorsal flank of 8-week-old Balb/c-Rag2-/-γC-/- male mice, as approved by Institutional Animal Care and Use Committees at KU Leuven. Eight weeks after the injection, tumors were surgically dissected from the mice. Samples were fixed in PBS containing 4% formaldehyde and embedded in paraffin. Serially 4 μm sections were stained with hematoxylin-eosin and characterized.

RNA extraction and RT-qPCR quantification

For the gene expression analysis of iPSCs-derived differentiated cells, total RNA was extracted using RNeasy kit (Qiagen, Hilden, Germany), according to the manufacturer's instructions. 1μg of RNA was used to prepare the corresponding cDNAs with Superscript III First-Strand synthesis system (Invitrogen). Real time PCR was performed using the Platinum SYBR green qPCR Supermix-UDG (Invitrogen). Relative gene expression was calculated by the 2-DDCt method, using GAPDH as housekeeping gene. RT-qPCR primers are listed in Supplementary Table S1.

Immunofluorescence

Human iPSCs or their differentiated progenitors were fixed for 20 minutes at 4°C in 4% paraformaldehyde and then washed three times in PBS. Cells were incubated for 20 minutes at room temperature in PBS containing 10% donkey serum (Serotec Ltd.) and subsequently incubated overnight at 4°C with primary antibody diluted in 1% donkey serum in PBS. For the dilutions of primary antibodies, see Table S1. Cells were then washed three times in PBS and incubated with Texas Red or fluorescein isothiocyanate-conjugated anti-mouse IgG (Sigma-Aldrich; 1:200 in 1% donkey serum in PBS) or rabbit IgG (Jackson

Laboratory, Bar Harbour, ME, http://www.jax.org; 1:400 in donkey serum in PBS) or goat IgG (Jackson Laboratory; 1:400 in donkey serum in PBS) for 2 hours at room temperature. Unbound secondary antibody was removed by three washes in PBS. Hoechst 33258 was added to the first wash (Sigma-Aldrich; 1:10,000).

Differentiation of iPSCs into hepatocyte-like cells

For the differentiation of human iPSCs into hepatocyte-like cells, an adapted protocol published by Roelandt P *et al* (J Hepatol 2012) was followed. Briefly, iPSCs were plated on Matrigel (BD Biosciences, San Jose´, CA, USA) coated 12 well plates with mTeSR1 medium (STEMCELL Technologies, Vancouver, CA) until they reached 70% confluence. Afterwards, cells were grown for 28 days in basal differentiation medium (Pauwelyn K *et al*, Plos One 2011) and different growth factors added sequentially [d0-d2 0 Activin A (100ng/mL) and Wnt3a (50ng/mL; R&D Systems Inc.); d2-d4 Activin A (100ng/mL); d4-d8 BMP4 (50ng/mL); d8-d12 aFGF (20ng/mL; R&D Systems Inc.); and d12-d28 HGF (20ng/mL; R&D Systems Inc.)]. To monitor hepatocyte differentiation, gene expression analysis and immunostaining for hepatocyte-specific markers was performed on d0 and d28. As functional assays for hepatocyte-like cells, albumin secretion were analyzed at day 0, 10 and 28 of differentiation and cytochrome 3A4/5 (CYP3A4/5) activity (with and without induction with phenobarbital) was analyzed at day 28 of differentiation, as previously described (Roelandt *et al*, J Hepatol 2012). For a detailed list of primers and antibodies used, see Supplementary Table S1 and S2.

Differentiation of iPSCs into neural progenitors and cortical cells

Human iPSCs were differentiated into cortical neurons following a protocol recently described by Espuny-Camacho et al. (Espuny-Camacho, Michelsen 2013). Briefly, dissociated iPSCs were plated at the density of 20000 cells/cm^2 in 12 well plates and 5cm dishes coated with hESC qualified Matrigel (VWR 734-1440) in mTeSR1 medium supplemented with ROCK inhibitor (final concentration 10μM, Calbiochem) for 2 days. Subsequently, iPSCs were grown for 16 days in DDM (Gaspard et al., 2009) supplemented with B27 and complemented with Noggin (100 ng/ml, R&D Systems Inc.) and until day 24 with DDM-B27 medium alone, changing the medium every 2 days. At day 24 the progenitors were manually dissociated in L-15 medium supplemented with 1mM glucose and then re-plated on poly-Lysin/Laminin coated coverslips and let them further differentiate until day 40 in DDM-B27 and ROCK inhibitor (10μM) without medium change. To monitor neuronal differentiation, gene expression analysis and immunostaining for neural specific markers was performed on d5, d11, d19, d24 and d40. For a detailed list of primers and antibodies used, see Supplementary Table S1 and S2.

Mutation analysis of the IDUA gene

Genomic DNA was extracted from human iPSCs using the Wizard Genomic DNA Purification kit (Promega, Madison, WI). Mutation analysis of the IDUA gene was limited to confirm the presence of mutations identified at diagnosis. The exons 2, 9 and 10 were amplified

and sequenced using intronic primers designed for both amplification and sequencing. Exons 2 was amplified in 25µl containing 100 ng of genomic DNA, Buffer 1X with MgCl2 1.5mM, dNTP mix 200mM, 15pmol of each primer, GC-RICH solution 1X and 0.5U of the proofreading PWO SuperYeld DNA Polymerase (ROCHE, Monza, Italy). Exons 9-10 co-amplification was carried out in 25µl volume containing 100 ng of genomic DNA, Buffer 1X with MgCl2 1.5mM, dNTP mix 200mM, 15pmol of each primer and 0.5U of the GoTaq DNA Polymerase (Promega). Cycling conditions were: initial denaturation at 96°C for 5 min, 30 cycles at the following conditions: denaturation at 96°C for 1 min, annealing at 67°C for exon 2, 65°C for exon 4 and 63°C for exons 9-10 for 1 min, extension at 72°C for 1 min, followed by final extension at 72°C for 7 min. PCR products were purified using an enzymatic reaction containing 5U of Exonuclease I (Celbio, Pero, Italy) and 1U of Alkaline Phosphatase (Promega) using the following conditions: 15 min at 37°C followed by 15 min at 80°C. Purified fragments were sequenced in both forward and reverse directions using BigDye v3.1 terminator technology and then purified with the BigDye XTerminator Purification Kit. Sequence reactions were carried out and purified according to the manufacturer's instructions and were analyzed on an ABI Prism 3130 Avant Automatic Sequencer (Applied Biosystems, Foster City, CA).

Specific α-L-iduronidase enzymatic activity

IDUA activity was determined according to Clements et al. (Clements PR, Brooks DA, Eur J Biochem 1985). Briefly, cells were resuspended in 150 mM NaCl and freeze-thawed 6 times. Protein extracts were

assayed for total protein content using the BCA assay. 5 µg of protein was added, in triplicate, to a solution containing 8 mM D-Saccharic acid 1,4-lactone and 2 mM 4-methylumbelliferyl-α-L-iduronide in 0.1 M sodium formate buffer, pH 3.2. Samples were incubated for 1 hr at 37°C before stopping the reaction by adding 1 ml of 0.5 M carbonate buffer, pH 10.7. The cleaved substrate was quantified on a Perkin Elmer fluorometer. The enzyme activity was calculated from a reference curve obtained by using 4-methylumbelliferone and was expressed as nmoles/hr/mg. Boxplot explanation: upper horizontal line of box = 75th percentile; lower horizontal line of box = 25th percentile; horizontal bar within box = median, square within box = mean; vertical lines out of the box = minum and maximum.

Quantification of GAGs

Human iPSCs were digested with proteinase K (0.5 mg/ml in 100 mM K2HPO4 pH 8.0; 1 ml/tube) at 56º C overnight. After digestion, proteinase K was inactivated at 90º C for 10 min. Debris was removed by centrifugation (5000g, 10 min, 4º C) and 100 ul cleared lysate used for sulfated GAGs quantification in the Blyscan Assay (Biocolor Ltd., UK). GAGs levels were normalized by the DNA content of each sample, and expressed as GAGs (ug)/ DNA (ug). Boxplot explanation: upper horizontal line of box = 75th percentile; lower horizontal line of box = 25th percentile; horizontal bar within box = median, square within box = mean; vertical lines out of the box = minum and maximum

Statistical analysis

All the data showed in the graphs are represented as mean of experiments and their relative standard deviations (SD). For comparison between groups, an unpaired 2-tailed Student t test was used. A p value less than .05 was considered statistically significant.

For IDUA enzymatic activity and GAGs quantification assay, the p-value refers to the wilcoxon non parametric test on the median (one side)

Results

Generation and characterization of MPS-iPSC lines

Using the approach described by Takahashi K *et al.* (Takahashi and Yamanaka 2006), we generated human iPSCs from fibroblasts and bone marrow (BM)-MSCs of 4 MPS IH patients. 3 out of 4 patient-derived cell sources were successfully reprogrammed and approximately 10 different cell lines were isolated from each patient. Three iPSC lines per patient were selected for full characterization. All the selected cell lines exhibited the typical human pluripotent stem cell morphology, including round cell shape, scant cytoplasm and large nucleoli (Fig. 1A, inset). The MPS-iPSC clones expressed the pluripotency markers Nanog, Oct-4, Sox2 and TRA-1-60 (Fig. 1A). The RT-qPCR results confirmed the high expression of the 4 endogenous pluripotency-specific genes and silencing of the transgenes (Fig. 1S-A). The number of transgene copies inserted in the genome of the isolated MPS-iPSCs was about 3 for each gene (Fig.1S-B). We performed *in vitro* differentiation into three germ layers of the MPS-iPSCs and detected proteins of the neuroectodermal (PAX6, SOX-1, SOX-2), mesendodermal (SOX-17, Brachyury, FOXA2) and extra-embryonic (CDX-2, GATA-4, SOX-7) cells (Fig. 1B). In addition, all the iPSC clones tested formed teratomas *in vivo* (Fig. 1C). Taken together, these results demonstrate that the MPS-iPSC lines generated from MPS-IH cells were successfully reprogrammed.

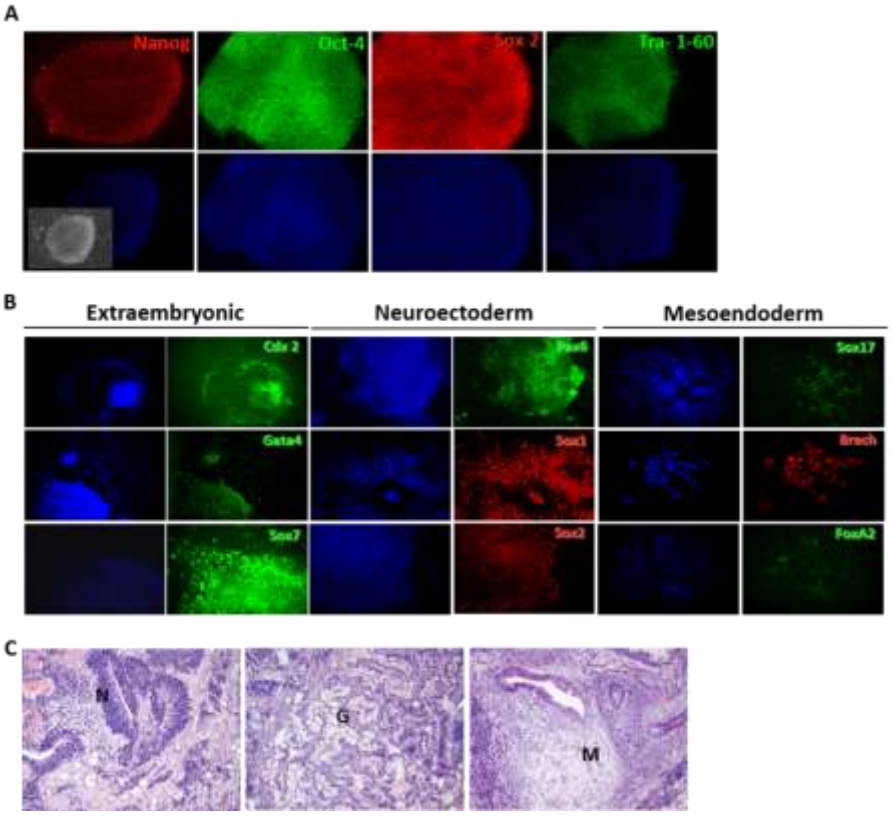

Fig. 1: Reprogramming of MPS IH fibroblasts and characterization of MPS-iPSC lines. (A) MPS-iPSCs express pluripotency markers. The picture (inset, magnification 10X) represents the morphology of an iPSCs clone at passage 3. The colony has the typical round shape, and the cells have scant cytoplasm and large nucleoli. The immunostaining was performed at passage 5 for the pluripotency markers NANOG, OCT4, SOX2, and TRA-1-60. Nuclei are stained blue with DAPI. Magnification 10X. (B) *In vitro* differentiation of human MPS-iPSCs. The immunostaining demonstrates that patient-derived iPSC lines differentiate *in vitro* in a chemically defined medium into derivatives of the three germ layers and into extra-embryonic tissues: extraembryonic (CDX-2, GATA-4, SOX-7), neuroectoderm (PAX6, SOX-1, SOX-2) and mesendoderm (SOX17, BRACHYURY, FOXA2). (C) Teratomas from human MPS-iPSCs. $2x10^6$ cells grown for 10 passages under described conditions were injected into the dorsal flank of Balb/c-$Rag2^{-/-}$ $\gamma C^{-/-}$ mice. The resulting tumors were harvested approximately 8 weeks after injection.

Hematoxylin and eosin stained sections of teratomas show the formation of cell types characteristic of all three germ layers including neural epithelium (N, neuroectoderm), glandular epithelium (G, endoderm) and mesenchyme (M, mesoderm).

Evaluation of disease-specific features on MPS-iPSCs

We next tested if the MPS-iPSC lines maintained the original characteristics of the disease-affected cell types. First, we analyzed the specific genotype of the MPS-iPSC lines. In all patient-derived iPSCs lines, the sequence analysis of the IDUA gene confirmed the mutations previously identified in the somatic counterparts used for the disease diagnosis (Fig. 2A). Patient 1 (Pt1) was homozygote for the p.P496R, a missense mutation in exon 10 (c.1487C>G) resulted in a non-conserved aminoacid change (Proline > Arginine) at position 496 of protein chain. Patient 2 (Pt 2) revealed a compound heterozygosity for p.Q70X and p.P496R mutations. The p.Q70X mutation (c.208C>T) in exon 2 caused a premature STOP codon at position 70 of protein chain. Patient 3 (Pt 3) was homozygote for the p.W402X mutation in exon 9 (c.1205G>A), which introduced a premature STOP codon at position 402 of protein chain.

IDUA enzymatic activity was significantly lower in MPS-iPSC lines compared to ND-iPSCs (median HD-iPSCs 13,60 nmol/h/mg, range from 4,85 to 54,10 *vs.* median MPS-iPSCs 1,15 nmol/h/mg, range from 0 to 11,30, p = 0.0043) (Fig. 2B, left panel). As expected, GAGs cellular content was significantly higher in patients than in ND (median HD-iPSCs 0,076 µg/µg DNA, range from 0 to 0,189 *vs.* median MPS -iPSCs 0,332 µg/µg DNA, range from 0,265 to 0,49, p = 0,0011) (Fig. 2B, right panel).

As expected, there was abnormal accumulation of GAGs in MPS IH teratoma-derived tissues compared to ND-iPSC derived teratomas. This was particularly evident in connective tissue of the teratomas, in which is possible to observe a disorganization of the tissue and the presence of swollen, enlarged, vacuolated cells (Fig. 2C, on right).

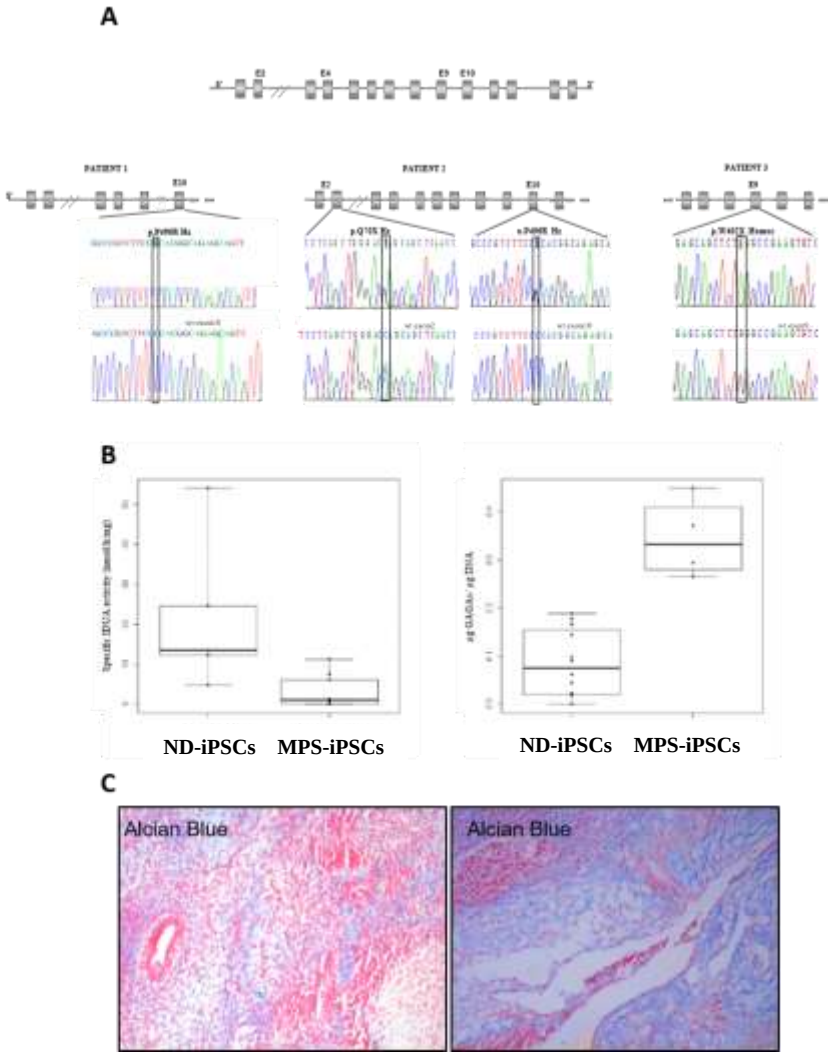

Fig. 2: Disease-specific features of MPS-iPSCs. (A) Molecular analysis of *IDUA* mutations. The automated sequencing of the IDUA coding region identified the

mutations in the genomic DNA of MPS-iPSCs generated from patient 1,2 and 3. The panel shows the positions of mutations (electroferograms higher) compared with the wild-type sequence (electroferograms lower). (B) IDUA activity evaluation. Specific IDUA enzymatic activity was measured in protein extracts of MPS-iPSCs and ND-iPSCs. Activity was expressed as nmoles of enzyme normalized against protein content (mg) and incubation time (hr). n= 10 MPS-iPSCs and 5 ND-iPSCs. The p-value refers to the wilcoxon non parametric test on the median (one side). (C) Accumulation of GAGs. Total GAGs levels were measured in each iPSC lines using the Blyscan Sulfated GAG assay. The content of GAGs, normalized to genomic DNA, was expressed as μg GAG/μg DNA in each sample. n= 4 MPS-iPSCs and 12 ND-iPSCs. The p-value refers to the wilcoxon non parametric test on the median (one side). (D) MPS-iPSCs (on right) and ND-iPSCs (on left) teratoma sections.

Lineage-directed differentiation of the MPS-iPSCs into disease-relevant cell types.

Subsequently, we investigated whether the MPS-iPSCs were able to differentiate into two disease relevant cell types, hepatocytes and neurons. Using the protocol described by Roelandt P. *et al.* (Roelandt P, Obeid S, J Hepatol 2012), we derived hepatocyte-like cells from MPS-iPSCs (Fig. 3A) and from ND-iPSCs. Immunostaining revealed that the differentiated MPS-iPSCs, similarly to ND-iPSCs, showed characteristics of hepatocyte-like cells, such as expression of the hepatic proteins albumin (ALB) and cytokeratin-18 (KRT18) and low expression of α-fetoprotein (AFP) (Fig. 3A). These results were confirmed by RT-qPCR for a number of hepatic marker genes, demonstrating no significant differences between MPS-iPSCs and ND-iPSCs (Fig. 3B). To provide further evidence that differentiation of MPS-iPSCs and ND-iPSCs was similar, we analyzed albumin secretion (Fig. 3C) and cytochrome P450 activity-with or without phenobarbital

induction- (Fig. 3D) of the iPSCs derived hepatocyte-like cells. In both assays, no differences among MPS-iPSCs and ND-iPSCs derived hepatocyte-like cells was detected. We also tested if the MPS-iPSC lines could be committed to cortical neuronal progeny, based on a protocol recently described (Espuny-Camacho, Michelsen 2013). The differentiated progeny derived from MPS-iPSCs expressed the typical neuronal markers Nestin, TuJ 1, FoxP2 and CTIP2 (cortical neurons) at the protein level (Fig. 4A). No significant differences in the expression profile of neural transcripts at different time points were detected between progeny from MPS-iPSCs and ND-iPSCs (Fig. 4B). Thus, we found that the differentiation capacity of MPS-iPSCs to hepatocyte-like cells and neurons was similar to that of ND-iPSCs, despite the fact that GAG accumulation occurred in undifferentiated MPS-iPSCs.

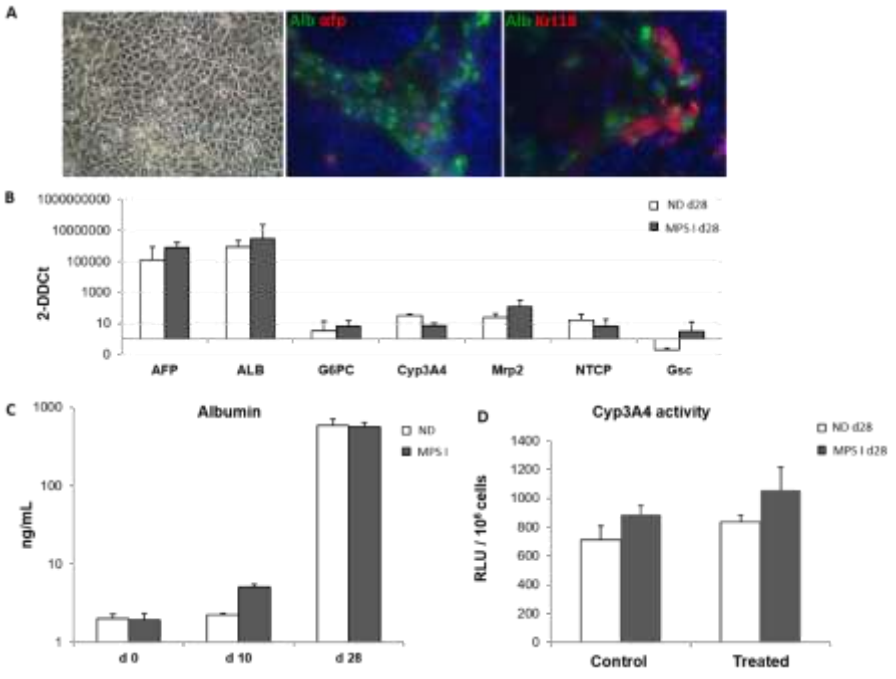

Fig. 3: Differentiation of MPS-iPSCs into hepatocyte-like cells. (A) After 28 days of culture in hepatic differentiation conditions, the differentiated iPSCs showed the morphology of hepatocyte-like cells, with cuboidal cell shape and clear nuclei (magnification 20X). Immunostaining of d28 hepatic progeny revealed the expression of ALB (in green), KRT18 and AFP (in red) in the differentiated MPS-iPSC lines. (B) Gene expression profile of hepatic markers (*GSC*, *AFP*, *ALB*, *G6PC*, *CYP3A4*, *MRP2*, *NTCP*) obtained at d28 by RT-qPCR, normalized to the housekeeping gene *GADPH*. Data are provided as fold change compared with levels on day 0. Bars are the means DDCt ± SD of 3 ND-iPSC samples *versus* 3 MPS-iPSC samples; each cell line was tested in two independent experiments. (C) Albumin secretion analyzed at different time points during hepatic differentiation of iPSCs. (D) CYP3A4 activity induced by phenobarbital (treated) of d28 hepatic differentiated progeny of iPSCs.

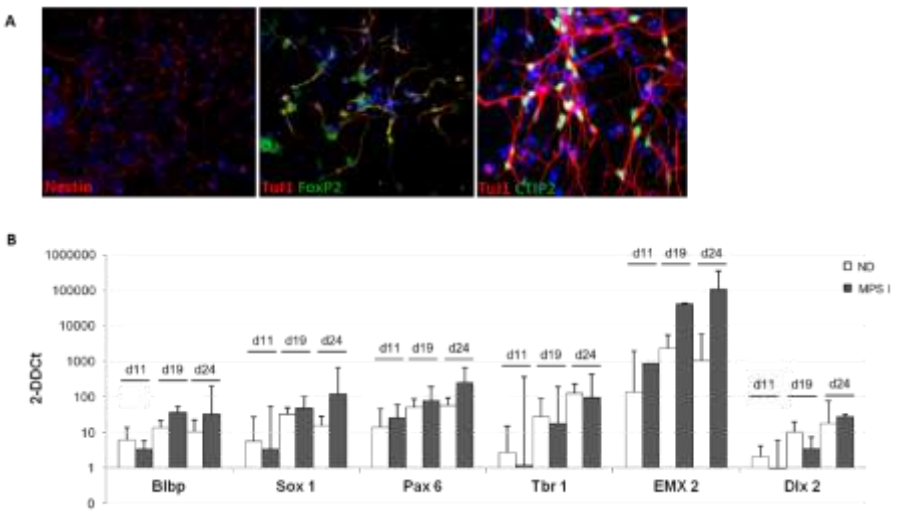

Fig. 4: Differentiation of MPS-iPSCs into neurons. (A) After 40 days of culture in neural differentiation conditions, the differentiated MPS-iPSCs express neuronal markers Nestin (in red), TUJ1 (in red), FOXP2 and CTIP2 (in green) by immunostaining. (B) Gene expression profile of neuronal markers (*TBR 1*, *EMX 2*, *DLX 2*, *BLBP*, *SOX 1*, *PAX 6*) in the progeny of differentiated iPSCs, obtained through RT-qPCR, normalised to the housekeeping gene *GADPH*, at different time points (d5, d11, d19 and d24). Data are provided as fold change compared with levels on day 5.

Bars are the means DDCt± SD of 3 ND-iPSC samples *versus* 2 MPS-iPSC samples. Each cell line was tested in independent experiments.

Discussion

The ability to generate pluripotent stem cells from somatic cells by cellular reprogramming (iPSCs generation), and subsequent re-differentiation to multiple cell types, has created the possibility for generating patient-specific differentiated cells to examine mechanisms underlying the disease phenotype. We here demonstrate that when iPSCs are generated from patients with Hurler syndrome and are re-differentiated towards neural and hepatic cells, cell types relevant to Hurler disease, apparently normal differentiation occurs despite the fact as in Hurler patients, significant accumulation of GAGs is seen in affected cells.

Tolar *et al.,* demonstrated in 2011, that fibroblasts or keratinocytes from Hurler patient could be reprogrammed to iPSCs, showing pluripotent characteristics, including ESC-like phenotypic features, embryoid bodies formation and teratoma generation (Tolar et al., 2011). Consistent with this study, we demonstrate here that iPSCs can be generated from somatic cells of patients with MPS-IH, and that retrain pluripotent characteristics. As a result of the lack of IDUA enzyme production, the MPS-iPSCs contained significantly higher levels of GAGs. Substantial accumulation of GAGs was also seen in teratomas *in vivo,* and this was most pronounced in the connective tissue: disorganization of the tissue and presence of lysosomal storage vacuoles. This finding is consistent with the clinical observation that GAGs accumulation affects the cytoskeleton (Hinek and Wilson 2000), and can also be found very extensively in perivascular mesenchyme in

all organs, and this even before birth (Crawfurd, Dean et al. 1973)Crow, Gibbs et al. 1983).

Tolar *et al.*, addressed the question whether iPSCs from Hurler patients could be efficiently differentiated towards hematopoietic cells, after genetic correction, as an autologous and therapeutic HSCs source. However, hematopoiesis in patients with MPS IH is essentially normal. By contrast, significant abnormalities are noted in a number of organs. Aside from the typical musculoskeletal manifestations, such as joint stiffness and contractures, and dysostosis multiplex, hepatomegaly and impaired mental development is common, due to GAGs accumulation in the liver, in the perivascular space, as well as in different neurons (Hinek and Wilson 2000). Using standard protocols for hepatocyte-like cell generation and cortical neuron generation, we found that the inherent differentiation ability of the MPS-iPSCs to both lineages appeared to be similar as what we found in ND-iPSCs, even if the differentiated MPS-iPSC progeny contained excessive amounts of GAGs.

Although the loss of IDUA lays at the basis of the disease, a number of studies have suggested that the abnormalities seen in different tissues are at least in part due to the aberrant binding of a number of growth factors and other extracellular molecules to the accumulated GAGs (Pan C, Nelson MS; Blood 2005). It is therefore interesting that hepatic differentiation from MPS-iPSCs was essentially indistinguishable from that of ND-iPSCs. Hepatic differentiation is accomplished using, among others, Activin A, Wnt3a, BMP4 and aFGF, all known to bind to GAGs. It will therefore be of interest to further examine the

hepatocyte differentiation to determine if subtle differences may be present between MPS and ND iPSCs progeny.

Severe Hurler syndrome is characterised by progressive mental retardation. The cascade of events leading from IDUA deficiency to neuropathology is unknown. Neuropathology in Hurler patients includes primary storage of GAGs in neurons but also the perivascular space, secondary accumulation of GM2 and GM3 gangliosides, severe neuroinflammation and consequent histological damage (Walkley 2004). It is well established that a number of lysosomal storage disorders are associated with neurological impairment, even if it is still not known whether this due to autonomous neuronal dysfunction. We found no obvious differences in cortical neuron development between MPS and ND iPSCs. Lemonnier *et al.* examined neural differentiation from iPSC generated from patients with mucopolysaccharidosis IIIB (MPSIIIB, Sanfilippo syndrome type B) (Lemonnier, Blanchard et al. 2011). In contrast to MPS-IH iPSC, MPS-IIIB iPSC could not be isolated and expanded unless the accumulating partially digested GAGs, to which FGF2 used for iPSCs expansion binds, were eliminated by enzyme supplementation. This was not seen for MPS-iPSCs made in this study nor by the Tolar *et al.* group (Tolar, Park et al. 2011). In MPS-IIIB, neural differentiation from iPSCs was possible, using floating neurosphere cultures but the neuronal progeny from MPS-IIIB progeny contained storage vesicles and disorganization of Golgi ribbons.

Here, we reported a successful derivation of human iPSCs from MPS IH patients and consequently differentiation to hepatocyte-like cells and cortical neurons, with efficiency similar to that of wild type iPSCs. In

conclusion, the ability to make patient-specific and differentiated progeny from Hurler patients will offer appropriate disease models for mechanistic studies and high-throughput screening in identical genetic backgrounds and represents an important first step towards the eventual clinical application in cell replacement therapy approaches.

Acknowledgments

We are indebted to Professor E. Cattaneo (Center for Stem Cell Research, Università degli Studi di Milano, Milan, Italy) for providing normal donor-derived iPSCs. We thank Dr F. Bertola (Consortium for Human Molecular Genetics, University of Milano-Bicocca, Monza, Italy) for molecular analyses of IDUA mutations.

Funding

This work was supported by the Italian Telethon Foundation to MS (TCP 07004). MS is Assistant Telethon Scientist at Dulbecco Telethon Institute (DTI). FG was recipient of a fellowship from DIMET PhD program, University of Milano-Bicocca.

References

Aldenhoven, M., J. J. Boelens, et al. (2008). "The clinical outcome of Hurler syndrome after stem cell transplantation." Biology of blood and marrow transplantation : journal of the American Society for Blood and Marrow Transplantation 14(5): 485-498.

Ballabio, A. and V. Gieselmann (2009). "Lysosomal disorders: from storage to cellular damage." Biochimica et biophysica acta 1793(4): 684-696.

Chang, C. J. and E. E. Bouhassira (2012). "Zinc-finger nuclease-mediated correction of alpha-thalassemia in iPS cells." Blood 120(19): 3906-3914.

Chung, S., X. Ma, et al. (2007). "Effect of neonatal administration of a retroviral vector expressing alpha-L-iduronidase upon lysosomal storage in brain and other organs in mucopolysaccharidosis I mice." Molecular genetics and metabolism 90(2): 181-192.

Clements PR, Brooks DA, Saccone GT and Hopwood JJ. (1985). Human alpha-L-iduronidase. 1. Purification, monoclonal antibody production, native and subunit molecular mass. Eur J Biochem 152:21-28.

Crawfurd, M., M. F. Dean, et al. (1973). "Early prenatal diagnosis of Hurler's syndrome with termination of pregnancy and

confirmatory findings on the fetus." Journal of medical genetics 10(2): 144-153.

Crow, J., D. A. Gibbs, et al. (1983). "Biochemical and histopathological studies on patients with mucopolysaccharidoses, two of whom had been treated by fibroblast transplantation." Journal of clinical pathology 36(4): 415-430.

DeKelver, R. C., V. M. Choi, et al. (2010). "Functional genomics, proteomics, and regulatory DNA analysis in isogenic settings using zinc finger nuclease-driven transgenesis into a safe harbour locus in the human genome." Genome research 20(8): 1133-1142.

Gatto, F., D. Redaelli, et al. (2012). "Hurler disease bone marrow stromal cells exhibit altered ability to support osteoclast formation." Stem cells and development 21(9): 1466-1477.

Hinek, A. and S. E. Wilson (2000). "Impaired elastogenesis in Hurler disease: dermatan sulfate accumulation linked to deficiency in elastin-binding protein and elastic fiber assembly." The American journal of pathology 156(3): 925-938.

Hockemeyer, D., F. Soldner, et al. (2009). "Efficient targeting of expressed and silent genes in human ESCs and iPSCs using zinc-finger nucleases." Nature biotechnology 27(9): 851-857.

Huang, H. P., P. H. Chen, et al. (2011). "Human Pompe disease-induced pluripotent stem cells for pathogenesis modeling, drug testing and disease marker identification." Human molecular genetics 20(24): 4851-4864.

J., N. E. F. a. M., Ed. (2001). The mucopolysaccharidoses. In: The Metabolic and Molecular Bases of Inherited Disease. New York, Mc Graw Hill.

Kawagoe, S., T. Higuchi, et al. (2011). "Generation of induced pluripotent stem (iPS) cells derived from a murine model of Pompe disease and differentiation of Pompe-iPS cells into skeletal muscle cells." Molecular genetics and metabolism 104(1-2): 123-128.

Lemonnier, T., S. Blanchard, et al. (2011). "Modeling neuronal defects associated with a lysosomal disorder using patient-derived induced pluripotent stem cells." Human molecular genetics 20(18): 3653-3666.

Meng, X. L., J. S. Shen, et al. (2010). "Induced pluripotent stem cells derived from mouse models of lysosomal storage disorders." Proceedings of the National Academy of Sciences of the United States of America 107(17): 7886-7891.

Metcalf, J. A., X. Ma, et al. (2010). "A self-inactivating gamma-retroviral vector reduces manifestations of mucopolysaccharidosis I in mice." Molecular therapy : the journal of the American Society of Gene Therapy 18(2): 334-342.

Muenzer, J. (2011). "Overview of the mucopolysaccharidoses." Rheumatology 50 Suppl 5: v4-12.

Pan C. (2005). "Functional abnormalities of heparan sulfate in mucopolysaccharidosis-I are associated with defective biologic

activity of FGF-2 on human multipotent progenitor cells". Blood. 2005 Sep 15;106(6):1956-64.

Park, I. H., R. Zhao, et al. (2008). "Reprogramming of human somatic cells to pluripotency with defined factors." Nature 451(7175): 141-146.

Peters, C. (2004). "Another step forward towards improved outcome after HLA-haploidentical stem cell transplantation." Leukemia : official journal of the Leukemia Society of America, Leukemia Research Fund, U.K 18(11): 1769-1771.

Porteus, M. H. and D. Carroll (2005). "Gene targeting using zinc finger nucleases." Nature biotechnology 23(8): 967-973.

Rashid, S. T., S. Corbineau, et al. (2010). "Modeling inherited metabolic disorders of the liver using human induced pluripotent stem cells." The Journal of clinical investigation 120(9): 3127-3136.

Roelandt, P., P. Sancho-Bru, et al. (2010). "Differentiation of rat multipotent adult progenitor cells to functional hepatocyte-like cells by mimicking embryonic liver development." Nature protocols 5(7): 1324-1336.

Smith, J. R., S. Maguire, et al. (2008). "Robust, persistent transgene expression in human embryonic stem cells is achieved with AAVS1-targeted integration." Stem cells 26(2): 496-504.

Takahashi, K., K. Tanabe, et al. (2007). "Induction of pluripotent stem cells from adult human fibroblasts by defined factors." Cell 131(5): 861-872.

Takahashi, K. and S. Yamanaka (2006). "Induction of pluripotent stem cells from mouse embryonic and adult fibroblast cultures by defined factors." Cell 126(4): 663-676.

Tenzen, T., F. Zembowicz, et al. (2010). "Genome modification in human embryonic stem cells." Journal of cellular physiology 222(2): 278-281.

Tolar, J., I. H. Park, et al. (2011). "Hematopoietic differentiation of induced pluripotent stem cells from patients with mucopolysaccharidosis type I (Hurler syndrome)." Blood 117(3): 839-847.

Traas, A. M., P. Wang, et al. (2007). "Correction of clinical manifestations of canine mucopolysaccharidosis I with neonatal retroviral vector gene therapy." Molecular therapy : the journal of the American Society of Gene Therapy 15(8): 1423-1431.

Vallier, L., T. Touboul, et al. (2009). "Signaling pathways controlling pluripotency and early cell fate decisions of human induced pluripotent stem cells." Stem cells 27(11): 2655-2666.

Visigalli, I., S. Delai, et al. (2010). "Gene therapy augments the efficacy of hematopoietic cell transplantation and fully corrects mucopolysaccharidosis type I phenotype in the mouse model." Blood 116(24): 5130-5139.

Walkley, S. U. (2004). "Secondary accumulation of gangliosides in lysosomal storage disorders." Seminars in cell & developmental biology 15(4): 433-444.

Zhu, H., M. W. Lensch, et al. (2011). "Investigating monogenic and complex diseases with pluripotent stem cells." Nature reviews. Genetics 12(4): 266-275.

Zou, J., M. L. Maeder, et al. (2009). "Gene targeting of a disease-related gene in human induced pluripotent stem and embryonic stem cells." Cell stem cell 5(1): 97-110.

Supplementary materials

Table S1. RT-qPCR Primers

Exogenous pluripotency genes		
hKLF4	F	GATGAACTGACCAGGCACTA
hKLF4	R	TCCTGTCTTTAACAAATTGGACT
hMYC	F	AAGAGGACTTGTTGCGGAAA
hMYC	R	TCCTGTCTTTAACAAATTGGACT
hOCT4	F	CCTCACTTCACTGCACTGTA
hOCT4	R	TCCTGTCTTTAACAAATTGGACT
hSOX2	F	CCCAGCAGACTTCACATGT
hSOX2	R	TCCTGTCTTTAACAAATTGGACT
Endogenous pluripotency genes		
hKLF4	F	GGTCGGACCACCTCGCCTTACAC
hKLF4	R	CTCAGTTGGGAACTTGACCA
hMYC	F	CTGAAGAGGACTTGTTGCGGAAAC
hMYC	R	TCTCAAGACTCAGCCAAGGTTGTG
hOCT4	F	CCTCACTTCACTGCACTTGTA

hOCT4	R	CAGGTTTTCTTTCCCTAGCT
hSOX2	F	ATGTCCCAGCACTACCAGAG
hSOX2	R	GCACCCCTCCCATTTCCC
PBGD	F	GGAGCCATGTCTGGTAACGG
PBGD	R	CCACGCGAATCACTCTCATCT
Hepatocyte differentiation		
AFP	F	CCTACAATTCTTCTTTGGGCT
	R	AGTAACAGTTATGGCTTGGA
ALB	F	TGGCACAATGAAGTGGGTAA
	R	CTGAGCAAAGGCAATCAACA
Cyp3A4	F	CCTCCCTGAAAGATTCAGC
	R	TGAAGAAGTCCTCCTAAGCT
G6PC	F	GTGTCCGTGATCGCAGACC
	R	GACGAGGTTGAGCCAGTCTC
Gsc	F	TCTCAACCAGCTGCACTGTC
	R	CCAGACCTCCACTTTCTCCTC
Mrp2	F	CGATATACCAATCCAAGCCTC
	R	GAATTGTCACCCTGTAAGAGTG
NTCP	F	AACCTCAGCATTGTGATGAC
	R	GTATTGTGGCCGTTTGGA
Neural differentiation		
Blbp	F	GGACTCTCAGCACATTCAAGAA
	R	CCACATCACCAAAAGTAAGGGT
Dlx2	F	ACGCTCCCTATGGAACCAGTT
	R	TCCGAATTTCAGGCTCAAGGT
Emx2	F	GCTTCTAAGGCTGGAACACG

	R	CCAGCTTCTGCCTTTTGAAC
Pax6	F	GTGTCTACCAACCAATTCCACAAC
	R	CCCAACATGGAGCCAGATG
Sox1	F	GCAAGATGGCCCAGGAGAA
	R	CCTCGGACATGACCTTCCA
Tbr1	F	ATGGGCAGATGGTGGTTTTA
	R	GACGGCGATGAACTGAGTCT

Table S2. Primary antibodies used for immunohistochemistry

AFP	1:4000; R&D Systems, MAB 1368
ALB	1:8000; Dako, A0001
Beta III tubulin (TuJ1)	1:1000; Covance, MMS-435P
Brachyury	1:100; Abcam, ab20680
Cdx-2	1:100; BioGenex, MU392A-UC
CTIP2	1:500; Abcam, ab18465
FoxA2	1:50; Abcam, ab5074
FoxP2	1:5000; Abcam, ab16046
GATA-4	1:100; Santa Cruz Biotechnology Inc, sc-25310
Hoechst 33258	1:10 000; Sigma-Aldrich
KRT18	1:250; Santa Cruz Biotech, SC31700
Nanog	1:100; R&D Systems Inc, AF1997
NESTIN	1:1000; Covance, MMS-570P
Oct-4	1:100; Abcam, ab18976

Pax-6	1:100; Covance (Cambridge BioScience) PRB-278P-100
Sox-1	1:100; R&D Systems Inc, AF3369
Sox-2	1:100; Abcam, ab15830
Sox-2	1:200; R&D Systems Inc, AF2018
Sox-7	1:100; Abcam, ab22584
Sox-17	1:200; R&D Systems Inc, AF1924
TRA-1-60	1:100; Santa Cruz Biotechnology Inc, sc-21705

CHAPTER 4:
Summary, conclusions and future perspectives

The general focus of the PhD thesis was to isolate and characterize cells of particular interest for Hurler pathology. To achieve this purpose, we took advantage from the innovative and increasingly promising iPSCs technique. They allowed us to reproduce developmental process and to create a perfect humanized *in vitro* disease-model, providing the possibility to verify possible impaired pathways due to the IDUA gene mutation.

In the first study, we investigated the involvement of the mesoderm compartment in MPS IH pathology, in particular of the MSCs and OBs cell population to assess their role in osteogenesis and osteoclastogenesis.

At first, we created a reproducible and standardized protocol to differentiate HD-iPSCs into osteoblasts, through the intermediate generation of *bona-fide* MSCs.

1. We isolated MSC-like cells that express the canonical mesenchymal cell surface markers, comparable to BM-MSCs; were able to adhere to plastic; and presented a comparable kinetic of grow as BM-MSCs, even though they demonstrated a more prolonged lifespan in culture.
2. Differentiation of MSC-like cells to osteoblasts was achieved, as confirmed by Alizarin Red staining and gene expression profile for osteogenic genes.
3. To complete the characterization of MSC-like cells, we also evaluated their ability to differentiate into adipocytes and chondrocytes. Oil Red-O staining confirmed the efficacy of the

designed adipocytes induction protocol. Partially differentiated chondrogenic pellets were obtained.

Secondly, we adopted the beforehand mentioned protocol to MPS-iPSCs to evaluate whether or not there was a compromised phenotype.

1. Four different lines were obtained from two MPS patients. MPS MSC-like cells showed a significant lower kinetic of growth compare to HD MSC-like cells. In particular, PT-2 MSC-like cells were not able to expand in culture.
2. Hydroxyapatite was produced by MPS-OBs but at a lower level compare to HD. Moreover, a significant downregulation of the osteogenic genes expression was reported.
3. Regarding the role of MPS MSC-like cells and OBs in the osteoclastogenesis process, we noticed an over expression of RANKL in MSC-like cells and an unusual pattern of production of RANKL and OPG during osteoblastic differentiation.

Overall, our data suggest the possibility that at early time points in disease pathogenesis physiologic alterations occurred. The later stages alterations of MPS disease pathogenesis that have been reported in literature may represent a consequence of an already compromised tissue. In our model, needs to be clarified whether the alterations observed are a consequence of IDUA gene disruption and GAGs storage within the cell cytoplasm. Moreover, we have to understand if the modifications reported in OB cells, in term of maturation and sustainment of osteoclastogenesis, is already linked to a dysfunction in MSC-like cells or they are two independent altered phenotypes.

In the second study, we investigated over the ectoderm and endoderm to explore the differentiation potential of MPS IH-iPSCs into other disease-relevant cell types, such as hepatocyte-like cells and neurons. We observed that:

1. Abnormal accumulation of GAGs in MPS IH-derived teratoma, particularly evident in the connective tissue, in which was possible to observe a disorganization of the tissue and the presence of swollen, enlarged, vacuolated cells.
2. MPS hepatocyte-like cells, with typical cuboidal morphology, expressed the characteristic genes and markers as HD-cells. Functional activity of differentiated cells has been performed, evaluating the ability to secrete albumin in the medium and the detoxification capacity after drug administration.
3. Similarly, iPSCs-MPS IH differentiated into neurons expressed their typical genes as HD iPSC-derived neurons.

In conclusion, MPS hepatocyte-like cells and neurons retrained similar morphological and functional features with normal iPSCs. This may suggest that neurological defect and hepatomegaly could occur at later stages, during the child's growth, because of a more prolonged accumulation of GAGs, and consequently, increased cell dysfunction. Interesting is the evident GAGs accumulation reported in the connective tissue of teratoma sections. These data are in accordance with our first study, underlying that an altered phenotype occurs in the mesoderm tissue already at early stage of development.

As future plans we propose to:

1. Increase the recruitment of HD and patient samples to further support our data.
2. Amplify MSCs and OBs characterization with functional assay:
    - ✓ Regarding their role in osteoclastogenesis, ELISA for quantitative determination of free human RANKL and OPG will be performed in MSCs and OBs.
    - ✓ For MSCs, we will assess cell cycles analysis, apoptosis test and telomerase activity assay.

      Capacity to generate bone *in vivo* will be assessed. Actually, there are already ongoing studies.

      Moreover, we propose a co-culture protocol (Gatto et al.) between MSC-like cells and CD34+ cells to evaluate if there are differences between HD MSC-like cells and MPS MSC-like cells in osteoclasts generation.
    - ✓ For OBs, we will quantify the production of extracellular matrix proteins such as COL1A2 and ALP with colorimetric and ELISA assay.
3. Preform gene-correction of MSC-like cells with the wild-type copy of the IDUA gene to understand if the affected phenotype of MPS MSC-like cells and OBs would be reversed. Doing that, we can assess whether or not these alterations are caused by IDUA gene mutation.

   Teratoma formation assay will be performed again to verify if the reduction of GAGs accumulation within the connective tissue will occur.